UNIVERSITY OF TORONTO

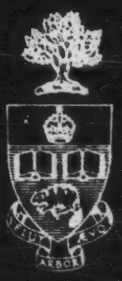
VELUT ARBOR ÆVO

DEPARTMENT OF CHEMICAL ENGINEERING
AND APPLIED CHEMISTRY

92-00197/

Liquid-Liquid Equilibria in Hydrogenation Processes for Bitumen and Coal

A Report Prepared by

John M. Shaw

Associate Professor
Department of Chemical Engineering and Applied Chemistry
University of Toronto
M5S 1A4

1990/06/22

CONTRACT SERIAL NO.
23440-9-9105

CONTRACTOR: UNIV. OF TORONTO

CONTRACT REQ' NO: 23440-9-9105

170 pp

MICROMEDIA

Table of Contents

Table of Contents 1

I Introduction 2

II Summary of Experimental Work 3
- Abstract 4
- Introduction 4
- Experimental 4
- Results and Discussion 5
- Conclusions 6
- References 6
- Tables 7
- Figures 8

III Prediction Complex Liquid-Liquid Equilibria 12
- Introduction 13
- Model Compounds for Coal Liquids 18
- Thermodynamic Model 19
- Pyrene/Tetralin/Light Gas Mixtures 22
- Phase Equilibrium Algorithm 24
- References 28

IV Project Summary
- Conclusions 32
- Recommendations for Future Work 33

V Appendix 34
- A: Phase Splitting and Synergism in Complex Hydrocarbon Systems
(MASc thesis written by L. Dukhedin-Lalla and approved by the University of Toronto during June 1990)

I Introduction

Under the terms of DSS contract # 23440-9-9105 we agreed to perform phase splitting experiments with both simple and complex hydrocarbon liquids pertinent to the development of optimal coal-oil coprocessing reactors and provide a theoretical framework for modelling the phase distribution results. Our experimental and theoretical findings are reported herein. The experimental aspects of the project are briefly summarized in Section II (L. Dukhedin-Lalla, P. M. Rahimi and J. M. Shaw) where partial phase diagrams for several model systems showing zones of liquid-liquid phase splitting and the association of phase splitting with synergistic phenomena are reported. Section II will be included in the proceedings of the upcoming ACS Symposium on coprocessing (Washington, August 1990). A detailed experimental exposition including an extensive literature survey, experimental methods, and complete experimental results is provided in Appendix A (a MASc thesis written by L. Dukhedin-Lalla, and approved by the University of Toronto during June 1990). Preliminary theoretical considerations and modelling results are reported in Section III (J. M. Shaw and S. Sayfaie). Over all conclusions and plans for future work comprise Section IV (J. M. Shaw). The various components of the report can be read separately as they are self contained documents. These documents represent the individual or collaborative efforts of L. Dukhedin-Lalla, P. M. Rahimi, J. M. Shaw and S. Sayfaie, as noted above.

II Summary of Experimental Work

PHASE SPLITTING AND SYNERGISM IN COAL OIL COPROCESSING AND COAL LIQUEFACTION

L. Dukhedin-Lalla+, P.M. Rahimi*, and J. M. Shaw+
+Department of Chemical Engineering, University of Toronto, Toronto, Canada, M5S 1A4
*CANMET, Energy Mines and Resources Canada, 555 Booth St., Ottawa, Canada, K1A OG1

ABSTRACT

The phase behaviour of complex hydrocarbon systems relevant to coal-oil coprocessing and direct coal liquefaction was investigated in the temperature range 600 to 700 K, using a batch autoclave apparatus. Bitumen and heavy oil + anthracene mixtures as well as model liquefaction solvents such as pyrene + tetralin are shown to exhibit phase splitting in this region. Gas phase constituents such as H_2, N_2, CH_4, C_2H_6 were found to influence the size and shape of the phase splitting zone but did not alter the phase behaviour per se. Significant fluctuations in the light oil yield obtained from laboratory and pilot scale models of coal/oil coprocessing and direct coal liquefaction processes are frequently attributed to synergism. In this paper, some aspects of synergism are related to phase splitting and the influence of phase splitting on reaction schemes. Preliminary criteria for solvent/diluent selection and operating conditions are proposed.

KEY WORDS: coprocessing, coal liquefaction, synergism

INTRODUCTION

Kinetic studies in heavy oil upgrading, coal/oil coprocessing and direct coal liquefaction are frequently conducted without due consideration for the physical properties of solvents or diluents under the reaction conditions employed (650 to 750 K, 4 to 30 MPa). Consequently, significant fluctuations in light oil yields obtained from laboratory and pilot scale studies, arising from apparently minor perturbations in operating conditions, are frequently attributed to synergistic phenomena [1-6]. As the reaction conditions associated with coprocessing and coal liquefaction typically intersect the critical region of one or more of the principal liquid constituents [7], complex phase behaviour can be anticipated [8, 9]. Phase splitting, for example, is a common phenomenon in the critical and subcritical regions [10]. In addition, hydrogen is a principal reagent in both coal dissolution [11] and oil hydrogenation reactions and hydrogen solubility in liquids is sensitive to composition [12]. Phase splitting and hydrogen solubility can have a direct and significant impact on observed rates for coal dissolution reactions [13, 14], for example, and these phenomena provide a satisfactory explanation for 20 wt % fluctuations in coal conversion arising in pyrene-tetralin mixtures under hydrogen [15] which had previously been attributed to synergism [1]. Results obtained by Rincon and Angulo [3, 4] and Fouda et al. [6] are also consistent with phase splitting [16]. The transition of the diluent or solvent from liquid to supercritical fluid is another phenomenon which can have a significant impact on reaction kinetics.

Many of the model compounds and liquids employed are unstable under the operating conditions investigated and the phase data presented are not equilibrium data per se. Catalysts are ubiquitous actors in these systems and their effect can only be minimized. Glass liners reduce the impact of trace pyrrhotite (a well known dehydrogenation catalyst) on reactor walls, but do not prevent catalytic hydrogenation due to catechol adsorption on stirrer surfaces [17]. Homogeneous isomerization, pyrolysis, and other reactions cannot be neglected at elevated temperatures. The degradation of pyrene [2, 15] and tetralin [18-21], for example, has been reported. Compound degradation cannot be ignored or prevented and phase compositions inevitably exhibit a time dependence.

EXPERIMENTAL

Experiments were conducted in a glass lined PPI autoclave having an inside diameter of 0.095 m and 0.3 m long. The autoclave, equipped with magnetically driven stirrer, internal cooling coil and three heated sample ports, was placed vertically in a 3000 W muffle furnace. All apparatus components were fabricated from type 316 stainless steel. The autoclave temperature was maintained within two degrees of a set point using an Athena temperature controller and a manually actuated internal cooling coil. All model compounds were reagent grade and supplied by Fluka. The anthracene oil was supplied by Allied-Signal and Athabasca bitumen and Venezuela heavy oil vacuum bottoms were supplied by CANMET. Their properties are listed in Table 1. After loading the autoclave with 150 g of liquid, air was removed by flushing and the autoclave was charged with hydrogen, methane, etc. to a preset pressure and heated at 6 K min^{-1} to the first set point. Once the temperature reached the set point, operating parameters were fixed for 0.5 h. Agitation facilitated the acquisition of phase data. However, it proved necessary to cease agitation 0.5 h before sample retrieval so that emulsions, if present, could break [15]. Samples were collected in ice cold sample vials and immediately diluted in toluene. Species that did not condense at 273 K were not collected. Following sample retrieval the autoclave was heated to subsequent set points and the procedure was repeated.

Samples were analyzed chromatographically and mass spectra were obtained using a Hewlett Packard 5987A radio frequency quadrupole mass spectrometer. Many peaks were not identified unambiguously. Samples (1 μl) were injected directly into a 30 m DB-17 column. Column operating conditions were: carrier gas, helium; temperature program, 373 K for three minutes, 373-548 K at 20 K min^{-1}. Additional GCMS analysis and ASTM standard boiling point data were provided by Shell Canada Ltd. Compositions are repeatable to within 2 to 3 mole %.

RESULTS AND DISCUSSION

Partial phase diagrams for the model systems pyrene + tetralin + (ethane, no gas, nitrogen, or methane) are shown in Figures 1 through 3 respectively. At low gas pressures a liquid-liquid zone appears in all cases at temperatures exceeding 640 K. This zone grows with temperature and at 698 K is quite broad eg. the zone is bounded by 0.25 and 0.60 mole % pyrene when no gas is added. Only ethane causes this zone to shrink at elevated temperatures Figure 1a. Phase splitting can also arise at elevated pressures. For example, with nitrogen (Figure 2), phase splitting arises from splitting of the liquid phase. The high pressure and low pressure zones combines at elevated temperatures. With methane, Figure 3, the vapour phase splits at elevated pressures but these two phases do not coexist with a third phase. Key transitions arising in these systems include: gas-liquid to gas-liquid-liquid at low or high pressure, gas-liquid-liquid to gas-liquid, fluid-fluid or fluid at elevated pressures. These systems are most susceptible to phase splitting at low pyrene contents.

Dukhedin-Lalla et al. [16] reported that the model solvent system indene-decalin did not undergo phase splitting and that the synergism observed by Chiba et al. [2] could not be explained by phase splitting of solvent components. However, decalin is unstable in mixtures with indene, or indene + anthracene oil, as shown in Table 2, and forms naphthalene or naphthalene derivatives at elevated temperatures. The solubility of pyrene like coal liquids in naphthalene at 673 K is 15 to 20 wt % depending on pressure and gas composition as shown in Figures 1 through 4. Chiba et al. [2] reported coal conversions of 53, 65, and 35 wt % in indene, indene (50 wt %) + decalin, and decalin at this temperature and attributed the fluctuation to synergism. The corresponding concentrations of the coal derived liquids in the solvents are 18, 22, and 13 wt %. These concentration values are based on the initial charges of coal (6 g) and solvent (18 g), to a 0.1 litre reactor and the physical properties of naphthalene. The impact of solvent expansion, and evaporation was included in the calculations. While the operating conditions and compositions for the phase and liquefaction experiments were not identical, the conversion of coal in "decalin", which corresponds to a coal derived liquid concentration in the solvent of 13 wt % compares favourably with the solubility limit for pyrene in naphthalene. The coal conversions reported by Chiba et al. [2] are consistent with phase splitting resulting from exceeding the solubility of coal derived liquids in the solvent where the solubility limit is a function of solvent composition. The decrease in coal conversion in solvents with a high "decalin" content can be explained in a manner analogous to the explanation of synergism in the pyrene-tetralin solvent system [15].

Complex mixtures of aliphatic and aromatic compounds also exhibit phase splitting as shown in Figure 4. Venezuela vacuum bottoms + anthracene oil and Athabasca bitumen + anthracene oil mixtures both exhibit phase splitting above 640 K for compositions in the 30 to 70 wt % range. As many of the species present could not be identified unambiguously or were retained by the column, the compositions shown in figure 4 are incomplete. Simple model systems do not mimic the behaviour of complex systems in this case. Pyrene-hexadecane mixtures, for example, only begin to phase split at 698 K for pyrene contents in excess of 75 wt %. Curtis et al. [5] reported coal conversions for a series of experiments which simulate the transition from coprocessing to coal liquefaction with complex solvents. The solvents comprised mixtures of Maya TLR (petroleum based) and V1067 (a bottoms recycle solvent from the

Wilsonville coal research facility). The authors showed that coal conversion decreased slightly, from 65 to 60 wt %, at 698 K as the V1067 content of the solvent increased from 0 to 35 wt %, with a large coincident increase in insoluble organic matter derived from the solvent. Then coal conversion began to increase rapidly to 75 and 90 wt % conversion at solvent compositions of 50 and 100 wt % V1067. The coal derived liquid content at the end of each of these experiments is 25, 50, 64, and 100 wt % respectively. These results are also consistent with phase splitting. The coal derived liquid content in the experiment where Maya TLR was used as a solvent is 25 wt %. Our results show that at 30 wt % mixtures of coal liquids and petroleum feed stocks phase split. So adding coal liquids to the solvent saturates the solvent with coal liquid thus inhibiting coal dissolution. A separate dispersed liquid phase is is then formed which leads to an increase in the production of insoluble organic matter (IOM) as the dispersed liquid becomes hydrogen starved due to poor liquid-liquid mass transfer and polymerization reactions dominate in this phase. If sufficient coal liquid is added to the solvent it becomes the continuous liquid phase and there is a sharp increase in coal solubility at this point because it is more soluble in coal derived solvent than in petroleum derived solvent. Consequently a greater fraction of the coal is solubilized and hydrogenated, coal conversion increases and the IOM produced by the coal based solvent decreases. In this case the continuous phase appears to change over at a coal liquid content of approximately 50 wt %.

Phase splitting is a fundamental characteristic of the coprocessing and coal liquefaction reaction environment and cannot be neglected in the design or interpretation of experiments, or the design of processes. In coprocessing, for example, care must be taken to ensure that the anticipated coal derived liquid concentration in the diluent does not exceed the solubility limit. Extant data [5, 6] and the present work place the solubility limit in the 25 to 30 wt % range but more dilute systems are preferred. Coal liquids exhibit phase splitting between 2 and 4 ringed compounds. Thus, in direct coal liquefaction, two optima appear to exist from the point of view of solvent selection which lead to different reactor design choices:

1. a heavy recycle solvent operated at a pressure sufficient to ensure adequate hydrogen availability,
2. a middle distillate operated at a pressure high enough to avoid the phase split zone.

The first optimum is best exemplified by the so-called German technologies whereas the second optimum has received little attention [22].

CONCLUSIONS

Phase splitting has been shown to arise in both simple and complex mixtures of aromatic, polynuclear aromatic and aliphatic compounds. This phenomenon is shown to account for fluctuations in coal conversions arising in coal oil coprocessing and coal liquefaction previously attributed to synergism. In particular, liquid yields from coal in coprocessing appear to be limited by the solubility of coal liquids in petroleum based solvents. In coal liquefaction the situation is more complex and a minimum of two solvent optima exist.

ACKNOWLEDGEMENTS

The authors wish to thank Shell Canada Ltd., Allied Signal Corp., and Mr. P. Sacco for their assistance. Funding provided by CANMET through DSS contract 23440-9-9405/01-SS and NSERC is gratefully acknowledged.

REFERENCES

1. Derbyshire, F. J., P. Varghese and D. D. Whitehurst, 1982. "Synergistic Effects Between Light and Heavy Solvent Components During Coal Liquefaction", Fuel, 61, 859-864.
2. Chiba, K., H. Tagaya, S. Sato and K. Ito, 1985. "Coal Liquefaction Using Indene-Tetralin and Indene-Decalin Mixtures as Solvent", Fuel, 64 , 68-73.
3. Rincon, J. E., and R. Angulo, 1986. "Petroleum heavy oil mixtures as a source of hydrogen in the liquefaction of Cerrejon coal", FUEL, 65, 899-902.
4. Rincon, J. E., and R. Angulo, 1987. "Synergism in coal liquefaction using petroleum heavy oil mixtures for the liquefaction of Cerrejon coal", Proc. 1987 Int. Conf. Coal Sci. , 375-8.
5. Curtis, C. W., K. Tsai and J. A. Guin, 1987. "Effects of Solvent Composition on Coprocessing Coal with Petroleum Residua", Fuel Processing Tech., 16, 71-87.

6. Fouda, S. A., J. F. Kelly and P. M. Rahimi, 1988. "The Effect of Coal Concentration on Coprocessing Performance", ACS Fuel Chem. Symp. Series, 33, 178-184.
7. Reid, R., J. Prausnitz, and B. Poling, The Properties of Gases and Liquids, 4th ed., Ch. 8, McGraw-Hill, 1987.
8. Subramaniam, B., and M. A. McHugh, 1986. "Reactions in Supercritical Fluids", Ind. Eng. Chem. Proc. Des. Dev. 25, 1-6.
9. Paulaitis, M. E., J. M. L. Penninger and R. D. Gray, 1983. Chemical Engineering at Supercritical Fluid Conditions Ann Arbor Science, Michigan
10. Adams, R. M., A. H. Knebel and D. E. Rhodes, 1979. "Critical Solvent Deashing", Chem. Eng. Prog. 75 (6), 44-48.
11. Pozzobon, R., S. Yushun and J. M. Shaw, 1990. "The Role of Hydrogen in Coal Particle Disintegration at Elevated Temperatures", CJChE (in press).
12. Shaw, J. M., 1987. "A Correlation for Hydrogen Solubility in Alicyclic and Aromatic Solvents", CJChE, 65, 293-298.
13. Shaw, J. M. and E. Peters, 1989. "The Role of Initial Reaction Conditions in Direct Coal Liquefaction",Ind. Eng. Chem. Res., 28, 976-982.
14. Shaw, J. M. and E. Peters, 1989. "A General Model for Coal Dissolution Reactions", Ind. Eng. Chem. Res., 28, 1795-1801.
15. Shaw, J. M., R. P. Gaikwad and D. A. Stowe, 1988. "Phase Splitting of Pyrene-Tetralin Mixtures Under Coal Liquefaction Conditions", FUEL, 67, 1554-1559.
16. Dukhedin-Lalla, L., P. M. Rahimi and J. M. Shaw, 1989. "Phase Splitting of Complex Hydrocarbon Mixtures", Fluid Phase Equilibria, 53, 415-422.
17. Yoshii, T. R. Yaginuma and H. Yoshikaura,1982. "Unusual Effects of Catechol on the Hydroliquefaction of Coal", FUEL, 61, 865-866.
18. Hooper, R. J., H. A. J. Battaerd and D. G. Evans, 1979. "Thermal Dissociation of Tetralin Between 300 and 450 °C" Fuel, 58, 132-138.
19. Benjamin, B. M., E. W. Hagaman, V. F. Raaen and C. J. Collin, 1979. "Pyrolysis of Tetralin", FUEL, 58, 386-390.
20. McNeill, R. I., D. C. Croanuer and D. C. Young, 1983. "Isomerization of Tetra-hydroaromatic Groups Under Coal Liquefaction Conditions", FUEL, 62, 401.
21. Penninger, J. M. L. and H. W. Slatboom, 1976. "Industrial and Laboratory Pyrolysis", Am. Chem. Soc. Symposium Series, 32, 444-449.
22. Shaw, J. M., and E. Peters. "Toward Optimal Reactor Designs for Direct Coal Liquefaction Processes", Proc. 36th Canadian Chemical Engineering Conf., October 1986.

TABLE 1: Physical Properties and Compositions of Oils (wt %)

		Anthracene Oil	Athabasca Bitumen	Venezuela (blend 24)
Specific gravity		(288.5 K) 1.092	(297 K) 1.046	(294 K) 1.026
Water, %		0.2	-	-
Xylene insoluble, %		0.08	-	-
Pentane insoluble, %		-	38.4	21.4
Distillation, % to	498 K	0.0	-	-
	543 K	7.9	-	-
	588 K	43.7	-	-
	628 K	80.5	-	-
	+628 K	19.0	-	-
	+798 K	-	99.3	95.1
Elemental analysis	C		84.3	84.3
	H		10.9	9.6
	N		0.8	0.7
	O		0.3	0.7
	S		3.5	6.0
Aromatic carbon, %			35.4	30.0
Mean molar mass			983	848

TABLE 2: Sample compositions obtained from ports located at the top (1) middle (2) and bottom (3) of the reactor for the system indene (25 wt %) + decalin (25 wt%) + anthracene oil (50wt %) + hydrogen (5 MPa)

COMPOUND (MOLE FRACTION)		648 K			673 K			698 K		
		PORT 1	PORT 2	PORT 3	PORT 1	PORT 2	PORT 3	PORT 1	PORT 2	PORT 3
INDENE or BENZENE derivative	(C_9H_{12})	0.641	0.536	0.533	0.542	0.543	0.269	0.269	0.224	0.205
DECALIN (cis & trans)	($C_{10}H_{18}$)	0.186	0.181	0.171	0.039	0.116	0.031	0.000	0.000	0.000
INDENE or BENZENE derivative	($C_{10}H_{12}$)	0.000	0.014	0.016	0.023	0.013	0.000	0.000	0.000	0.000
SPIRO (4,5) DECANE	($C_{10}H_{18}$)	0.030	0.033	0.035	0.000	0.015	0.000	0.000	0.000	0.000
TETRALIN	($C_{10}H_{12}$)	0.000	0.011	0.012	0.010	0.000	0.000	0.000	0.000	0.000
NAPHTHALENE	($C_{10}H_8$)	0.073	0.091	0.119	0.228	0.171	0.450	0.575	0.584	0.608
NAPHTHALENE derivative	($C_{11}H_{10}$)	0.011	0.013	0.018	0.032	0.021	0.046	0.040	0.050	0.034
NAPHTHALENE derivative	($C_{12}H_{12}$)	0.000	0.000	0.000	0.022	0.000	0.000	0.000	0.000	0.000
ACENAPHTHENE	($C_{12}H_{10}$)	0.017	0.028	0.028	0.016	0.023	0.000	0.000	0.000	0.000
DIBENZOFURAN	($C_{12}H_8O$)	0.009	0.018	0.013	0.019	0.023	0.039	0.000	0.032	0.000
9-H FLUORENE	($C_{13}H_{10}$)	0.011	0.024	0.015	0.030	0.030	0.053	0.036	0.033	0.053
DIBENZOFURAN derivative	($C_{13}H_{10}O$)	0.000	0.002	0.002	0.000	0.000	0.000	0.000	0.000	0.000
ANTHRACENE	($C_{14}H_{10}$)	0.021	0.017	0.031	0.024	0.028	0.061	0.080	0.035	0.058
PYRENE or FLUORANTHENE	($C_{16}H_{10}$)	0.000	0.012	0.008	0.015	0.016	0.051	0.000	0.042	0.018
2 RINGED		0.941	0.899	0.903	0.896	0.879	0.796	0.884	0.858	0.847
3 RINGED		0.058	0.089	0.089	0.089	0.104	0.153	0.116	0.100	0.111
4 RINGED		0.000	0.012	0.008	0.015	0.016	0.051	0.000	0.042	0.041

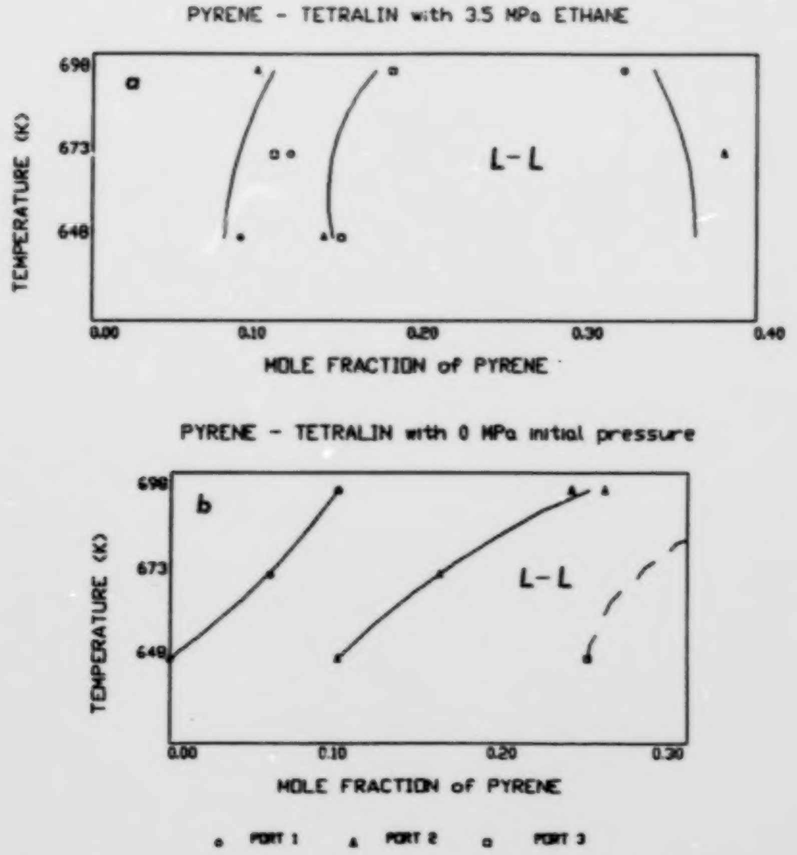
PYRENE - TETRALIN with 3.5 MPa ETHANE

PYRENE - TETRALIN with 0 MPa initial pressure

FIGURE 1: Partial phase diagrams for the systems pyrene + tetralin + ethane (a), and pyrene + tetralin (b)

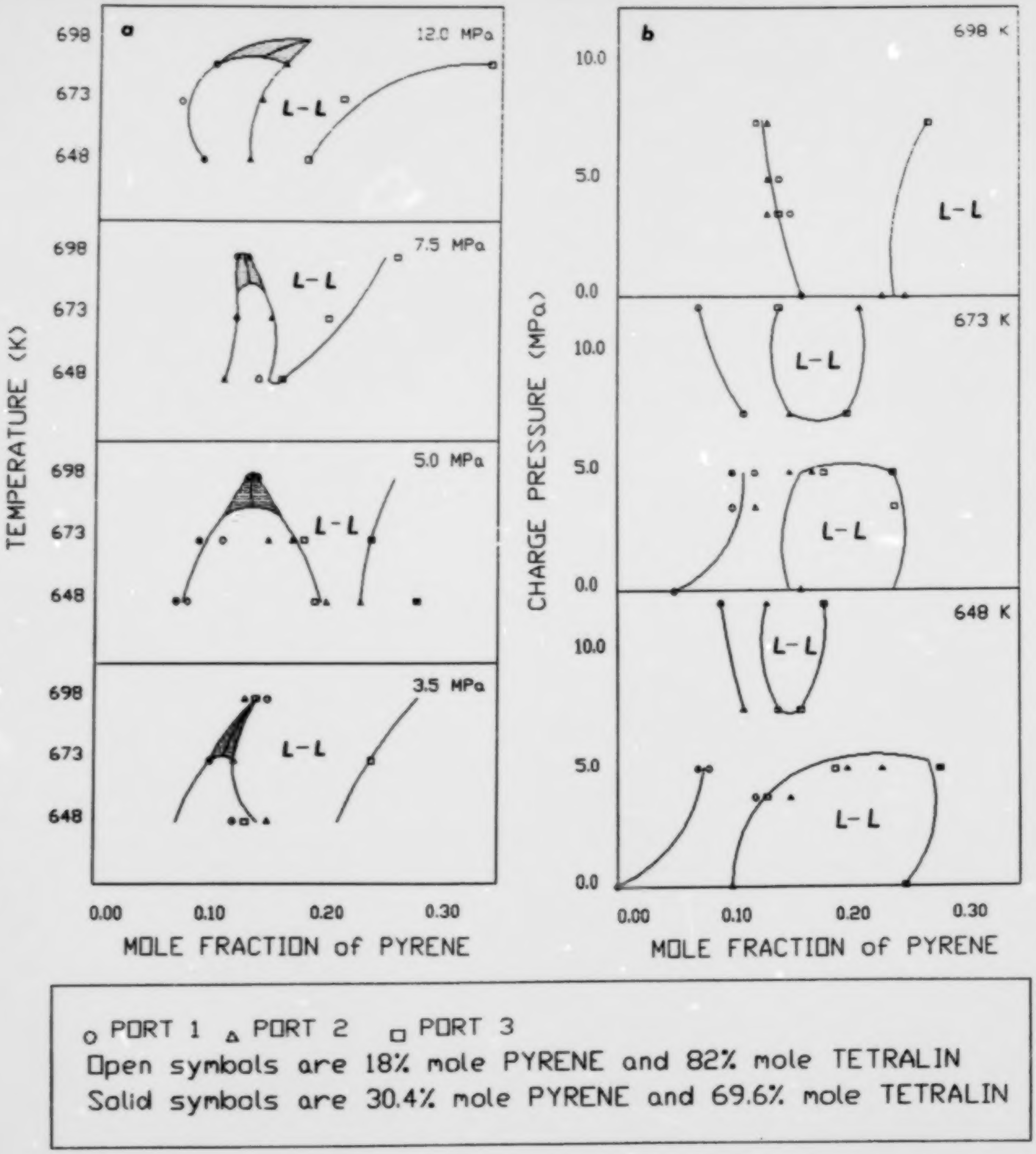

FIGURE 2: Partial phase diagram for the system pyrene + tetralin + nitrogen showing isobars (a) and isotherms (b)

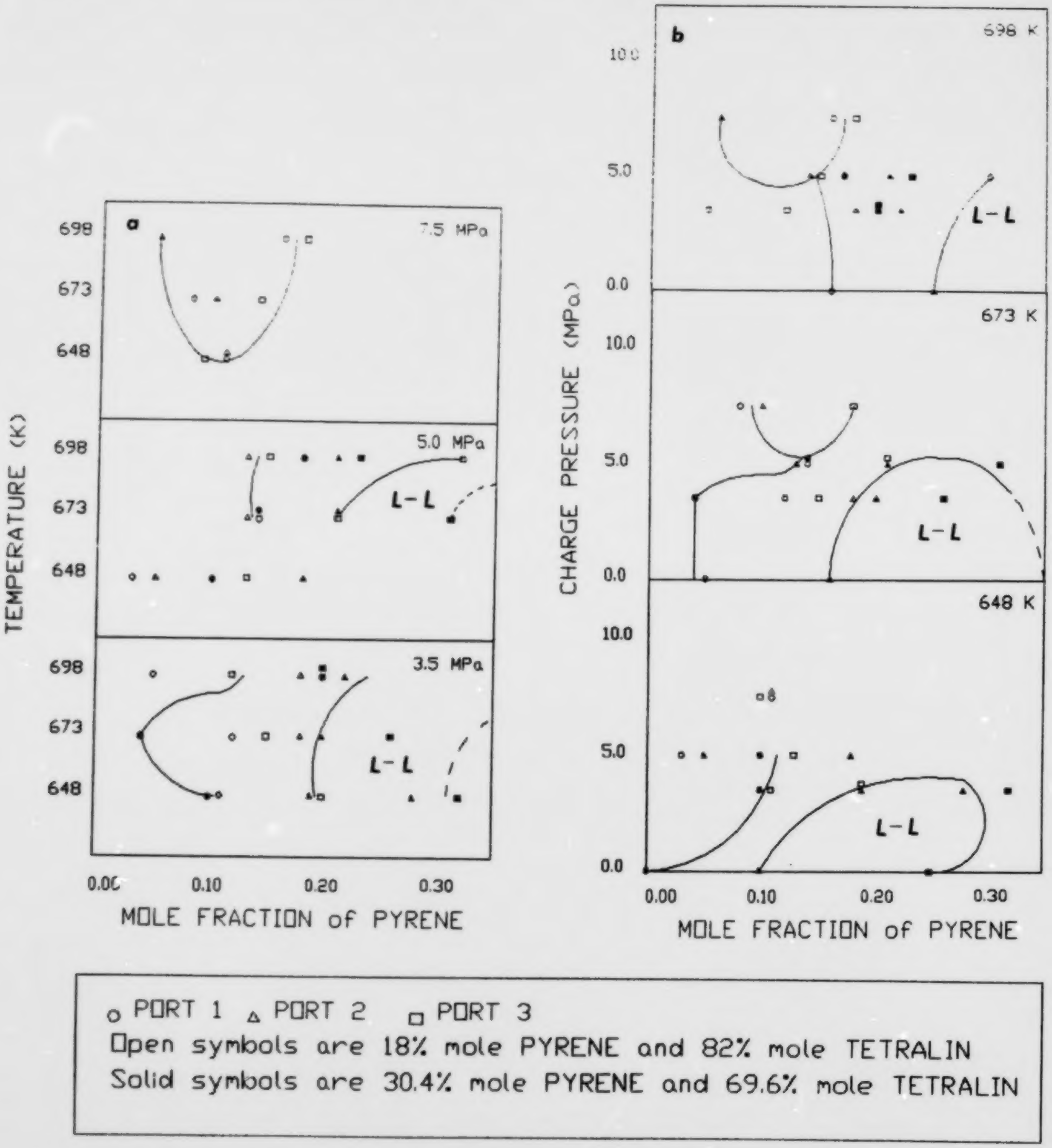

FIGURE 3: Partial phase diagram for the system pyrene + tetralin + methane showing isobars (a) and isotherms (b)

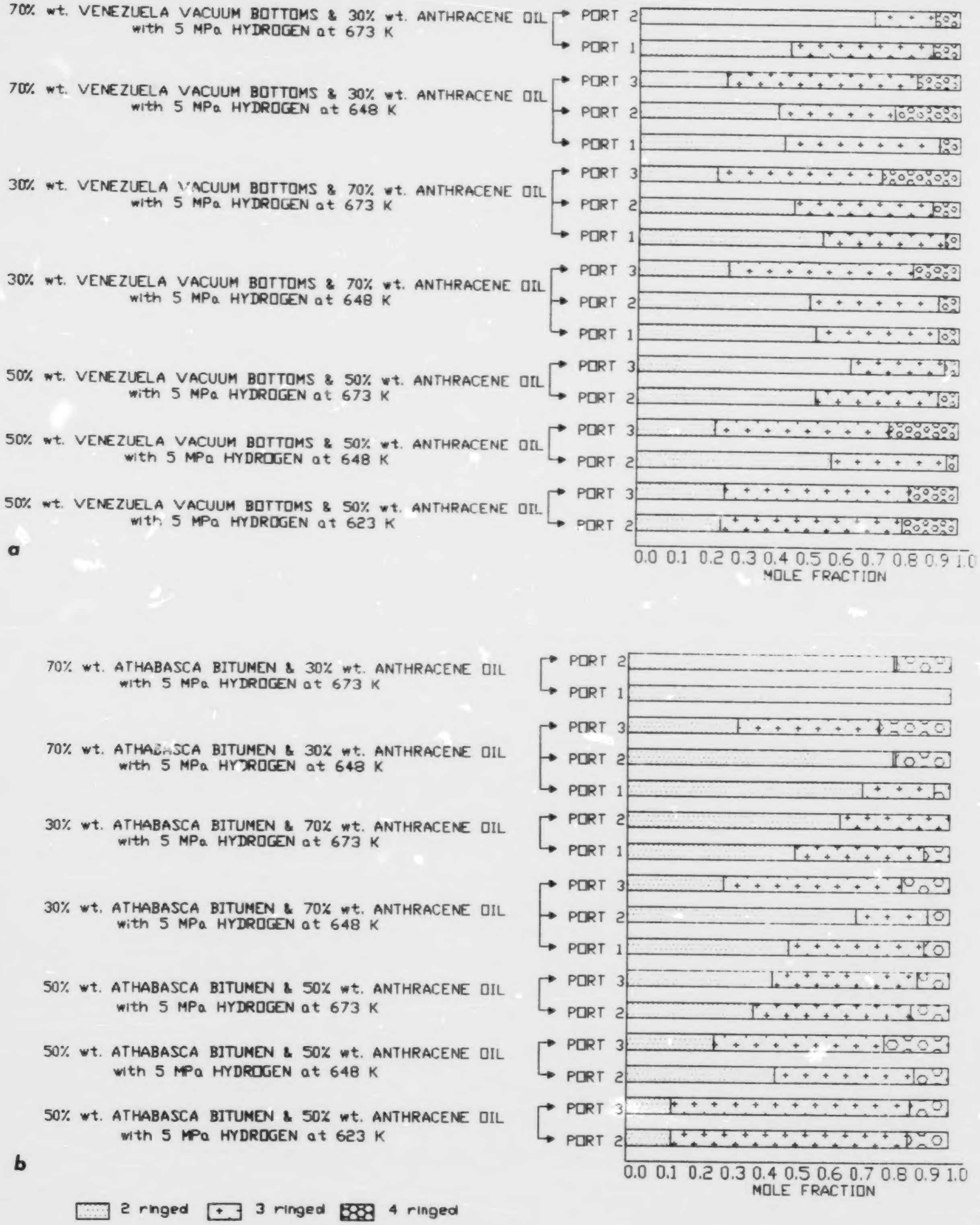

FIGURE 4: Sample compositions obtained from ports located at the top (1) middle (2) and bottom (3) of the reactor for Venezuela vacuum bottoms + anthracene oil + hydrogen mixtures (a), and Athabasca bitumen + anthracene oil + hydrogen mixtures (b)

III Prediction Complex Liquid-Liquid Equilibria

INTRODUCTION

It may appear that thermodynamics is restricted to equilibrium conditions. A little consideration, however, reveals that by defining path, reversible and irreversible processes, the concept of time is implicitly introduced into classical thermodynamics.

Let us examine how the concept of time can be introduced into the second law. The second law of thermodynamics is based on the postulate of existence of a state function, entropy. The entropy change of a system is due to the entropy production within the system, S_p, and entropy flow to the system, S_f. The second law can be stated as

$$dS/dt = dS_p/dt + dS_f/dt \quad (1)$$

together with

$$dS_p/dt \geq 0 \quad (2)$$

It is customary to write the above equation in the following form (Glansdorff and Prigogine, 1971)

$$dS = dS_p + dS_f$$

$$dS_p \quad 0$$

since in thermodynamics time is always taken as increasing in the positive direction (Denbigh, 1981). For a closed system in contact with a heat bath, the above equations reduces to the classical Carnot-Clausius inequality

$$dS \geq Q/T$$

where Q denotes heat absorbed by the system, and T is the temperature of the heat bath. This equation, however, states that the differential of a quality is greater than another quantity which has no differential. To overcome this mathematical shortcoming, it is preferred to retain dt in eqs. (1) and (2). Thence, the Carnot-Clausius equation becomes

$$dS/dt \geq q/T \tag{3}$$

where q is the heating rate. It is worth nothing that the heating rate in eq. (3) is the same quantity appearing in the Fourier law of heat transfer

$$q = -K.\ \mathrm{div}\ T \tag{4}$$

Furthermore, eq. (4) has less practical application without applying the first law of thermodynamics

$$dU/dt = w + q$$

where U and w denote, respectively, internal energy of the system and power. This law enables us to measure heating rate experimentally (Astarita, 1975).

One of the restrictions of classical thermodynamics, is its restriction to equilibrium conditions. However, most real systems are not at equilibrium. On the other hand, all scientific theories are based on some simplifying assumptions. In fact, if it is desired to develop a theory free from assumptions, sooner or later one is faced with fundamental problems without any hope of overcoming them. Moreover, the generality of a theory lies in these assumptions. A theory is applicable to more classes of physical systems if the assumptions are less restrictive. In addition, these assumptions should be self-consistent. The rest of this section is devoted to three different approaches to non-equilibrium thermodynamics.

The simplest approach is to assume that the properties of the system depend only on the instantaneous values of some variables. Based on this assumption, one can measure the non-equilibrium values of the variables and apply the known equilibrium equations. Evidently, this approach is not applicable to all real physical systems and is very restrictive. For example, the composition, temperature, and pressure of a reacting system can be measured experimentally at non-equilibrium conditions at a particular time. The state of the system is then completely determined by applying classical thermodynamics. This approach has been applied to coal model components which will be discussed in the next section. It is worth mentioning that this approach is expected to apply when the system is near equilibrium. While for systems far from equilibrium, it may not describe the system adequately.

It is worth mentioning that there is no general rule for determining how far a system is from equilibrium and the system under consideration should be examined thoroughly before applying this method. For example, the composition of a reacting system may be measured experimentally at different time intervals. If the composition changes dramatically, then it may be concluded that the system is far from equilibrium.

As a second alternative, it can be assumed that the properties depend on the past history of the system, i.e. present state of the system depends on the immediate previous state, and develop the required non-equilibrium theory. Evidently, this approach applies to much more complex systems and many real systems.

According to the Duhems' Theorem the equilibrium state of a closed system formed initially from given masses of species is completely determined by any two independent variables (Smith and Van Ness, 1975). The most appropriate variables for the Helmholtz free energy are temperature and volume:

$$A = a(T,V) \tag{5}$$

Consider a system enclosed by motionless wall, i.e. constant volume, surrounding by a heat bath and charged with n reacting species. Evidently, the Helmholtz free energy is also a function of the extent of reaction

$$A = a(T,V,\underset{\sim}{\xi}) \tag{6}$$

where $\underset{\sim}{\xi}$ denotes extent of reaction vector. If the properties of the system are also a function of instantaneous values of the variables, there is no need to enforce any restrictions upon the system volume and temperature. In other words, equation (6) is also applicable to a reacting system enclosed by an adiabatic and moving wall. If, however, the properties of the system are affected by the past history of the variables, the Helmholtz free energy is also a function of the time derivative of temperature and volume:

$$A = a(T,V,\underset{\sim}{\xi},\dot{T},\dot{V}) \qquad (7)$$

Finally, representation of a non-equilibrium system can be achieved by assuming local equilibrium, i.e. by conceptually dividing the system to small parts (cells) and assuming local equilibrium within each part (Glansdorff and Prigogine, 1971).

MODEL COMPOUNDS FOR COAL LIQUIDS

Model components are important in understanding the properties of coal and coal liquids, developing correlations for property prediction, studying complex reactions, and investigating future processes (Tsonopolos et. al., 1986). Many components are employed for these purposes. Two species of interest in this work, pyrene and tetralin, are among them.

Recently, Dukhedin-Lalla (1990) showed that mixtures of pyrene/ tetralin with methane, ethane, and nitrogen exhibit phase splitting. The experiments were conducted at high temperatures and pressures. The main object of this work is to investigate the simplest way to represent these results.

THERMODYNAMIC MODEL

Two common methods for thermodynamic description of solutions are Equations of State (EOS) and Excess functions. To employ the latter approach, either a mathematical model or Group Contribution method (GCM) should be used. Since coal liquids are complex mixtures containing thousands of molecules with different structure, the problem involved in determining group concentration may restrict the application of GCM. Moreover, the applicability of current GCMs is restricted to low temperatures and pressures, since the parameters have been regressed from equilibrium data at these conditions. Also, this method cannot distinguish some isomers. For these reasons, in spite of some reported success of its application (Behmanesh and Allen, 1989), this approach was not considered as a potential method.

It is well-known that the thermodynamic properties of liquid mixtures depend on temperature, pressure, and composition. At conditions remote from the critical point, however, the effect of pressure is small. For this reason, only composition and temperature appear as independent variables in mathematical models of excess Gibbs free energy functions (Van Ness et. al., 1978). Nevertheless, the effect of pressure is reflected through the pointing correction. In critical and supercritical regions, however, the pointing correction cannot properly represent the effect of pressure.

Two commonly used mathematical models of excess Gibbs energy are presented in Table-1. It is worth mentioning that the characteristic energy parameters in both equations are treated as a function of temperature only (Prausnitz et al., 1986). For example, in the NRTL equation as a linear function (Renon and Prausnitz, 1968) while in the UNIQUAC equation as a weak function of temperature (Anderson and Prausnitz, 1978). For the above reasons, in this work, the EOS approach was selected as a potential method.

Name	g^E	Binary parameters
NRTL'	$\frac{g^E}{RT} = x_1 x_2 \left(\frac{\tau_{21} G_{21}}{x_1 + x_2 G_{21}} + \frac{\tau_{12} G_{12}}{x_2 + x_1 G_{12}} \right)$ where $\tau_{12} = \frac{\Delta g_{12}}{RT} \qquad \tau_{21} = \frac{\Delta g_{21}}{RT}$ $\ln G_{12} = -\alpha_{12}\tau_{12} \qquad \ln G_{21} = -\alpha_{12}\tau_{21}$	Δg_{12}, Δg_{21}, α_{12}
UNIQUAC'	$g^E = g^E \text{ (combinatorial)} + g^E \text{ (residual)}$ $\frac{g^E \text{ (combinatorial)}}{RT} = x_1 \ln \frac{\Phi_1}{x_1} + x_2 \ln \frac{\Phi_2}{x_2} + \frac{z}{2} \left(q_1 x_1 \ln \frac{\theta_1}{\Phi_1} + q_2 x_2 \ln \frac{\theta_2}{\Phi_2} \right)$ $\frac{g^E \text{ (residual)}}{RT} = -q_1 x_1 \ln [\theta_1 + \theta_2 \tau_{21}] - q_2 x_2 \ln [\theta_2 + \theta_1 \tau_{12}]$ $\Phi_1 = \frac{x_1 r_1}{x_1 r_1 + x_2 r_2} \qquad \theta_1 = \frac{x_1 q_1}{x_1 q_1 + x_2 q_2}$ $\ln \tau_{21} = -\frac{\Delta u_{21}}{RT} \qquad \ln \tau_{12} = -\frac{\Delta u_{12}}{RT}$ r and q are pure-component parameters and coordination number $z = 10$	Δu_{12} and Δu_{21}

Table 1- Excess Gibbs Energy of binary mixtures from NRTL and UNIQUAC equations (Reid et. al., 1987).

One of the unusual phenomenon in phase equilibria is the so-called *barotropic effect* or density inversion (Gangoli and Thodos, 1977). It should be emphasized that the EOS is capable of representing this phenomenon which was first observed by Kamerlingh-Onnes in 1907 for the helium-hydrogen system. Fig-1 depicts the calculated solid-liquid and liquid-fluid density inversion for the xenon-naphthalene system (McHugh and Krukonis, 1986).

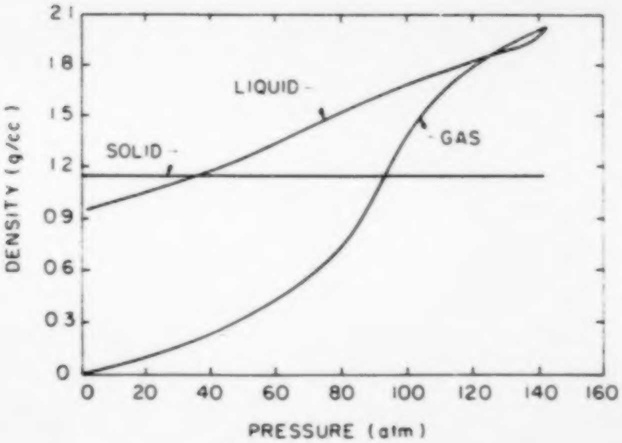

Fig. 1- Calculated density for the xenon-naphthalene system using Peng-Robinson EOS along the solid-liquid-vapour line (McHuge and Krukonis, 1986)

PYRENE/TETRALIN/LIGHT GAS MIXTURES

In order to use EOS, acentric factor, critical temperature and pressure of pure species are required. For mixtures, interaction parameters between each pair of components are also needed. The data presented by Dukhedin-Lalla (1990) contains *undefined* components. There are, however, well-established methods for estimating the properties of petroleum cuts. In spite of different structure and chemical properties of coal liquids and oil (the former being more aromatic, i.e. lower H/C ratio, with significant amount of heteroatoms while the later is more aliphatic), similar methods can be used for coal liquids (Tsonopoulos et. al.,1986).

Therefore, the critical pressure and temperature of undefined components may be obtained from normal boiling point and specific gravity by the equation of Riazi and Dubert which is recommended in the API technical book (Tsonopoulos et. al., 1986) or other correlations (e.g. see Kesler and Lee, 1976). ASTM D2887-84 should be used to obtain the normal boiling point of undefined components (Green, 1976, Pannel and Sood, 1982), while

$$\begin{aligned} S = {} & 0.553461 + 1.15156(t_b/1000) \\ & -0.708142(t_b/1000)^2 \\ & +0196237(t_b/1000)^3 \end{aligned}$$

may be used to calculate the specific gravity (Tsonopoulos et. al., 1986). In the above equation, S and t_b denote specific gravity and normal boiling point (F), respectively.

The acentric factor can be calculated by adjusting it until the calculated normal boiling point for the undefined components matches the experimental one, or by using Lee-Kesler (1976) correlation.

Currently, we are examining the published methods for evaluating binary interaction parameter between different components (Graboski and Daubert, 1978a, 1978b, 1979, Moysen et. al., 1983, Nishimumi et. al., 1988, 1990).

PHASE EQUILIBRIUM ALGORITHMS

In order to use most existing phase equilibrium algorithms, the number of phases of the system should be known in advance. There are three restrictions which all systems at equilibrium should satisfy, namely; mass balance, equality of chemical potentials of each component in different phases, and the lowest possible Gibbs free energy at a given temperature and pressure. Most existing routines may fail to predict the equilibrium composition of a given feed at a specified temperature and pressure, if the number of phases is over or under estimated, even though the state of the system is completely specified according to Duhem's Theorem.

This last point was the motivation to review the stability criterion.

The theoretical aspect of thermodynamic stability was treated over a century ago by Gibbs in his pioneering paper "On the Equilibrium of Homogeneous Substances." Recently, Baker et. al. (1982) considered the properties of Gibbs energy surface and showed that the tangent hyperplane of the Gibbs surface of a stable system does not intersect the free energy hypersurface at any point except those points which is tangent to free energy hyperplane. The number of equilibrium phases is equal to the number of tangent points. Nevertheless, no mathematical formulation was presented in their paper. Michelsen (1982a, 1982b) present an algorithm for flash calculations using the tangent plane criterion. Nghiem (1984, 1985) applied this criterion to multiphase equilibrium and saturation pressure and temperature computation. The numerical procedure is discussed by Nghiem et. al. (1983).

As a preliminary test, various feed compositions of the compounds reported by Dukhedin-Lalla (1990) with a very rough estimate of binary interaction parameters were examined by plotting P-T diagrams and calculating the critical point(s). Most tested systems exhibit two critical points. Also the stability limit of one system was calculated (fig. 2) by the procedure outlined by Heidemann and Khalil (1980). The arrowhead in this figure shows the direction of increasing volume. Moving in this direction, the region to the right of the stability limit curve is unstable. It should be emphasized that no binary interaction parameters (Kij) was used for the mixture depicted in fig 2.

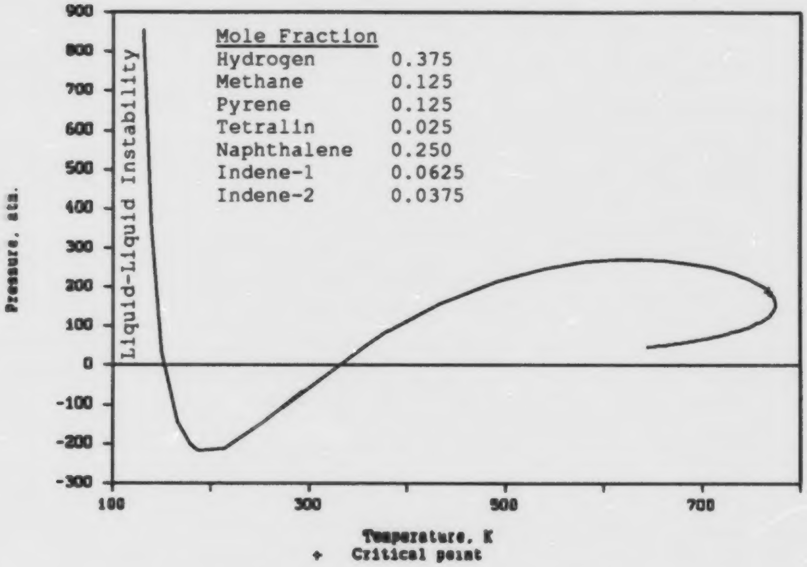

Figure 2- Calculated stability limit[1]
(Kij = 0.0)

---

[1] The second critical point is not shown since it is out of the range of the figure.

Our experience, however, reveals that the results are sensitive to the binary interaction parameters, as was anticipated. Therefore, fig. 2 should be treated only as a qualitative outcome. This figure shows the potential of the predictive nature of the method since no experimental data was used in constructing the stability limit curve. Moreover, we expect to obtain quantitative results, after close examination of reported binary interaction-parameter estimation-methods.

REFERENCES

Anderson T.F., and J.M. Prauznitz, 1978, *Ind. Eng. Chem. Process Des. Dev.*, 17, 4, 552.

Astarita G., 1975, "An Introduction to Non-linear Continuum Thermodynamics," Società Editrice di Chimica, Milano.

ASTM Standards, 1987, Section 5, Volume 05.02, 657.

Baker L.E., A.C. Pierce, and K.D. Luks, Oct. 1982, *Soc. Pet. Eng. J.*, 731-42.

Behmanesh N., and D. Allen, 1989, Fifth International Conferenc on Fluid Properties & Phase Equilibria for Chemical Process Design, Alberta, Canada, April 30-May 5, 94.

Denbigh K.G., 1981, "The Principles of Chemical Equilibrium," Cambridge University Press, N.Y., 4th ed.

Dukhedin-Lalla L., M.A.Sc. Dissertation, University of Toronto, 1990.

Gangoli N., G. Thodos, 1977, *Ind. Eng. Chem. Prod. Res. Dev.*, 16, 3, 208.

Gibbs J.W., 1876, *Transactions of the Connecticut Academy*, 3, 108, as reprinted in "The Scientific Papers of J. Willard Gibbs," Vol. 1, Dover, New York, 1961.

Glansdorff P., and I. Prigogine, 1971, "Thermodynamic Theory of Structure, Stability and Fluctuations," John Wiley & Sons Ltd.

Graboski M. S., and T. E. Daubert, 1979, *Ibid.*, 18, 2, 300.

Graboski M. S., and T. E. Daubert, 1978b, *Ibid.*, 448.

Graboski M. S., and T. E. Daubert, 1978a, *Ind. Eng. Chem. Process Des. Dev.*, 17, 4, 443.

Green L.E., 1976, *Hydrocarbon Processing*, 55, 5, 205-207.

Heideman R.A., and A.M. Khalil, 1980, *AICHE J*, 26, 5, 769-779.

Kesler M.G., and B.I. Lee, 1976, *Hydrocarbon Processing*, 55, 3, 153-158.

McHugh M., and V. Krukonis, 1986, "Supercritical Fluid Extraction," Butterworth Publishers.

Michelson M.L., 1982b, *Fluid Phase Equilibria*, 9, 21-40.

Michelson M.L., 1982a, *Fluid Phase Equilibria*, 9, 1-19.

Moysan J.M., M.J. Huron, H. Paradowski, and J. Vidal, 1983, *Chem. Eng. Sci.*, 38, 7, 1085-1092.

Ngheim L.X., K. Aziz, and Y.K. Li, 1983, *Soc. Pet. Eng. J.*, 23, 521-30.

Nghiem L.X., Y.K. Li, and R.A. Heidman, 1985, *Fluid Phase Equilibria*, 21, 39-60.

Nishimui H., T. Arai, and K. Takeuchi, 1988, *Fluid Phase Equilibria*, 42, 43-62.

Nishiumi H. and H. Gotoh, 1990, *Fluid Phase Equilibria*, 56, 81-88.

Pannell R.B., and A. Sood, 1982, *J. Chromat. Sci.*, 20, 433-435.

Prauznitz J.M., R. N. Lichtenthaler, and E.G. Azevedo, 1986, "Molecular Thermodynamics of Fluid Phase Equilibria," Printice-Hall Inc. 2nd ed.

Reid C.R., J.M. Prausnitz, and B. E. Poling, 1987, The Properties of Gases and Liquids," McGraw-Hill, 4th ed.

Renon H., and J.M. Prausnitz, 1968, *AICHE J*, 14, 1, 135.

Smith J.M., and H.C. Van Ness, 1975, "Introduction to Chemical Engineering Thermodynamics," McGraw-Hill, Inc, 3rd ed.

Tsonopoulos C., J.L. Heidman, and S.C. Hwang, 1986, "Thermodynamic and Transport Properties of Coal Liquids," John Wiley & Sons, Inc.

Van Ness H.C., F. Pedersen, and P. Rasmussen, 1978, *AICHE J*,24, 6, 1055.

IV Project Summary

Conclusions

1. Both simple and complex mixtures of aromatic and polynuclear aromatic compounds and their derivatives are subject to phase splitting. Mixtures shown to exhibit phase splitting include: pyrene-tetralin, bitumen-anthracene and heavy oil-anthracene.

2. Mixtures containing significant mole fractions of 2 and 4 ringed compounds are most susceptible to phase splitting.

3. Light gas constituents affect the phase splitting zone in two ways:
   - the more soluble the gas under the experimental conditions the larger the phase splitting zone. Thus, the phase splitting zone for liquids in the presence of ethane > methane > nitrogen > hydrogen at a fixed temperature and low to moderate pressures.
   - gases with low solubility tend to drive the mixtures to supercritical conditions at elevated pressures where fluid or fluid-fluid behaviour predominates. Supercritical fluids can be excellent media for reaction purposes.

4. Although it has not proven possible to duplicate experimental conditions for experiments reported in the literature, all extant yield data for coprocessing and coal liquefaction which have been attributed to synergism are consistent with phase splitting.

5. A computational approach for predicting liquid-liquid equilibrium has been identified. However, the computations are complex and the temperature/pressure/composition space identified for phase splitting is extremely sensitive to the values of interaction parameters. Interaction parameters can exhibit a strong temperature dependence and various parameter values have been reported for the same molecular interactions. Only qualitative predictions can be made at the present time.

6. On a more practical level, it is worth noting that as AMOCO has changed its operating conditions to temperatures in excess of 740 K, there are no longer proposed coprocessing reactors operating in the temperature range most susceptible to liquid-liquid phase splitting. Consequently, the phase splitting phenomenon reported here may be limited to preheaters or product separation vessels.

Recommendations for Future Work

1. Interaction parameters for model compounds and petroleum/coal liquid cuts suitable for coprocessing and coal liquefaction reaction environments should be evaluated.

2. Phase diagrams for model and complex liquids should be predicted quantitatively as a design aid.

3. Phase equilibria associated with preheaters for coprocessing and coal liquefaction processes should be investigated. Phase splitting may or may not arise in preheaters, depending on the extent of reaction realized, and the time available.

V Appendix

Phase Splitting and Synergy
in
Complex Hydrocarbon Systems

by

Leisl Dukhedin - Lalla

A Thesis submitted in conformity with the requirements
for the Degree of Masters of Applied Science in the
University of Toronto

Department of Applied Chemistry and Chemical Engineering
University of Toronto

c Copyright by Leisl Dukhedin - Lalla 1990

ABSTRACT

The phase behaviour of complex hydrocarbon systems associated with heavy oil upgrading, coal/oil coprocessing and direct coal liquefaction systems were investigated. Partial phase diagrams for the pyrene - tetralin system with nitrogen, methane and ethane in the range of 623 K - 698 K and 0 - 12 MPa have been generated. Similar experiments with bitumen/heavy oil/anthracene oil mixtures were also performed. Operating conditions for the processes mentioned above are usually within the critical and subcritical region of one or more of the constituents in these systems. The onset of phase splitting is a common phenomenon in these regions. Phase splitting is reported with the pyrene - tetralin and bitumen, heavy oil - anthracene mixtures at temperatures in excess of 648 K. Previously reported fluctuations in conversions with these model systems have been attributed to synergistic phenomena. In this thesis, some aspects of the synergism are connected to phase splitting in terms of shifts in hydrogen solubility and coal dissolution properties as liquid - liquid immiscibility arises. Preliminary predictions for optimum solvent design and operating conditions are proposed.

Acknowledgements

The success of this project has been as a result of the efforts of many people. I would especially like to thank Professor John Michael Shaw for his supervision, encouragement and unrelenting patience (for all the experiments that "coked") throughout this undertaking.

I would also like to thank Mr. Sun Yushum and Mr. Tom Shepherd for their assistance during many experiments. To all my family and friends who have given support and motivation during the many seemingly hopeless days.

Table of Contents

Abstract ii

Acknowledgments iii

Table of Contents iv

List of Figures vi

List of Tables ix

1. Introduction 1

2. Literature Survey

2.1 Synergism 4

2.2 Phase Splitting 13

2.3 Liquid - liquid equilibrium 16

3. Experimental

3.1 Materials 24

3.2 Equipment 26

3.3 Control and Safety 28

3.4 Operation 33

3.5 Analysis 34

3.6 Experimental Considerations 35

4. Results

4.1 Experimental Considerations 40

4.2 Material Instability 43

4.3 Phase Splitting

4.3.1 Model Compounds 48

4.3.2 Heavy Oils 50

5. Discussion

5.1 Gas Phase Composition 75

5.2 Phase Splitting Systems 77

5.3 Synergy and Phase Splitting 77

5.4 Solvent Design 80

6. Conclusions and Recommendations 82

7. References 84

8. Bibliography 87

Appendices

Appendix A : Sample composition of model solvents 88

Appendix B : Sample composition of heavy oils 100

Appendix C : Calibration curves 114

Appedix D : Sample calculation for port placement 119

List of Figures

Figure 2.1 : Effect of temperature and pressure on Monterey coal conversion for pyrene - tetralin solvents (60 min. reaction time) 6

Figure 2.2 : Coal conversion of Yallourn with various solvents and operating conditions 8

Figure 2.3 : Coal conversion with different solvents as a function of temperature and residence time 11

Figure 2.4 : Coal conversion with different solvents as a function of a)temperature and b)pressure 12

Figure 2.5 : Coal conversion and oil production in blends of coal liquids and petroleum solvents 14

Figure 2.6 : Partial phase diagram for the pyrene - tetralin solvent system showing the two phase liquid region at 700 K 17

Figure 2.7 : The impact of solvent composition on coal conversion (solid line - elevated pressure, broken line - low hydrogen pressure) for binary solvents type A,B,C and D) 18

Figure 2.8 : Phase transition during phase splitting 18

Figure 2.9 : Equilibrium curve for liquid - liquid 22
equilibrium in binary systems at constant pressure

Figure 2.10 : Six types of classes of binary pressure -

temperature diagrams 23

Figure 3.1 : Apparatus 27

Figure 3.2 : Density profile for tetralin with no gas 29

Figure 3.3 : Density profile for Athabasca bitumen a) with no gas and b) with hydrogen 30

Figure 3.4 : Density profile for Venezuela Vacuum Bottoms (blend 24) with a) no gas and b) with hydrogen 31

Figure 3.5 : Temperature program used in GC - MS for model solvent systems 37

Figure 3.6 : Temperature program used in GC - MS for heavy oil solvent systems 38

Figure 4.1 : Three main processes occurring in tetralin degradation 47

Figure 4.2 : Tetralin degradation with nitrogen 52

Figure 4.3 : Tetralin degradation with methane 53

Figure 4.4 : Tetralin degradation with a) no gas b) ethane 54

Figure 4.5 : Partial phase diagram (isobars) for pyrene - tetralin with nitrogen 55

Figure 4.6 : Partial phase diagram (isotherms) for pyrene - tetralin with nitrogen 56

Figure 4.7 : Partial phase diagram (isobars) for pyrene - tetralin with methane 57

Figure 4.8 : Partial phase diagram (isotherms) for pyrene -

tetralin with methane 58

Figure 4.9 : Partial phase diagram (isobars) for pyrene - tetralin with a) ethane and b) no gas 59

Figure 4.10: Composition (in terms of 2,3 and 4 or more fused ringed material) retrieved from ports 1,2 and 3 of the reactor for Venezuela Vacuum Bottoms(blend 24) and Anthracene oil with hydrogen 60

Figure 4.11: Composition (in terms of 2,3 and 4 or more fused ringed material) retrieved from ports 1,2 and 3 of the reactor for Athabasca Bitumen and Anthracene oil with hydrogen 61

List of Tables

Table 3.1 : Physical properties of gases 24

Table 3.2 : Physical properties of model solvent compounds 24

Table 3.3 : Physical properites of oils 25

Table 4.1 : Systems that did not exhibit phase splitting. All systems were charged with 5 MPa hydrogen (cold) 62

Table 4.2 : 18 mole % Pyrene - 82 mole % Tetralin with 7.5 MPa Nitrogen (cold) at 623 K 63

Table 4.3 : Pyrene - Tetralin with Nitrogen 64

Table 4.4 : Pyrene - Tetralin with Methane 65

Table 4.5 : Pyrene - Tetralin with Ethane 66

Table 4.6 : Pyrene - Tetralin with no gas 67

Table 4.7 : 50 wt. % Venezuela Vacuum Bottoms (blend 24) and 50 wt. % Anthracene oil with 5 MPa Hydrogen 68

Table 4.8 : 30 wt. % Venezuela Vacuum Bottoms (blend 24) and 70 wt. % Anthracene oil with 5 MPa Hydrogen 69

Table 4.9 : 70 wt. % Venezuela Vacuum Bottoms (blend 24) and 30 wt. % Anthracene oil with 5 MPa Hydrogen 69

Table 4.10 : 50 % Athabasca Bitumen and 50 wt. % Anthracene oil with 5 MPa Hydrogen 70

TAble 4.11 : 30 % Athabasca Bitumen and 70 wt. % Anthracene oil with 5 MPa Hydrogen 71

Table 4.12 : 70 % Athabasca Bitumen and 30 wt. %

Anthracene oil with 5 MPa Hydrogen 71

Table 4.13 : 25 wt. % Indene - 25 wt. % Decalin - 50 wt. % Anthracene oil with 5 MPa Hydrogen 72

1. INTRODUCTION :

The optimization of light oil yields from heavy oil upgrading, coal/oil co-processing and direct coal liquefaction has been widely researched. Recently, a great deal of attention has been paid to significant fluctuations in light oil yields from laboratory studies. Minor variations in operating conditions, such as temperature, pressure and composition, have led to appreciable changes in coal/pitch conversions. This seemingly unpredictable behaviour has been attributed to synergistic phenomena. It is the objective of this project to elucidate some aspects of the reported synergism by investigating the phase behaviour of similar complex hydrocarbon systems under operating conditions achieved during processing. Phase behaviour such as phase splitting leading to liquid/liquid and supercritical fluid/fluid equilibria are addressed. In most of the processes mentioned operating conditions are usually within the critical region of one or more of the components in the system. Typically very complex phase behaviour is associated with subcritical and supercritical fluids and this fact has not been previously considered in kinetic studies for these processes. This unpredictable phase behaviour must be considered for a variety of reasons before reactor design, solvent design and operating conditions can be optimized.

A literature survey of some of the systems previously connected with synergistic behaviour is provided. This list is not exhaustive. The systems cited are diverse and represent examples of synergy in direct coal liquefaction, heavy oil upgrading and coal/oil coprocessing.

Initially model solvent systems, such as pyrene-tetralin, indene-decalin and naphthalene-decalin, used in direct coal liquefaction were investigated since these systems had been the first associated with synergistic behaviour. Although these models solvent systems are indeed 'simple' systems they provide an initial approach to understanding the behaviour of real systems during processing. The pyrene-tetralin system is especially useful model system since it is not only a well known solvent system but it also is a good coal liquefaction model. One of the major characteristics of coal liquids are their high aromaticity, and pyrene is representive of a four ring aromatic coal liquid and tetralin of a two ring aromatic/hydroaromatic coal liquid. Both of these compounds are also present in substantial amounts in many process streams. It was the objective of this project to investigate the pyrene-tetralin system with a variety of gases in order to determine the effect of the gas phase on the phase behaviour. The pyrene - teralin mixture was investigated with methane, nitrogen and ethane since these are typical components found in process streams. The next step in the investigation involved performing similar experiments but with 'real' solvent systems. Two heavy oil - anthracene oil mixtures were chosen since these systems had been previously associated with synergism. One objective of this research was to generate partial phase diagrams for these systems thereby allowing some predictions for optimum solvent and operating systems.

Heavy oil upgrading, coal/oil co-processing and coal liquefaction have been established as three distinct fuel processing technologies. In some very important aspects they are indeed very different. However in terms of processing conditions and materials they are quite similar. It is hoped that results of this work will be applicable to all technologies (Dukhedin - Lalla et al., 1989a,b and 1990).

2. LITERATURE SURVEY

2.1 Synergism

The following literature survey consists of a series of investigations which make reference to synergistic phenomena and hence provide the background and starting point for this project.

Derbyshire et al., (1982) conducted coal conversion experiments with binary model compound solvents; pyrene - tetralin and tetralin - 2-methylnaphthalene. The dissolution of a bituminous Monterey and subbituminous Bell Ayr coals using these solvent systems was investigated. Figures 2.1:a,b,c,d are a summary of the results which exhibited non-additive behaviour. With a 70% wt. pyrene - 30% wt. tetralin system at 700 K and 6.7 MPa hydrogen pressure a maximum coal conversion (THF soluble materials) of 92% wt. was obtained. But with pure tetralin and pure pyrene, at the same temperature and pressure, coal conversions were 83% wt. and 78% wt. respectively. At a higher hydrogen pressure of 12.1 MPa and 700 K conversions were 78%, 92% and 89% wt. for pure pyrene, 70% wt. pyrene - 30% wt. tetralin and pure tetralin respectively. It was concluded that coal conversions were unaffected by increasing hydrogen pressure in the range of 6.7 - 12.1 MPa. This non-additive behaviour was attributed to interactions of pyrene,tetralin and hydrogen gas. At 673 K synergism was not observed and coal conversion showed a linear relationship from 86% to 90% at 12.1 MPa from 0% wt. to 100% wt. tetralin solvent. At 6.7 MPa and 673 K conversions increased from 73% to 92% from 0% wt.to 100% wt. tetralin content whereby it intersected the higher temperature curve at approximately 50 % wt. tetralin. From this work it can be concluded that the synergistic effect occurs at 700 K for a 70% wt. pyrene - 30% wt. tetralin solvent system and was unaffected by changes in initial hydrogen pressure. Non-additive behaviour was not apparent in the 2-methylnaphthalene and tetralin mixtures. Derbyshire et al., (1982) suggested that the synergistic effects can be accounted for by the interactions of the pyrene - tetralin - hydrogen system and their possible effect on pyrene hydrogenation which would led to better overall rates of hydrogen transfer to the coal and consequently higher coal conversion.

Chiba et al., (1985) performed similar experiments with indene-decalin and indene-tetralin mixtures as coal liquefaction solvents. Experiments were conducted under a hydrogen pressure of 5 MPa at 673 K and 713 K with a Yallourn coal for a nominal reaction time of 60 minute with 24 g of material in a 0.1 L autoclave and a solvent to coal ratio of 3:1. Figures 2.2a and 2.2b are a graphical representation of these results. A similar synergistic effect was observed. For the indene-tetralin systems an optimum conversion of 90% wt. THF soluble materials at 673 K was achieved at a composition of 88% wt. tetralin and 12% wt. indene. With pure indene and pure tetralin coal conversions were approximately 50% wt. and 80% wt. respectively. At a 50% wt.-50% wt. indene-decalin system at 673 K an optimum conversion of approximately 65% wt. and at 713 K the same mixture showed a maximum conversion of 73% wt. Pure decalin conversions were approximately 40% wt. at 673 K and 50% wt. at 713 K and pure indene conversions at both temperatures were approximately 50% wt. Chiba et al., (1985) suggested two possible mechanisms for explaining the synergistic effect. The first being the bimolecular reaction of indene with tetralin and decalin

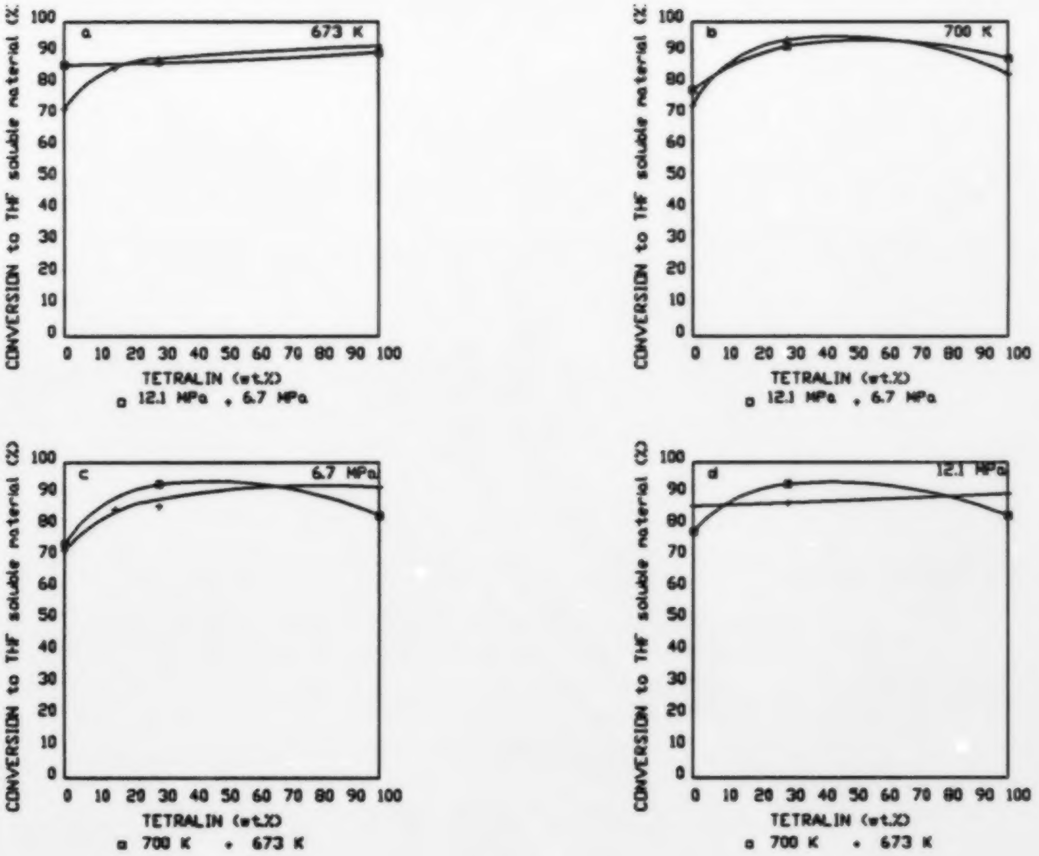

Figure 2.1 : Effect of temperature and pressure on Monterey coal conversion for pyrene - tetralin solvents (60 min. reaction time). (From Derbyshire et al., 1982).

leading to active intermediates which promote coal liquefaction as active hydrogen donors, acceptors and scavengers for coal radicals present in the reactions. The second mechanism proposes that coal radicals are scavenged by indene and stabilized as lower molecular weight compounds.

Rincon et al., (1986) conducted experiments with petroleum heavy oil and anthracene oil and reported synergistic phenomena. Anthracene oil has been shown to be a fairly good solvent for thermal dissolution of coal while petroleum heavy oil is richer in hydrogen and acts as a good hydrogen donor. A positive synergistic effect was attained during coal liquefaction experiments with Cerrejon coal without hydrogen in a 3:1 ratio of solvent to coal with approximately 40 g of material in a 0.3 L autoclave. The effect of temperature and reaction time were investigated. Figures. 2.3a,b and c are a summary of the results obtained. Petroleum heavy oil (PHO) showed the lower conversion while anthracene oil (AO) was better with a maximum conversion to THF soluble material of approximately 35% at 713 K. At the higher temperatures conversions were the lowest due to'coking' or carbonization reactions. The 50% wt. - 50% wt. of AO to PHO yielded the highest conversions. At 673 K and residence times of 10 min., 30 min. and 60 min. the conversions were 60%, 70% and 85% respectively. This work clearly showed that synergistic phenomena is not restricted to model solvents but is also associated with complex solvents.

Rincon et al., (1986) proposed that while petroleum heavy oil has a high availability of donatable hydrogen its low solubility of coal fragments leads to poorer coal conversion. Alternatively anthracene oil has a high solubility for coal

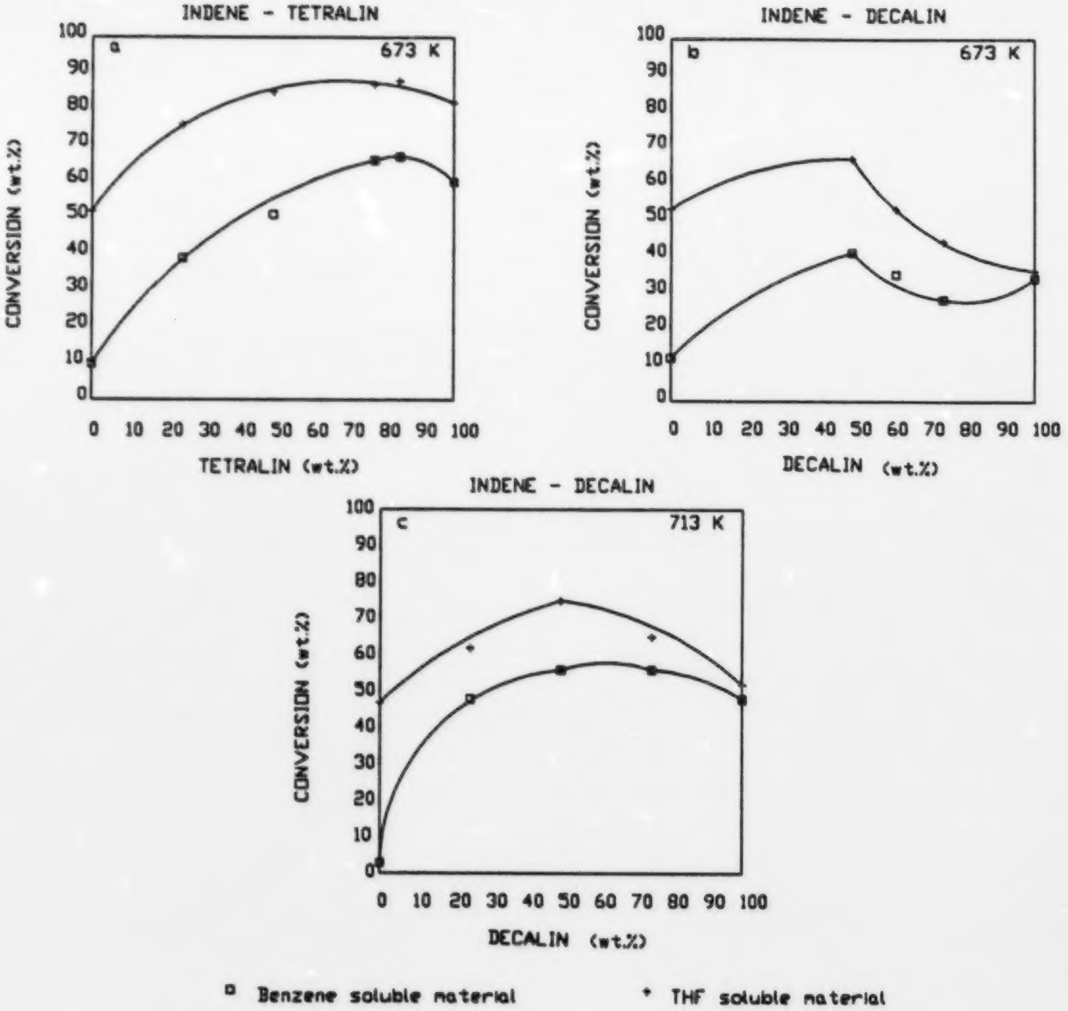

Figure 2.2 : Coal conversion of Yallourn with various solvents and operating conditions. (From Chiba et al., 1985)

fragments but its low hydrogen donor capacity gives rise to low yields. It was suggested that the attributes of both solvents operating simultaneously give rise to the observed synergism.

Rincon et al., (1987) continued this work and performed similar experiments the results of which are shown in Figure 2.4. This work shows slightly different results from the previous work. The difference was accounted for by the change in experimental conditions. The initial experiments were performed in a tubing bomb while the results reported in this work were conducted in an autoclave. The major difference arises from a change in the heat transfer mechanism. The results from an investigation of coal conversion as a function of temperature at an autogenous pressure are reported in Figure 2.4b. The 50% wt. - 50% wt. of petroleum heavy oil and anthracene oil showed the highest coal conversion (THF solubles) of approximately 57% at 633 K. However at the higher temperatures the anthracene oil solvent gave better conversions than the petroleum heavy oil and the 50% wt. - 50% wt. mixture. At the higher temperatures problems with 'coking' led to negative conversions. The next step in the study investigated coal conversions as a function of different hydrogen pressures. The synergistic effect was maintained at pressures lower than 6.9 MPa. At the higher pressures the conversions were only slightly higher with the anthracene oil as a solvent.

Curtis et al., (1987) performed a variety of coal/oil coprocessing experiments to study the effect of solvent composition on coal conversion and oil production. A coal derived solvent V1067 (highly aromatic) with Maya TLR (top long resid, highly aliphatic) solvent was coprocessed with Illinois No. 6 coal at five different weight percentages of V1067 in Maya TLR at 698 K and at a hydrogen pressure of 8.5 MPa with a coal to solvent ratio of 1:2. Experiments were conducted with 10 g of material in a 50 ml microreactor. The results of these experiments are reproduced in Figure 2.5. Coal conversions decreased from 60% to 45% in the range of 0% to 35% additions of V1067 in Maya TLR. Conversions then increased from 60% to 85% approximately within the 35% to 100% range of V1067 in Maya TLR. Oil production showed a more erratic behaviour with the basic trend being a decrease from 12.5% to -10% production in the range of 0% to 100% V1067 in Maya but at the 50% wt. of V1067 in Maya TLR the oil production showed an increase to 10% and then continued in the downward trend. Curtis et al., suggested that such complex and unpredictable behaviour is a result of intermolecular interactions between the coal and solvent system.

Fouda et al., (1988) performed experiments in coal/ oil co-processing and also observed a synergistic effect. The effect of coal concentration on co-processing showed a synergistic increase in distillate yield at coal concentrations of approximately 3%. This effect was considered a catalytic contribution due to better dispersion of catalyst in the presence of coal. At coal concentrations of approximately 30% wt. a decrease in distillate yield from pitch was observed. Distillate yields decreased from approximately 65% wt. to 50% wt. as coal concentrations increased from 30% wt. to 40% wt.. From this work it was concluded that at low coal concentrations the effect of coal derived liquids is not appreciable therefore conversion decreases as the amount of coal present increases. While at higher coal concentrations the conversion increases as coal concentrations

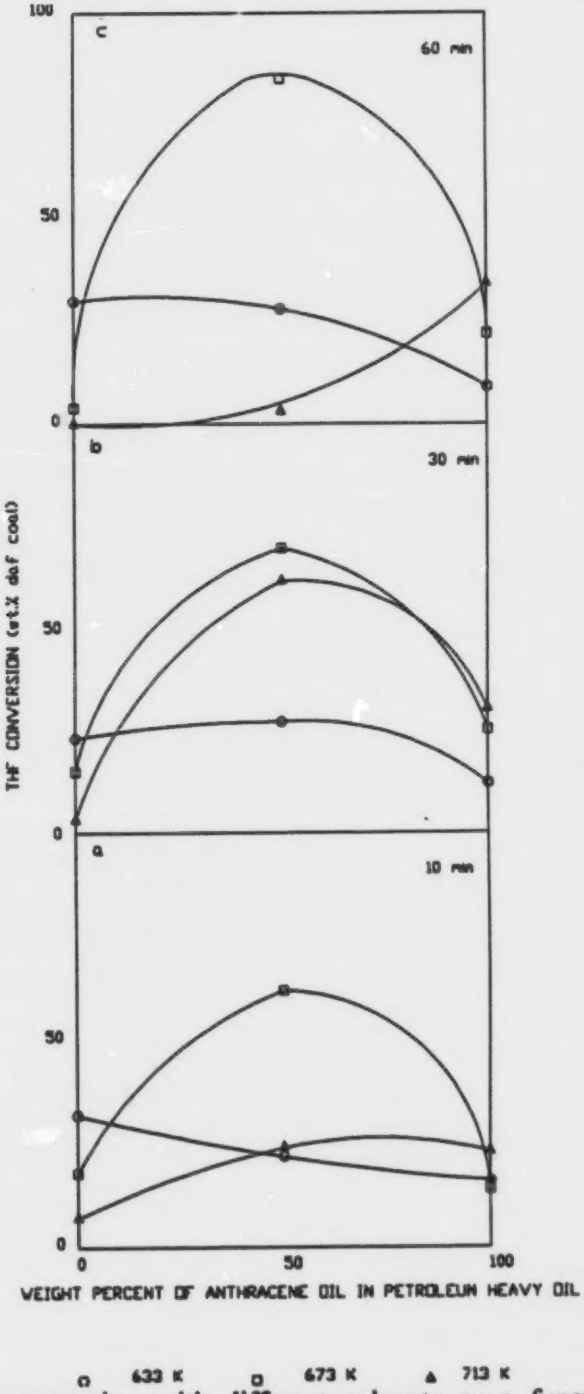

Figure 2.3 : Coal conversion with different solvents as a function of temperature and residence time. (From Rincon et al., 1986)

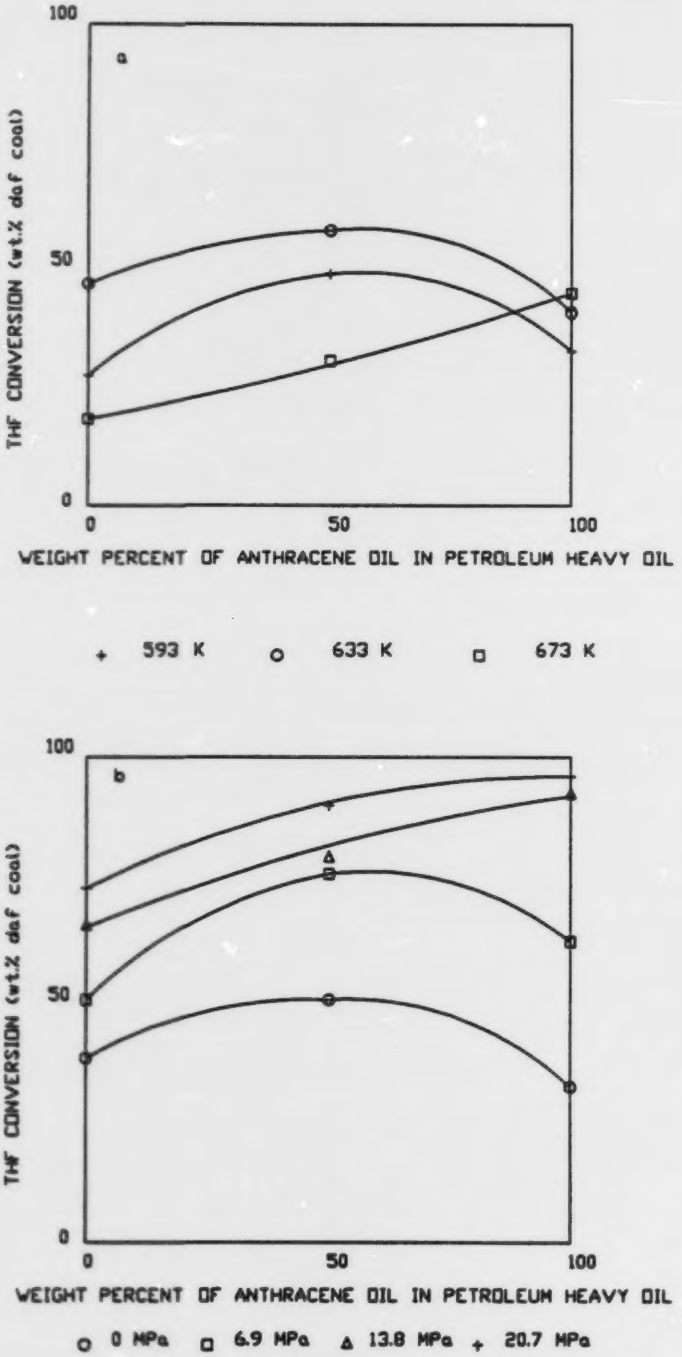

Figure 2.4 : Coal conversion with various solvents as a function of a) temperature and b) pressure. (From Rincon et al., 1987)

increases due to the presence of coal derived liquids. It was proposed that these two mechanisms occur during processing.

2.2 Phase Splitting

Shaw et al., 1988 investigated the role of phase splitting as related to the synergistic phenomena being reported. Experiments were performed with a pyrene, tetralin and hydrogen system. The phase behaviour of this mixture over the temperature range of 620 K - 700 K and hydrogen charge pressures of 0 MPa to 5.5 MPa was investigated. Phase splitting of a single liquid into two separate liquid phase was observed. The results showed the presence of a heavier pyrene rich phase and a lighter pyrene poor phase. A partial phase diagram (see Figure 2.6) of pressure versus pyrene % wt. shows the existence of two liquid phases.

Shaw et al., (1988) then connected the non-additive phenomena previously described by Derbyshire et al., (1982) to the phase splitting behaviour exhibited by the hydrogen - pyrene - tetralin system. The hydrogen - pyrene - tetralin system is miscible at 675 K but at higher temperatures, 700 K, becomes only partially miscible. The observed synergistic behaviour of the solvent system was only apparent at temperatures greater than 700 K . Hydrogen is approximately eight times more soluble in tetralin than in pyrene in the temperature range of 675 K - 700 K (Shaw 1987). If one assumes that the solvent are a single liquid phase and the coal dissolution properties of the solvent is independent of the composition then in the temperature range of 675 K - 700 K coal conversions are expected to increase as tetralin concentration increases. This is consistent with the results obtained by

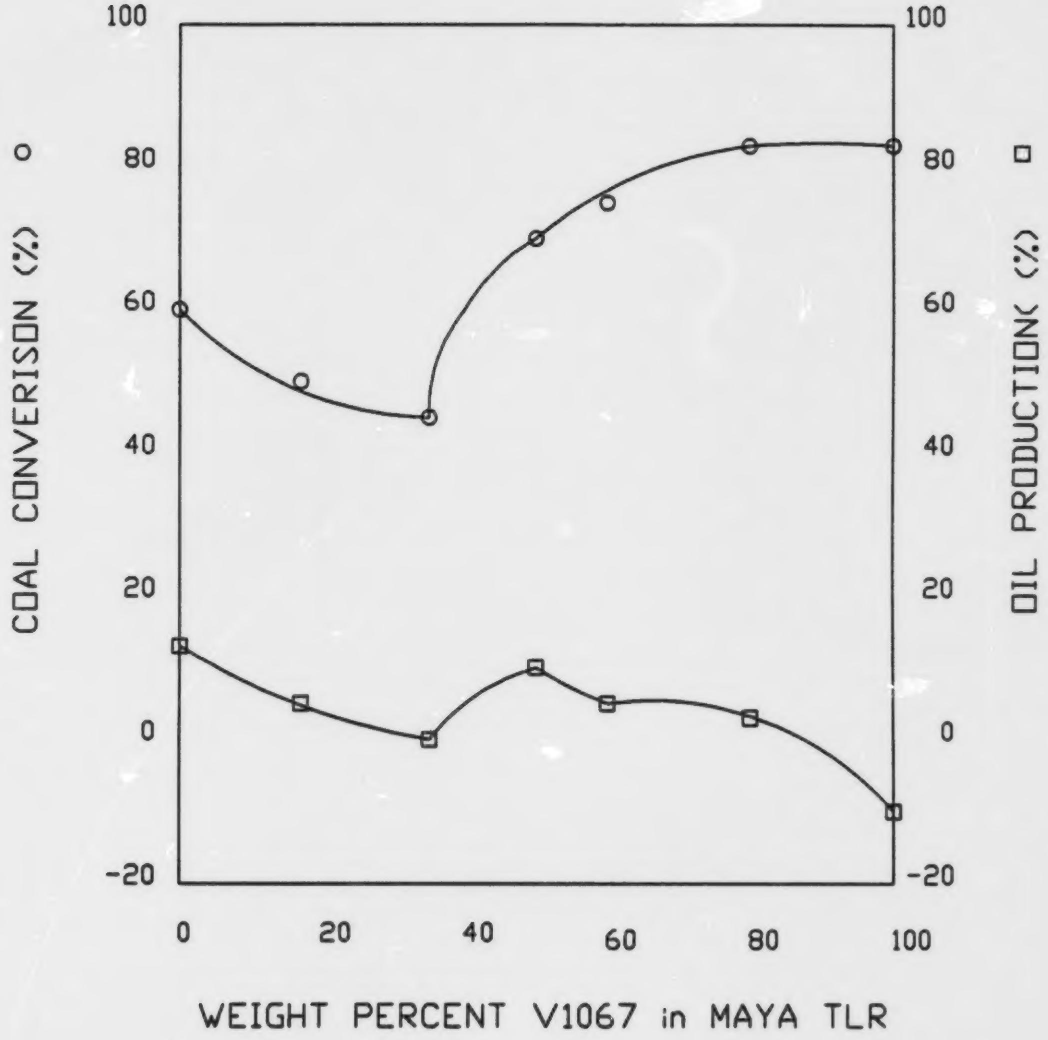

Figure 2.5 : Coal conversion and oil production in blends of coal liquids and petroleum solvents. (From Curtis et al., 1987)

Derbyshire et al., (1982) at 675 K.

Shaw et al., (1988) proposed four types of solvent behaviour which considers the existence of more than one liquid solvent phase and the effect of solvent composition on coal conversions. The four types of behaviour are shown in Figure 2.7. Type 'A' behaviour assumes one continuous solvent phase and that solvent component B has a higher hydrogen solubility than solvent component A. As the amount of the component A increases coal conversion increases. Work reported by Shaw and Peters (1989) show that at low hydrogen pressures coal reactions become mass transfer limited even in the presence of a good hydrogen donor solvent since it is the availability of molecular hydrogen that becomes the determining step. Consequently the effect of solvent composition should be less at higher hydrogen pressures if the solvent phase is a continuous. This behaviour was observed with the pyrene -tetralin - hydrogen system at 675 K. Type 'B' behaviour considers the case where component A has good coal dissolution properties but low hydrogen solubility and component B has good hydrogen solubility. The case where coal liquids are soluble in both components and a partially miscible binary solvent exist is considered first. Coal conversion increases as the amount of component B increases whereby a plateau is encountered as the A-rich phase persists. A step change in conversion occurs as the continuous phase switches to a B-rich phase followed by an increase in coal conversion. At higher hydrogen pressures the effect is reduced. Type 'C' behaviour considers the case where coal dissolution products are less soluble in component B than in component A and as before B has a higher hydrogen solubility than A. The effect of solvent composition becomes unpredictable since coal derived components that are not soluble in the continuous liquid phase may either be hydrogenated or polymerized during further reaction. The shaded area shows the possible range of coal conversion. If type 'C' and type 'B' behaviour are combined then type 'D' behaviour is proposed. Figure 2.8 shows the proposed phase transitions that can occur during phase splitting where a "B" rich phase dispersed phase exist in an "A" rich continuous phase and as the mass fraction of component B increases the continuous phase switches and becomes a "B" rich one. This representation of the phase splitting phenomena is a simplified one and demonstrates the extreme cases. At 700 K where the pyrene - tetralin hydrogen system exhibited phase splitting Derbyshire et al., (1982) observed coal conversions that are consistent with type 'D' behaviour. Tetralin is known as a good hydrogen donor with high hydrogen solubility but demonstrates poor physical solvating properties for coal liquids where as pyrene has a lower hydrogen solubility but is a good physical solvent for coal derived material. If a tetralin rich phase was the predominant continuous phase at 700 K then one would expect coal conversions to decrease as the mass fraction of tetralin increased since the heavier pyrene rich dispersed phase would tend to polymerize forming 'coke' as a result of hydrogen starvation due to poor liquid -liquid mass transfer rates. The difference in hydrogen solubility, hydrogen donor ability and dissolution properties in each phase would effect conversions.

2.3 Liquid - Liquid Equilibrium

This section presents typical liquid - liquid equilibrium often encountered in

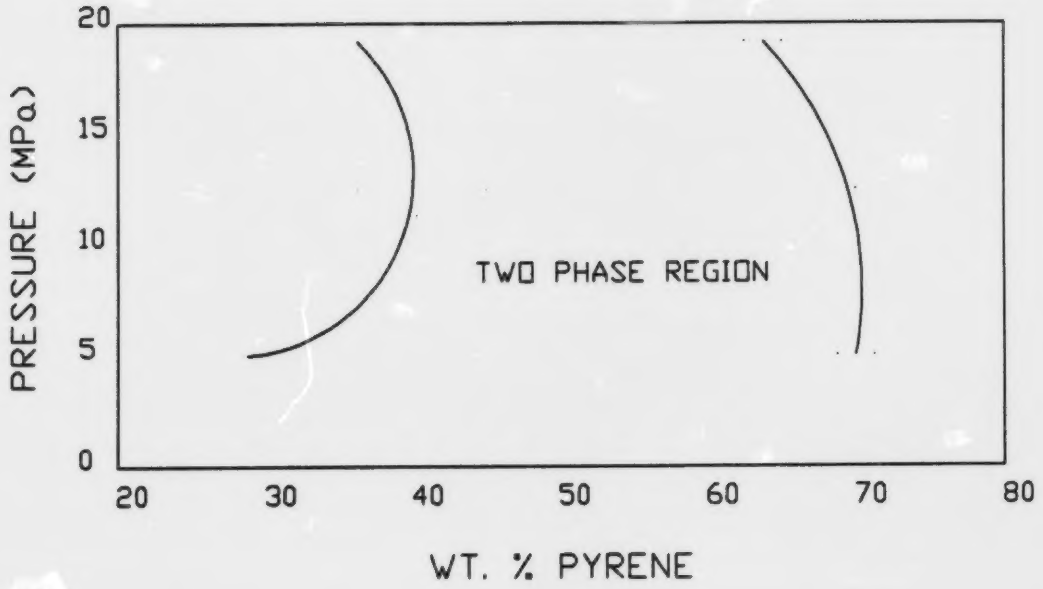

Figure 2.6 : Partial phase diagram for pyrene - tetralin solvent system showing two phase liquid region at 700 K. (From Shaw et al.,1988).

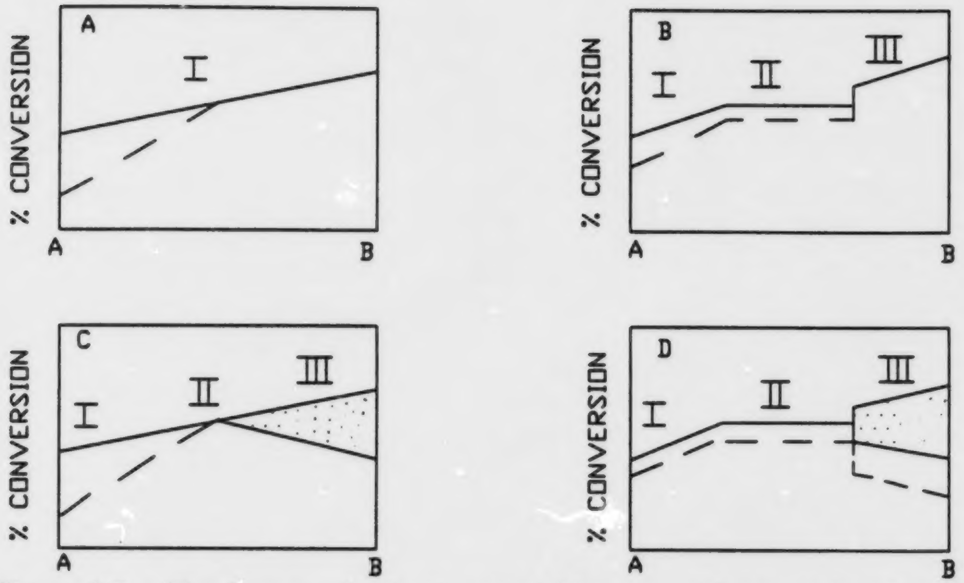

Figure 2.7 : The impact of solvent composition on coal conversion (solid line - elevated pressure, broken line - low hydrogen pressure) for binary solvent types A,B,C and D. (Shaw et al., 1988)

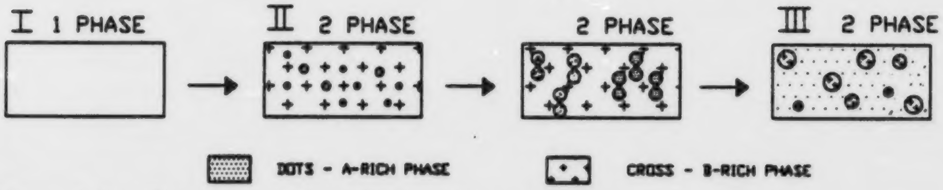
I 1 PHASE
II 2 PHASE
2 PHASE
III 2 PHASE
DOTS - A-RICH PHASE
CROSS - B-RICH PHASE

Figure 2.8 : Phase transition during phase splitting.

binary systems. By categorizing the systems being investigated as binary two phase systems a very simplified view of a rather complex situation is being considered. These systems are not binary and the number of phases present is not always clearly apparent. In following paragraph the word "critical" is used to denote the point at which liquid - liquid immiscibility arises which may not necessarily be in the critical region of the mixture and must not be confused with critical phase behaviour.

A two component two phase system has two degrees of freedom. By keeping one variable constant (usually pressure) the curves shown in Figure 2.9 are typical equilibrium curves encountered in liquid - liquid equilibrium (Novak et al., 1987). The most common equilibrium curve is shown in Figure 2.9a. This systems shows the existence of an upper critical solution temperature (UCST). Miscibility of the two liquids increases as temperature increases and the UCST represents the temperature at which the properties of both liquid phases are identical (at constant pressure). At temperatures greater than Tc the system exists as a homogenous phase and at temperatures less than Tc two phases appear. Figure 2.9b depicts the reverse situation where liquid - liquid immiscibility arises as temperature increases and this systems has a lower critical solution temperature. A system that exhibits a closed miscibility curve is shown in Figure 2.9c where phase splitting is bracketed by a temperature range. Figure 2.9d is a system with both lower and upper critical solution temperatures but unlike Figure 2.9c. two separate equilibrium curves are formed.

The high pressure phase behaviour of mixtures in their critical region was reviewed by Subramaniam and McHugh (1985). Scott and van Konyenburg presented (see FIgure 2.10) six classes of binary phase behaviour using pressure - temperature diagrams. Type I behaviour represents the simplest possible binary P - T diagram. The liquids are miscible in all proportions and a continuous critical mixture curve exist. C1 and C2 represent the critical points of the more volatile component and less volatile component respectively. In all cases shown in Figure 2.10 the overall mixture compositions varies along the critical mixture curve.

In type II behaviour the liquids are no longer totally miscible at all pressures and temperatures. This plot is similar to type I behaviour except at temperatures lower than the critical points of both components liquid - liquid immiscibility arises. Liquid - liquid - gas behaviour ends at the upper critical end point (denoted by the triangle) where one of the liquid phases becomes identical to one of the liquid phases.

In type III behaviour the critical line is not continuous. The line emerging from C1 exhibits a two phase region until it intersects the upper critical end point. At which point LLG behaviour arises. The lines starting at C2 represent gas - gas, gas - liquid and fluid - fluid equilibria.

In type IV phase behaviour the branch of the critical mixture line starting at C2 intersects a region of liquid - liquid equilibria at lower critical solution temperature. At this point the two liquid phases become identical and exist with the gas phase. The branch of the critical line starting at C1 intersects the LLG line at an upper critical end point. From the lower critical end point to the upper critical end point LLG exist.

Type V phase behaviour is similar to type IV except LLG phase behaviour does not arise at subcritical temperatures. In this case the LLG line is also bracketed by the upper and lower critical end points. In type VI behaviour the critical mixture line is similar to type I behaviour however, outside the envelope at lower temperatures a three phase region exist which has a lower and upper critical end point and is bounded by a liquid - liquid line. And as pressure is increased liquid - liquid or fluid - fluid behaviour arises.

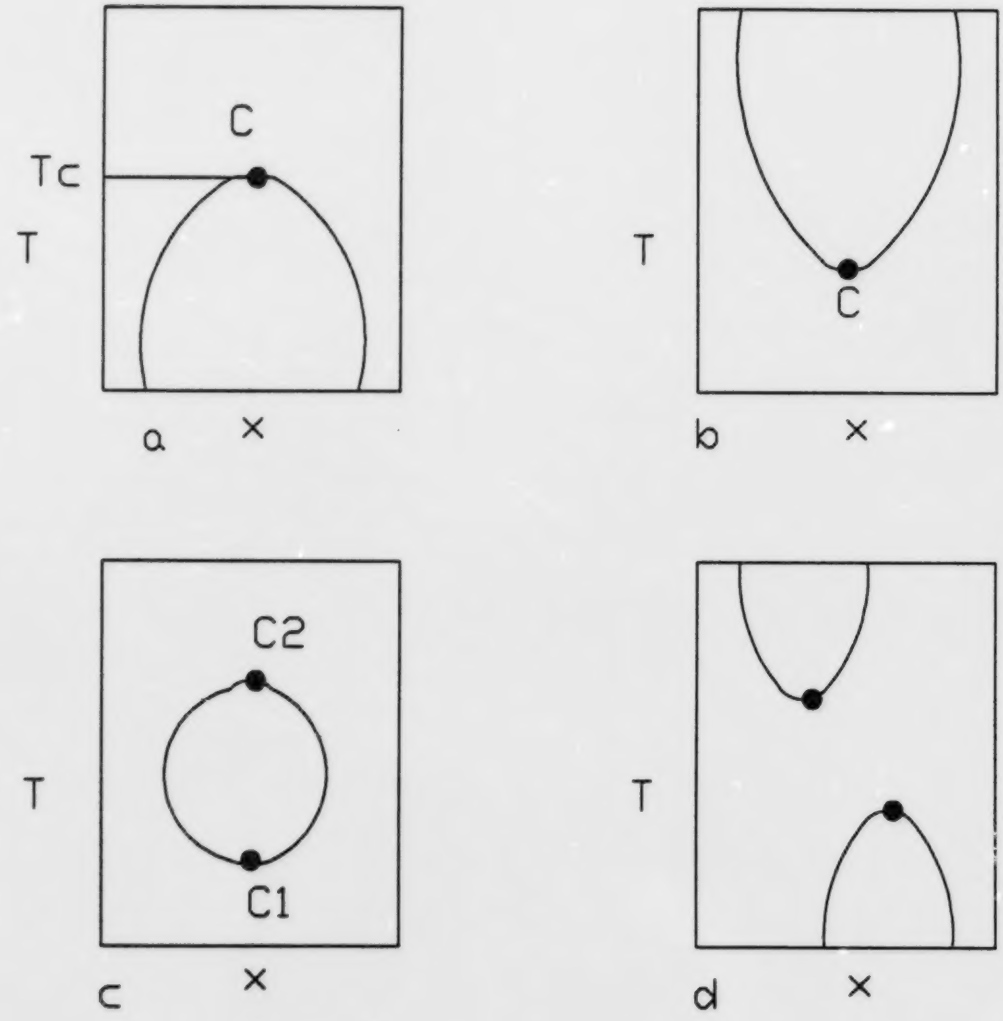
C
Tc
T
a
x
T
C
b
x
C2
T
C1
c
x
T
d
x

Figure 2.9 : Equilibrium curves for liquid - liquid equilibrium in binary system at constant pressure, types a,b,c and d

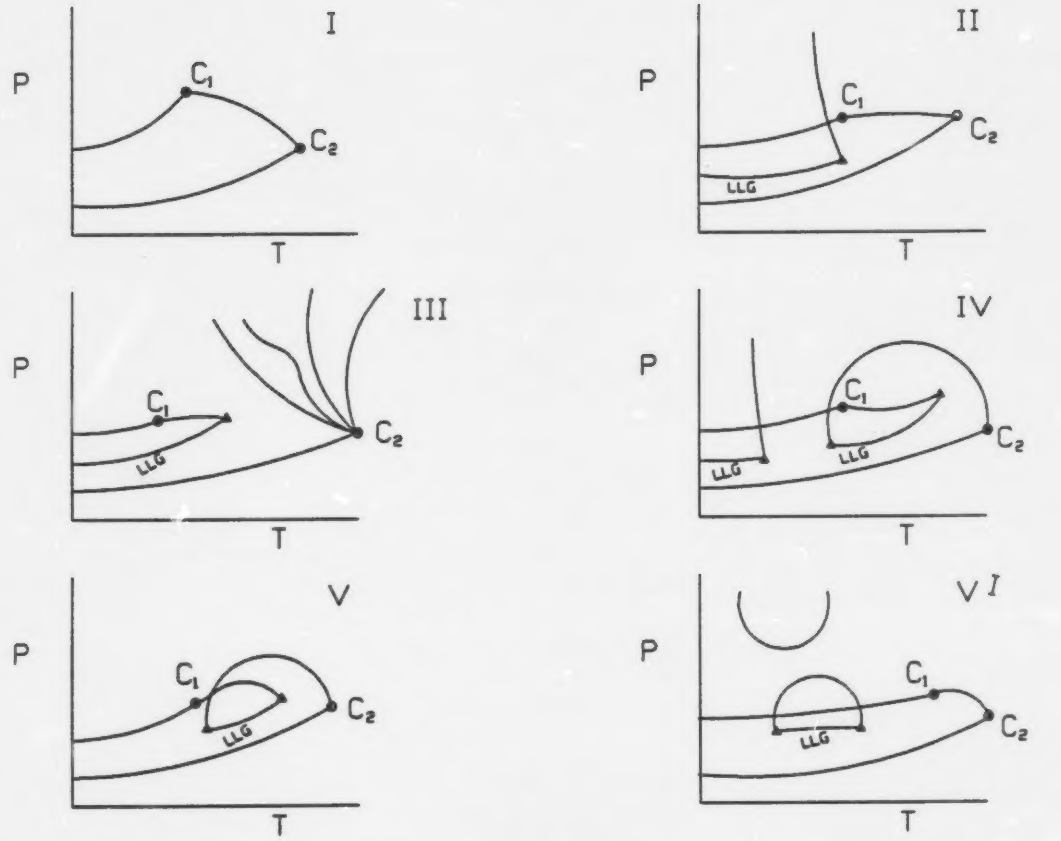
I
P
C1
C2
T
II
P
C1
C2
LLG
T
III
P
C1
LLG
C2
T
IV
P
C1
LLG
LLG
C2
T
V
P
C1
LLG
C2
T
VI
P
C1
LLG
C2
T

Figure 2.10 : Six types of pressure - temperature diagrams for bianry mixtures, in the critical region

3. EXPERIMENTAL

3.1 Materials

Physical properties of the materials used in experiments are given in Tables 3.1 to 3.3.

Table 3.1 : Physical properties of gases

	HYDROGEN	NITROGEN	METHANE	ETHANE
FORMULA	H_2	N_2	CH_4	C_2H_6
MOLECULAR WEIGHT	2.016	28.013	16.043	30.071
CRITICAL TEMPERATURE (K)	33	148	190	305
CRITICAL PRESSURE (MPa)	1.29	3.39	4.61	4.83

Nitrogen and hydrogen were supplied by Canadian Oxygen Ltd. and methane and ethane were supplied by Canada Liquid Air Ltd.
All gases were commercial grade.

Table 3.2 : Physical properties of model solvent compounds

	DECALIN	INDENE	NAPHTHALENE	PYRENE	TETRALIN
PURITY (%)	95	98	95	98 - 95	97
MOLECULAR	138.25	116.16	128.19	202.26	132.22
FORMULA	$C_{10}H_{18}$	C_9H_8	$C_{10}H_8$	$C_{16}H_{10}$	$C_{10}H_{12}$
MELTING POINT (K)	--	—	354	429	—
BOILING POINT (K)	(cis) 469 (trans) 460	456	491	666	481
CRITICAL TEMPERATURE (K)	702	698	748	892	719
CRITICAL PRESSURE (MPa)	3.6	3.8	4.05	2.6	3.5

All model solvent compounds were supplied by Fluka, Chem. Fabrik CH9470 Buchs Switzerland

Table 3.3 : Physical properties of heavy oils

	Anthracene Oil	Athabasca Bitumen	Venezuela (blend 24) Vacuum Bottoms
Specific gravity	1.092 (15.5 °C)	1.046 (24°C)	1.026 (21 °C)
water %	0.2	--	--
xylene insoluble %	0.08	--	--
pentane insoluble %	--	38.4	21.4
Distillation, % to	--		
498 K	0.0	--	--
543 K	7.9	--	--
588 K	43.7	--	--
628 K	80.5	--	--
+628 K	19.0	--	--
+798 K	--	99.3	95.1
Elemental analysis			
C	--	84.3	84.3
H	--	10.9	9.6
N	--	0.8	0.7
O	--	0.3	0.7
S	--	3.5	6.0
Aromatic carbon %	--	35.4	30.0
Mean molar mass	--	983	848

Anthracene oil was supplied by Allied - Signal Chemical Co. and Athabasca bitumen and Venezuela (blend 24) vacuum bottoms were supplied by CANMET

3.2 Equipment

A schematic of the apparatus is shown in Fig.3.1. Experiments were conducted in a 2 L autoclave manufactured by Pressure Product Industries and designed for a maximum working pressure of 34.5 MPa at 673 K and 51.7 MPa at 295 K. The reactor system is constructed of 316 stainless steel. The autoclave is 0.095 m in diameter and 0.3 m in length and is placed vertically in a 3000 W muffle furnace. The muffle furnace was later replaced by a 4000 W band heater. In an attempt to reduce the amount of materials used in any one experiment a stainless steel insert with an inner diameter of 0.05 m and a length of 0.24 m was employed. The insert is held in place by the inner cooling coils. This allowed the amount of material used in an experiment to be reduced from approximately 500 g to 180 g. The reactor is equipped with a permanent magnetic driver coupled with a belt drive. A two bladed turbine with a diameter of 0.03 m and placed 0.03 m from the base of the insert completes the stirring mechanism.

Samples are retrieved from the reactor via three heated sample ports. These ports are typically (for model solvents) placed at 0.25 m, 0.14 m and 0.00 m from the top of autoclave. In order to place the sample ports the densities of the materials used in experiments was measured. The densities of tetralin, Athabasca bitumen and Venezuela blend 24 vacuum bottoms as a function of temperature were determined. The impact of hydrogen pressure on the densities was also investigated. These results are shown in Figures 3.2 to 3.4. For a detailed analysis of sample port placement refer to Appendix D.

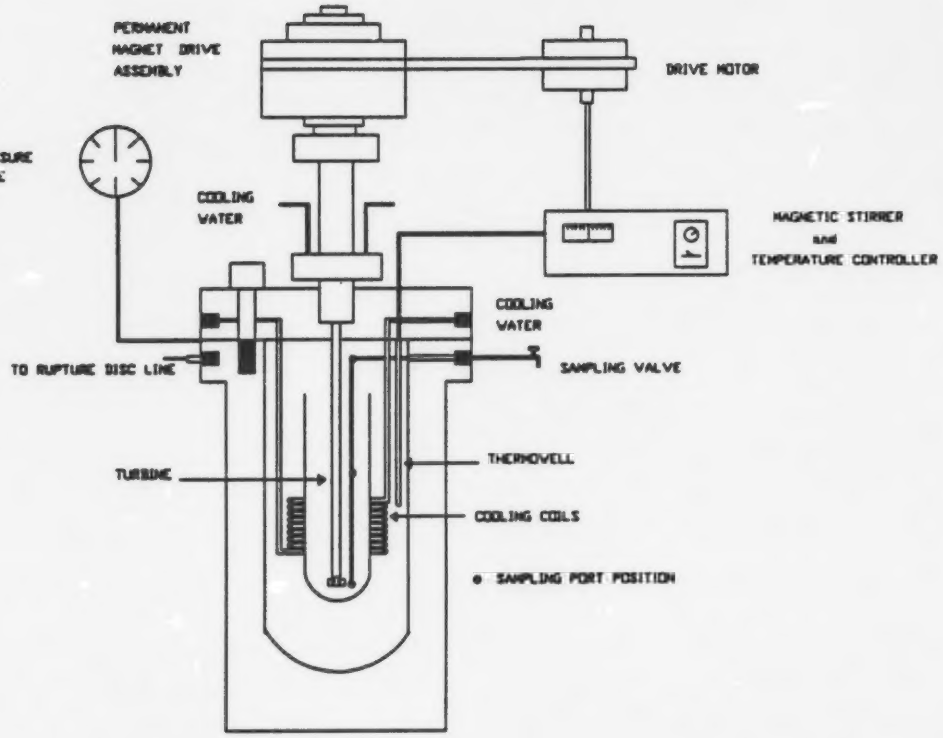
PERMANENT MAGNET DRIVE ASSEMBLY
DRIVE MOTOR
PRESSURE GAUGE
COOLING WATER
MAGNETIC STIRRER and TEMPERATURE CONTROLLER
COOLING WATER
TO RUPTURE DISC LINE
SAMPLING VALVE
TURBINE
THERMOWELL
COOLING COILS
● SAMPLING PORT POSITION

Figure 3.1 : Apparatus

The sample ports were placed in order to obtain a gas sample and two liquid phase samples. Each sample port is equipped with a needle valve ensuring precision control during sampling. This is especially important when sampling across large pressure differences. The two liquid sample port valves are connected to a 3-way high pressure block which is attached to the reactor. The gas sample port valve is directly connected to the reactor.

The temperature in the reactor is measured by a thermocouple (TYPE-K) placed in a permanent thermowell. Pressure is monitored in two ways, a pressure line from the reactor is connected to a pressure gauge and to a pressure transducer which interfaces with a computer. A computer is especially useful when trying to detect small leaks during pressure testing since it is capable of measuring smaller increments. The reactor is pressurized or vented by a 3 - way high pressure block connected to a series of valves. The 3 - way high pressure block connects two 2 - way valves to the reactor system, one valve is connected to the particular gas cylinder being used in the experiment while the valve is attached to a venting pipe which is placed in the ventilation system. This set up permits easy pressurizing, venting and purging of the system during start-up and shut-down. The reactor is sealed with eight 12.7 cm bolts and a 316 stainless steel O - ring gasket.

The autoclave is welded to a support system which is bolted to the floor and encased in a stainless steel hood.

3.3 Control and Safety

The temperature in the reactor is controlled to within 2 K of the setpoint by an Aethena controller which has a maximum setpoint of 698 K.

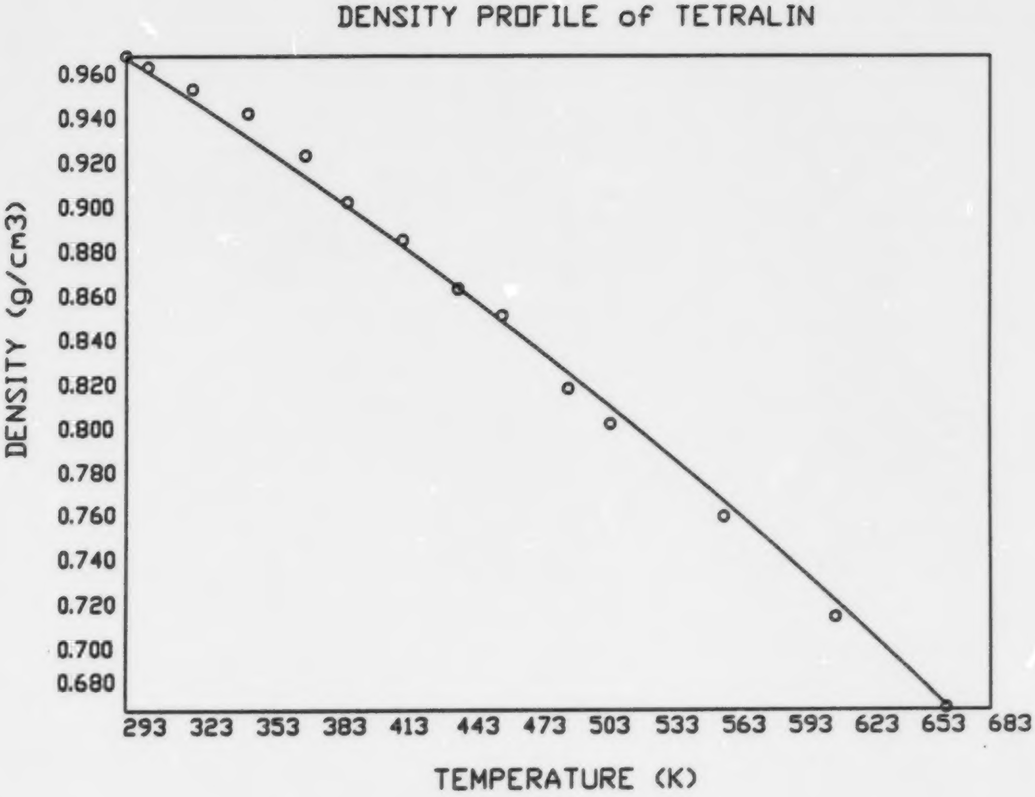

Figure 3.2 : Density profile for tetralin with no gas

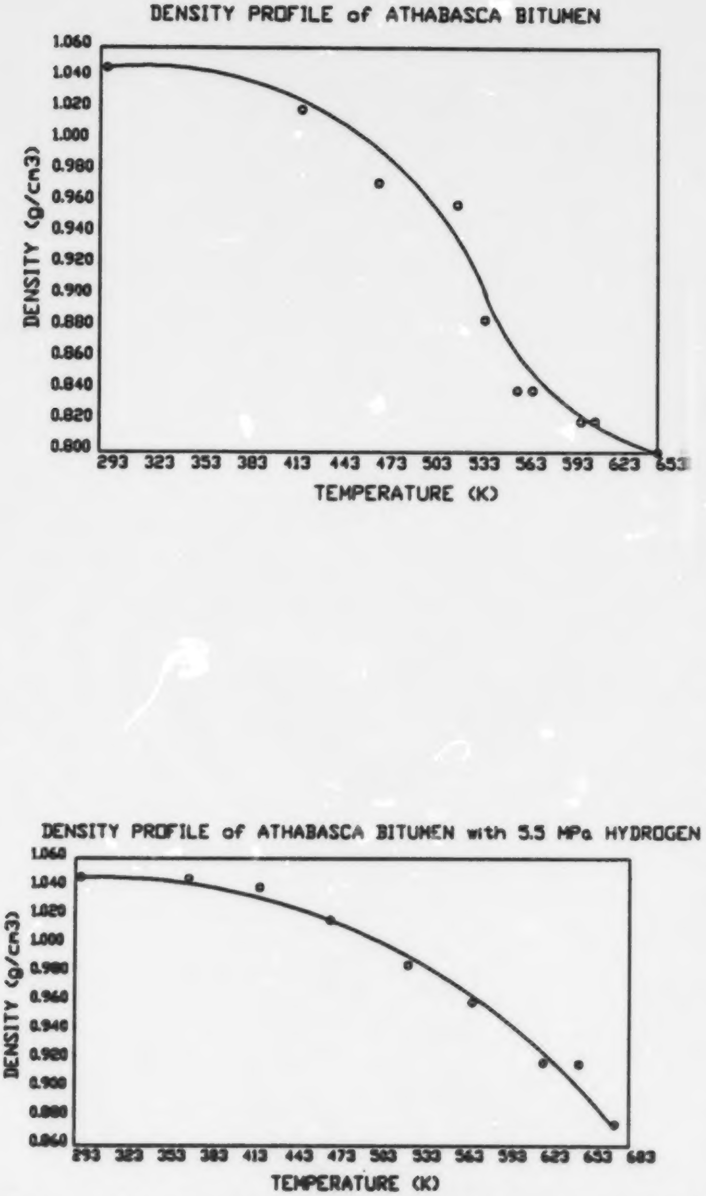

Figure 3.3 : Density profile for Athabasca bitumen a) with no gas and b) with hydrogen

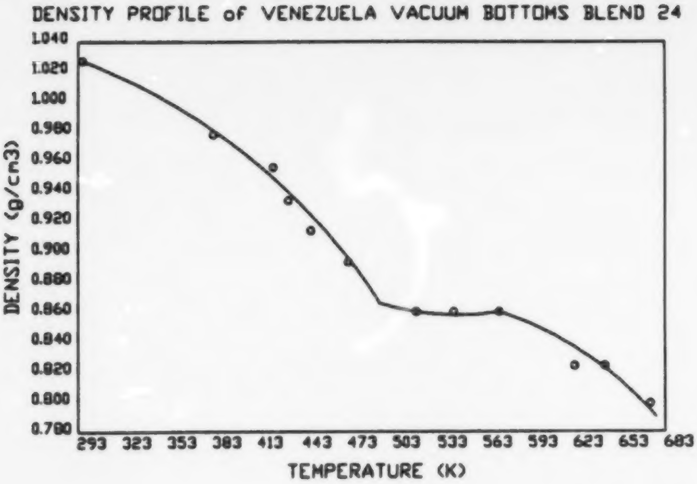

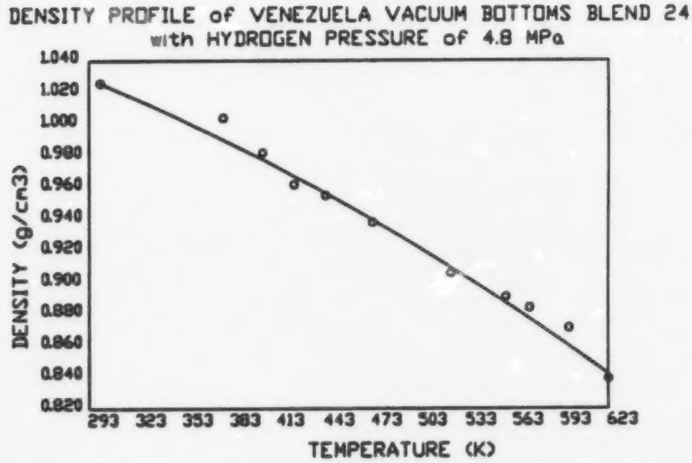

Figure 3.4 : Density profile for Venezuela Vacuum Bottoms (blend 24) with a) no gas and b) with hydrogen

The heating tape used with the sample ports is connected to variable rheostat controller. The magnetic driver is controlled by a Reliance Electric variable speed controller (range 0 - 2500 rpm). The stirrer is also equipped with a tachometer which allows for easy monitoring of the stirrer. A water cooling jacket surrounds the magnetic stirrer shaft to protect the mechanism from thermal damage. In the event of a possible hazardous situation arising from an increase in temperature in the reactor rapid cooling can be achieved by an internal water cooling coil. The cooling water is a manually controlled by valves.

The reactor is also equipped with a stainless steel rupture disc with a bursting range of 49.8 MPa at 295 K and 34.5 MPa at 672 K. Excessive overpressure in the reactor will burst the rupture disc. The rupture disc line is attached to a blow out cylinder which ensures proper containment of the material. The rupture disc is set at a bursting range below the maximum allowable working pressure which prevents failure of the equipment in the event of overpressure. The entire reactor system is contained in a large stainless steel container which is equipped with its own ventilation system.

An emergency switch on the control panel is connected to the power supply for the system. In the case of an emergency this switch provides immediate shut down of all electrical parts which includes the heater, magnetic stirrer and heating tape. During sampling and cleaning of the reactor personnel are fitted with gas mask, safety goggles, overalls and gloves.

3.4 Operation

In any particular experiment the reactor is charged with 180 g of material placed in the insert. With the O - ring gasket in place the reactor is then sealed with eight bolts tightened in a star pattern. The bolts are treated with *Silver Goop* to prevent seizure. The system is then evacuated by an aspirator connected to the venting line and purged with nitrogen followed by the gas being employed in the particular experiment. The reactor is then pressurized to the required pressure and pressure tested. Leaks are detected with Snoop solution and careful monitoring of the pressure by means of the pressure gauge and pressure transducer. After ensuring that the system is free of leaks the magnetic driver belt is attached, cooling water lines connected to the stirrer cooling jacket and inner cooling coils, and the thermocouple is placed in the thermowell. The system is now ready for start-up.

The valve to the cooling water line for the magnetic stirrer jacket is opened, the heater is activated and the heating tape is switched on. The temperature controller is set for the first set point. If model solvent compound are being employed then the magnetic is invoked at this point but if any of the heavy oil systems are being used then the system is heated to 473 K before the stirrer is switched on.

Once the set point is reached the magnetic stirrer is switched off and the temperature is maintained at the set point for 0.5 hours. This allows for an equilibration period of the system before sampling. The sample lines are purged, usually less than 2 ml is removed, before a final sample is retrieved. Samples are collected in ice cold vials and immediately diluted in toluene. A typical sample would be approximately 1 ml diluted in 5 ml of toluene. This simple sampling procedure is very efficient for experiments with model compound solvents. Materials which have boiling points lower than 273 K are not collected. After sampling is completed the stirrer is turned on and the temperature controller is adjusted for the next set point, and the entire procedure is repeated.

At the end of an experiment the heater, heating tape and stirrer are switched off. Both cooling water valves are turned on and left running. When the system is at room temperature the autoclave is depressurized by means of the venting line. The bolts are loosened and the motor belt is removed whereupon the autoclave is ready for cleaning. The waste material from the reactor is placed in a sealed container for waste disposal. All parts are dismantled and cleaned with tetrahydorfuran. Sampling lines are changed accordingly. The procedure for cleaning, charging and assembling the reactor usually requires approximately 6 hours depending on the success of the pressure testing and whether the sample lines are replaced. The actual run time for the experiment is approximately 6 hours.

3.5 Analysis

Samples were analyzed by gas chromatography. Preliminary screening of the samples were performed with a Shimadzu (GC - 6AM) gas chromatograph. The gas chromatograph uses a flame ionization detector and a 0.75 m OV-101 column. The column was operated with nitrogen as the carrier gas set at a flow rate of 40 ml/min and FID conditions were hydrogen gas flow of 0.6 kg/cm^3 and air flow of 0.6 kg/cm^3. A temperature program of 433 K for 2 min, 433 K to 528 K at 20 K/min and a final temperature of 528 K held for 2 min was used. 1 ul samples (as originally diluted) were injected into the column. Initially the sensitivity is set at 1, after the solvent peak has emerged the sensitivity is set to 10^3. The gas chromatograph is interfaced with a computer which allows some preliminary data analysis.

Detailed analysis was performed with a Hewlett - Packard 5987A radio frequency quadruple gas chromatograph mass spectrometer (GC-MS). The GC-MS was used to simultaneously identify and quantify the samples. The GC-MS is equipped with a 30 m DB-17 column. Samples were further diluted 10 ul in 1 ml of toluene and a 1 ul sample of this solution is then injected into the GC-MS. The system is completely computer operated. The computer procedure is menu driven but requires some patience in mastering the techniques. Different temperature programs were investigated and the following programs were found to be the most efficient. For the model compounds the temperature program shown in Figure 3.5 was used. The program has a total run time of 16.75 min. The heavy oil systems required a less steep temperature program to ensure proper separation. The program used has a total run time of 43 min and is shown in Figure 3.6.

3.6 Experimental Considerations

Previously (Shaw et al., 1988) experiments were conducted without the insert and for any one experiment approximately 500 g of material was required. In order to reduce the amount of material used in an experiment an insert was constructed. The insert was designed to fit snugly in the inner cooling coils, and this proved to be a successful design which did not significantly alter the results of the experiments. One advantage to the insert was that materials were placed slightly away from the reactor walls where heat transfer problems had led to 'coking' or carbonization reactions. The thermowell is also situated next to the insert hence ensuring valid temperature readings. Although the 'coking' problems had been reduced by the use of the insert it was still a significant problem. At this stage a glass liner was placed within the insert and this proved to be a very successful method of reducing the 'coking' reactions.

During the course of the project the heater was replaced. The 3000 W muffle furnace was removed and a 4000 W band heater was installed. The change in heating system altered the rate of heating. For example in a typical experiment with pyrene-tetralin system 2.5 hrs was required to reach a set point 623 K with the 3000 W furnace. With the 4000 W furnace in 1.5 hrs the same set point was attained. Such a change in heating mechanism may alter the reaction pathways and the rate of degradation. The outcome of any such changes will be discussed in the following result section.

One of the most challenging aspects of the experimental work was the positioning of the sample ports, especially the positioning of the second sample port. This position is reflective of where phase splitting occurs and hence the location of the upper liquid phase. The location of this sample port was predicted using the densities of the components and other simplifying assumptions. In order to remove the need for such an estimation the design of a floating sampling port was considered whereby the sampling line would float on the upper liquid level. This

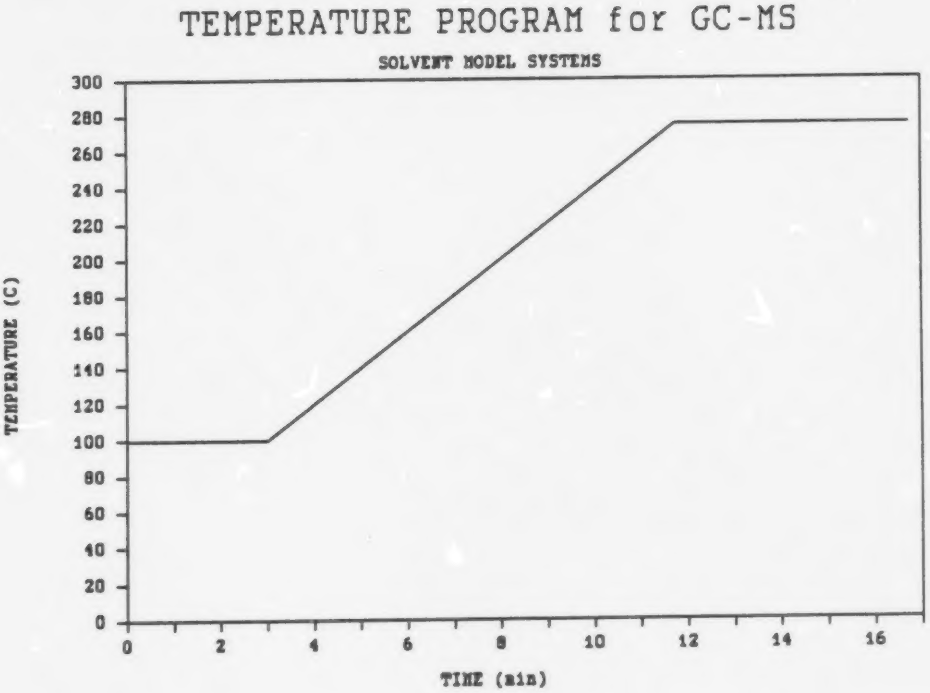

Figure 3.5 : Temperature program used in GC-MS for model solvent systems

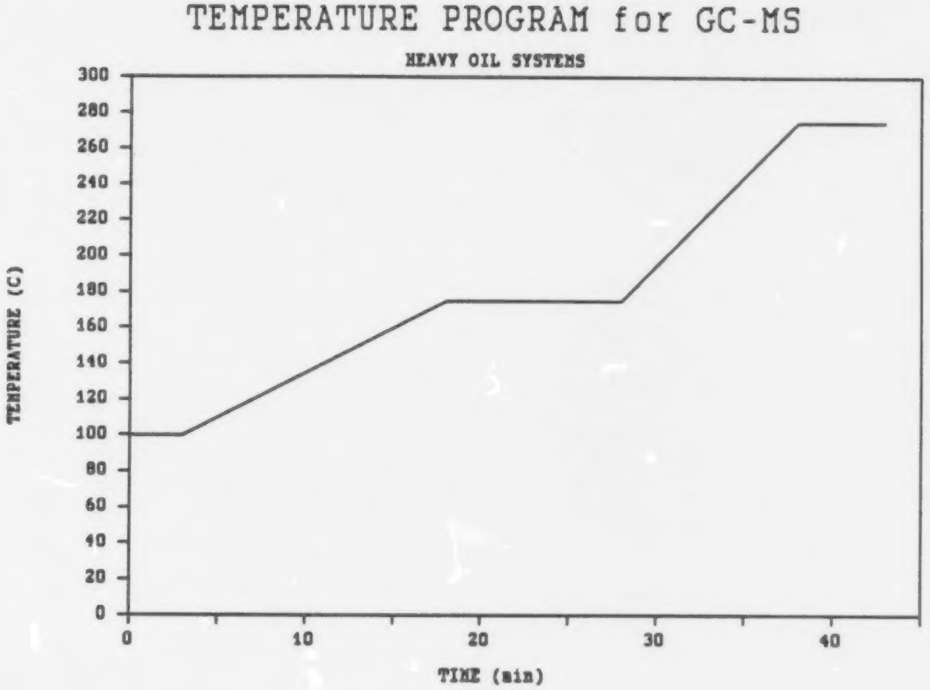

Figure 3.6 : Temperature program used in GC-MS for heavy oil systems

was attempted with three different approaches ; teflon tubing, flexible tubing and a glass donut shaped float. Each attempt was unsuccessful. The teflon tubing disintegrated under the mildest reaction conditions, a sturdy connection between the flexible tubing and the rest of the sample line could not be obtained and finally the glass float was too heavy and too fragile.

4. RESULTS :

4.1 Experimental Considerations

A summary of results are presented in Figures 4.5 to 4.10 and Tables 4.1 to 4.13. Detailed tables of all results appear in appendices A and B. These results are qualitative and do not represent absolute compositions and hence can only be used to demonstrate trends arising in the various systems. All mole fractions reported were determined on toluene free basis, and a gas free basis i.e any light gases such as methane, nitrogen, hydrogen etc. and any other material not condensable above 273 K were not analyzed. Materials heavier than pyrene were also not analyzed.

In using gc - ms analysis peaks were not identified unambiguously. The Hewlett Packard HP5987A gc - ms system identifies any particular peak with a certain probability of fit. Peaks such as indene, naphthalene, tetralin, decalin and pyrene were however definitively identified using standards. In some instances peaks were identified with 99% probability of fit, for example in the heavy oil systems the compound dibenzofuran was identified to such a probability. In other cases identification proved more challenging. A peak appearing at a retention time between 3.35 to 3.45 minutes was commonly identified as any of the following peaks : 2,3 dihydro-1-H-indene, propenyl benzene, structural isomers of ethenyl-methyl benzene etc. with all compounds being C_9H_{10} and all being identified with the same probability. Similarly a peak appearing at 3.85 to 4.05 minutes was identified as structural isomers of 1-methyl 2,3 dihydro-1-H-indene, structural isomers of ethenyl-ethyl-benzene and structural isomers of methyl propenyl benzene where all compounds were $C_{10}H_{12}$. These peaks are therefore referred to as benzene and indene derivatives in the tables. The problem was even greater with the heavy oil systems, due to the wide variety of components, when compared with the model systems. At first it was thought that a less steep temperature program would allow for better separation and consequently easier identification however a change in temperature program did not rectify the problem. The lack of definitive compound identification is not uncommon since it is well documented (Gudzinocz et al., 1977) that mass spectrometry techniques are not always efficient for identification of isomers.

Quantitative analysis was achieved using standards. Three standards of known concentration were prepared with the following compounds : indene, decalin (cis and trans), tetralin, naphthalene and pyrene. Samples of calibration curves of peak area versus moles for each component were generated and appear in Appendix C. These calibration curves were generated for both temperature curves used in analysis. Usually samples were analyzed in batches and for each batch calibration curves were obtained. It is interesting to note the response factor (area to mole ratio) was very similar for each component. Using linear regression the slopes of the calibration lines were calculated and for a particular set were $9.72x10^{-15}$, $7.8x10^{-15}$, $6.1x10^{-15}$, $8.65x10^{-15}$ and $4.26x10^{-15}$ (peak area/mole) for indene, trans and cis decalin, tetralin, naphthalene and pyrene respectively. Since these values were all in the same order of magnitude it was possible to make good approximations for response factors of compounds for which it was not possible to generate calibration curves.

The onset of phase splitting is usually encountered upon approaching the critical region of one or more of the components in a system. Liquid vapour transitions in a pure fluid and liquid - liquid transition in an initially miscible liquid mixture are examples of phase changes that have critical points. Rapid shifts in transport and thermodynamic properties of these systems lead to surprising macroscopic phenomena. Greer and Moldover (1981) and Gulari, Saad and Bae (1987) have studied thermodynamic anomalies and the effect of critical phenomena on transport properties in the critical and supercritical region. They have documented liquid-like fluctuations in the vapour phase and vapour-like behaviour in the liquid phase close to the critical points. The most important aspect of these findings relative to this research is the shifting in the density variables (mass density and mole fraction of each chemical component). Close to a critical point, even at equilibrium, exists different domains of density and concentration in a fluid. Stanley (1971) in "Introduction to Phase Transitions and Critical Phenomena " have shown this type of behaviour in a binary mixture of cyclohexane - aniline. At temperatures well above the critical temperature a single clear phase exists. As the temperature is lowered the fluid takes on a dramatic flow which is termed "critical opalescence". When the temperature is just below the critical temperature although there is a distinct meniscus between gas and liquid phases there are many clusters of higher density material existing in the gas phase above the meniscus and, vice versa. Due to these fluctuations the location of the different phases in a mixture close to the supercritical is not easily predicted. In some cases the results show a greater concentration of pyrene in what is expected to be a gas phase, an example of this is the sample retrieved from the upper sample port with the pyrene - tetralin system with 3.5 MPa ethane. This "gas" phase sample showed the highest concentration of pyrene. At first this result seems erroneous but when one considers the possible fluctuations in densities and concentrations such findings are possible, and is indicative of subcritical and supercritical fluid.

The presence of emulsions was also another problem that was detected upon analysis of the results. In order to maximize mass and heat transfer rates and thereby obtain phase data the experimental apparatus was equipped with a stirrer. Shaw et al., 1988 investigated different equilibration periods and stirring rates which would reduce the existence of possible emulsions without increasing the amount of degradation. An optimum period of 30 minutes was suggested. In most experiments emulsion separation was not a problem but since these experiments were conducted with smaller volumes than those used by Shaw et al., 1988 emulsions were encountered more frequently.

4.2 Material Instability

At elevated temperatures the pyrene-tetralin mixtures were susceptible to degradation. The pyrene proved to be the more stable component with only small amounts of dihydropyrene produced as an evident hydrogenation product. The tetralin however showed more extensive degradation and because of this instability pyrene was treated as a trace component and used to generate all phase diagrams produced. Although pyrene is not susceptible to hydrogenation it is very susceptible to dehydrogenation and consequently "coke" formation. Figures 4.2, 4.3 and 4.4 are plots of tetralin content as a function of temperature and pressure.

Tetralin dehydrogenates primarily to naphthalene with indene and benzene derivatives produced as other degradation products. Figure 4.2 traces the tetralin content in the pyrene - tetralin system with methane. Clearly degradation is temperature dependent with decreasing tetralin content as temperature increases. Samples retrieved from the top sample port, usually a gas sample, showed the greatest tetralin degradation. At 698 K samples from the top port did not contain any tetralin and this result was consistent at all pressures and both pyrene - tetralin mixtures. At 648 K tetralin degraded to primarily naphthalene with small amounts of other degradation products present. As temperature increased degradation was more extensive with both naphthalene and tetralin being converted to benzene and indene derivatives (see Appendix A). From the results, tetralin degradation does not exhibit any apparent dependency on increasing methane charge pressure. At a charge pressure of 7.5 MPa methane tetralin degradation in samples from port 2 and 3 was the lowest compared to samples retrieved from these ports at lower pressures. Experiments performed with the 30.4% mole pyrene - 69.6% mole tetralin showed the greatest tetralin degradation with an almost complete lack of tetralin in all samples at 698 K.

Figures 4.3 and 4.4 show tetralin degradation with nitrogen, ethane and no gas. All trends demonstrated with methane were also apparent in systems with the other gases. Degradation was greatest at 12 MPa nitrogen. Upon comparing tetralin degradation in the presence of the various gases there was no outstanding difference and even close inspection of the degradation products did not reveal any marked difference from one gas to another. If one compares the three experiments conducted with 18% mole pyrene - 82% mole tetralin and 3.5 MPa nitrogen, methane and ethane there is no significant difference in tetralin degradation.

Benjamin et al., (1979) studied the pyrolysis of tetralin at 773 K. They reported trace amounts of naphthalene and 1-methyl 2,3 dihydro-indene when tetralin was heated at 673 K for 1 hr. However when tetralin was heated at 773 K for 1 hr. extensive decomposition was observed with approximately 75% of the tetralin being degraded. Naphthalene was the major product with small amounts of 1-methyl 2,3 dihydro-indene, 2,3 dihydro-indene, ethylbenzene and toluene. They found that the degradation of tetralin to naphthalene is very slow in the absence of suitable catalyst and in the absence of any solvent mixture. Penninger and Slatboom (1976) reported an equilibrium between naphthalene, hydrogen and tetralin. Benjamin et al., (1979) agreed that although tetralin degrades to naphthalene the reverse reaction does not occur even at 823 K or at 673 K with an initial hydrogen pressure of 12.4 MPa.

Work done by Hooper et al., (1979) showed that tetralin degrades appreciable at temperatures greater than 648 K. They found that in the temperature range 673 K to 723 K the reaction to produce 1-methyl 2,3 dihydro-indene was dominant but this reaction did not occur to any measurable degree until some dehydrogenation of tetralin to naphthalene had occurred. They suggested three main processes (see Figure 4.1)

In this work tetralin degradation was more extensive than that previously reported. Degradation was evident at temperatures greater than 623 K. The results agree more closely to the work presented by Hooper et al., (1979) than to that of Benjamin et al., (1979). Similar degradation products were found and the three main processes proposed readily agree with the results. The reverse reaction of naphthalene to tetralin was not observed and the existence of an equilibrium between naphthalene, tetralin and hydrogen was not evident. The production of 1-methyl 2,3 dihydro-indene as the dominant reaction at temperature in the range of 673 K to 713 K was not apparent and in most cases naphthalene was the main degradation product.

Material instability is a function of many parameters. Heating rate, equilibration period, stirring rate, catalyst and "memory" effects in the equipment are just a few of the parameters to be considered when dealing with material instability. Stirring rate and equilibration periods were constant for all experiments but the heating rate, the inadvertent introduction of catalysts and any "memory" effects could not be controlled. Since the equipment was also used for experimental work with heavy oil systems the introduction of catalyst in the form of sulphur compounds could not be prevented (metal sulphides being well known hydrogenation catalysts, Wilson et al., 1982). The existence of pyrrhotite and other similar dehydrogenation catalysts may explain the extensive tetralin degradation observed and the presence of naphthalene as the more dominant product in most cases. A glass liner was used in an attempt to reduce this effect but since a liner was only used in the insert the problem was not completely alleviated. Similarly siliceous and carbonaceous deposits, though non-catalytic, may alter reaction paths and consequently affect material instability (Wilson et al., 1982). It was also noted that experiments performed with new glass inserts also showed a greater degree of tetralin degradation but a reduction in coking reactions.

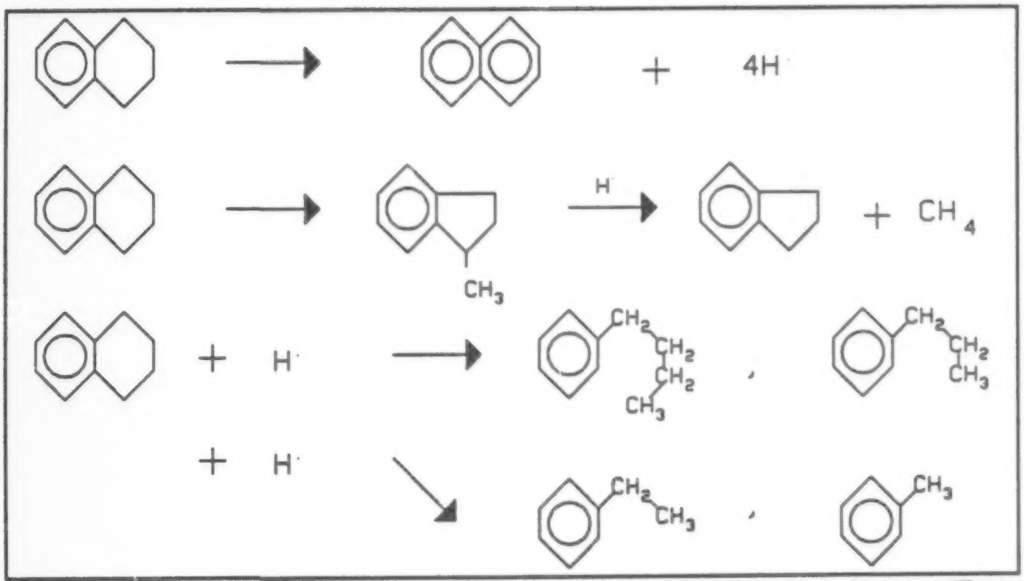
+ 4H·
H·
+ CH₄
CH₃
+ H·
+ H·
CH₂
CH₂
CH₂
CH₃
CH₂
CH₂
CH₃
CH₂
CH₃
CH₃

Figure 4.1 : Three main processes occurring in tetralin degradation. (From Hooper et al., 1979)

So far the change in heating mechanism has not been yet considered and the experiments conducted with the 18% mole pyrene - 82 % mole tetralin and methane at 3.5 MPa, 5.0 MPa and nitrogen at 12 MPa were performed with the 3000 W muffle furnace. While all other pyrene - tetralin experiments were performed with the 4000 W band heater. The results do not show any appreciable change or any apparent difference in tetralin degradation when comparing the two heaters.

The formation of carbonaceous material (material insoluble in tetrahydrofuran) was the single greatest problem in obtaining samples. For example, the experiment with pyrene - tetralin with no gas was conducted three times in order to obtain samples from the bottom sample port (port 3) and each attempt was unsuccessful due to coking and consequent plugging of sample lines. In most cases coking was not a problem at temperatures below 673 K and predominantly only affected sample retrieval from port 3. One would expect that in a reaction environment which has good mixing and sufficient labile hydrogen that coking reactions would not be a significant problem. However extensive polymerization can be explained as a result of phase splitting and is dealt with in the following section.

4.3 Phase Splitting

4.3.1 Model Compounds

Table 4.1 is a list of all model compound systems investigated which did not exhibit phase splitting at temperature specified, for example, a mixture of 60% wt. decalin and 40% wt. naphthalene did not exhibit phase splitting at temperatures lower than 673 K. In each case the specified temperature was the highest temperature at which samples were obtained. Phase splitting phenomena was detected by comparing samples retrieved from the three sample ports, if these samples showed a marked difference in composition then this signified the existence of two liquid phases.

Results for pyrene - tetralin - nitrogen systems investigated are given Table 4.3. Partial phase diagrams for this system are shown in Figures 4.5 and 4.6 as isobars and isotherms respectively. Samples obtained at temperatures lower than 623 K did not exhibit phases splitting. This was consistent for all experiments and a typical example of such results is given in Table 4.2 where samples obtained at 623 K do not exhibit phase splitting while those obtained at 648 K do show the presence of two liquid phases. Fig 4.6 at 648 K and 673 K show the existence of gas - liquid - liquid behaviour at all pressures investigated. As the temperature increases to 698 K the gas and "lighter" liquid phase combine and exist in fluid - fluid equilibrium with the "heavier" liquid phase. This phenomena is more easily demonstrated by the isobar (Figure 4.5). The shaded region in this diagram represents the region where the transition from gas - liquid - liquid equilibrium to fluid - fluid equilibrium occurs, the area is shaded since the exact temperature of the transition is not known.

The results of the pyrene - tetralin - methane system are shown in Figures 4.7 and 4.8. The behaviour of this system is much more complex and is not as easily described as the nitrogen system. A gas - liquid - liquid equilibrium exists with the methane system at 648 K and 3.5 MPa. At 648 K as the pressure increases to 5 MPa there does not appear to be three distinct phases and as the pressure increases to 7.5 MPa only one phase is present. At 673 K gas - liquid - liquid equilibrium exists for pressures up to 5 MPa and as the pressure increases the gas phase split and fluid - fluid equilibrium is evident. Unlike the nitrogen system where at all pressures gas - liquid - liquid behaviour undergoes a transition to fluid - fluid equilibrium for temperatures greater than 673 K the methane only exhibits this type of behaviour at 7.5 MPa. And gas - liquid -liquid behaviour persists for temperatures above 673 K at pressures lower than 7.5 MPa. The dotted lines in these diagrams represents a "heavier" phase line although not sampled in these experiments does exist as shown by Shaw et al., 1988. These lines have been included but there exact location is not known. With the methane system the existence of emulsions proposed to be a significant problem, for example, the samples retrieved at 698 K with the 3.5 MPa system (solid symbols) appears to be an emulsion.

Figure 4.9 represents the results obtained with ethane at 3.5 MPa and with the absence of any initial gas phase. These results are very similar and show gas - liquid - liquid behaviour in the temperature range between 648 K to 698 K.

4.3.2 Heavy Oils

Characterisation of the heavier oil systems proved to be challenging due to the complexity of the systems. The components were therefore divided into the following groups : 2 fused-rings (e.g naphthalene), 3 fused-rings (e.g anthracene) and 4 and greater fused rings (e.g pyrene). Analysis of greater than 4 fused ringed material was not possible using gc - ms. The sample composition retrieved from each port is presented in the form of a bar graph.

Figure 4.10 and Tables 4.6 to 4.8 show the results from an investigation of 30%, 50% and 70% wt. Venezuela vacuum bottoms (blend 24) in anthracene oil with 5 MPa hydrogen. At temperatures lower than 623 K phase splitting did not occur in any of the systems investigated and an example of this is shown 50% wt. system. In this system the amount of 2,3 and 4 fused ringed systems samples retrieved from ports 2 and 3 are the same. Due to experimental difficulty samples from port 1 were not obtained in the 50% wt. system and excessive coking in the 70% wt. system at 673 K prevented samples from port 3. At temperatures above 648 K phase splitting occurs in all the mixtures investigated. In most cases where phase splitting has arisen port 3 shows a greater amount of 4 fused ring compared to port 1 and 2. Investigations with 30, 50 and 70 % wt. athabasca bitumen in anthracene oil with 5 MPa hydrogen show very similar results. Phase splitting occurs at temperatures greater than 648 K and higher concentrations of 4 fused ring material in the lower port is also shown. With both heavy oil systems sample compositions are very similar except with the 70 wt. % heavy oil in anthracene oil. The Athabasca bitumen demonstrated greater problems with polymerization reactions and subsequently greater concentrations of 2 fused ringed material in ports 1 and port 2. Clearly phase splitting phenomena is not restricted to model solvent systems and is also encountered in more complex solvent systems.

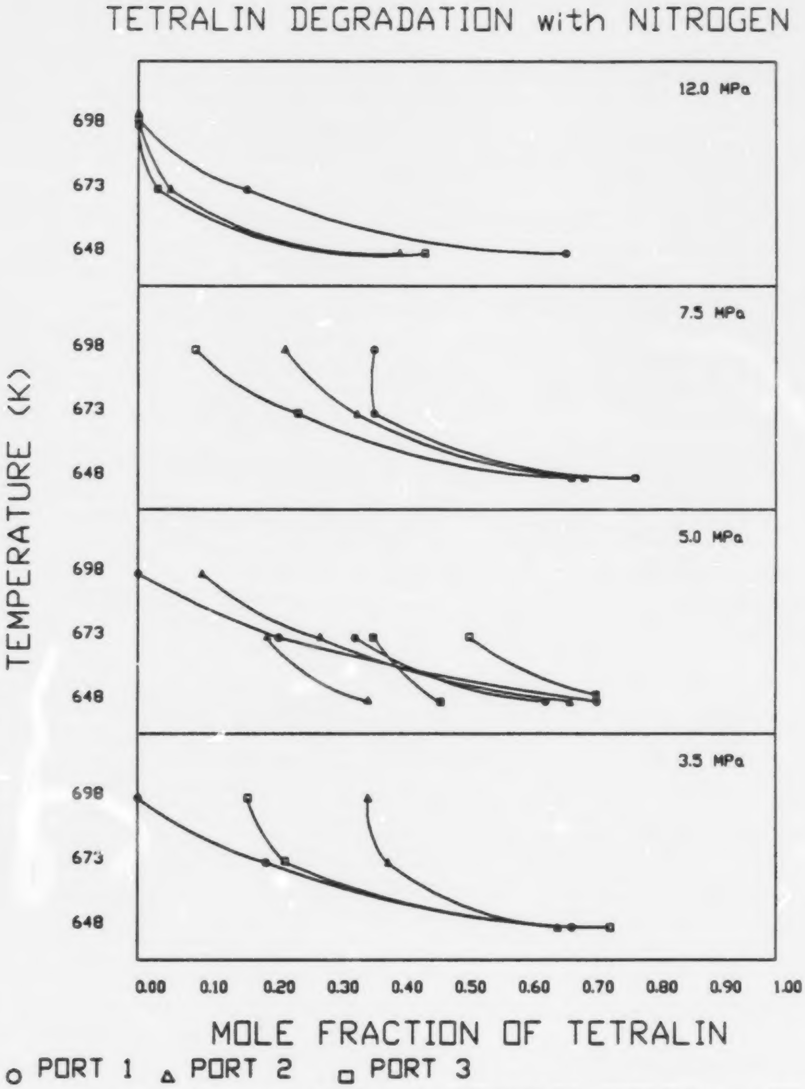

Open symbols are 18% mole PYRENE and 82% mole TETRALIN

Solid symbols are 30.4% mole PYRENE and 69.6% mole TETRALIN

Figure 4.2

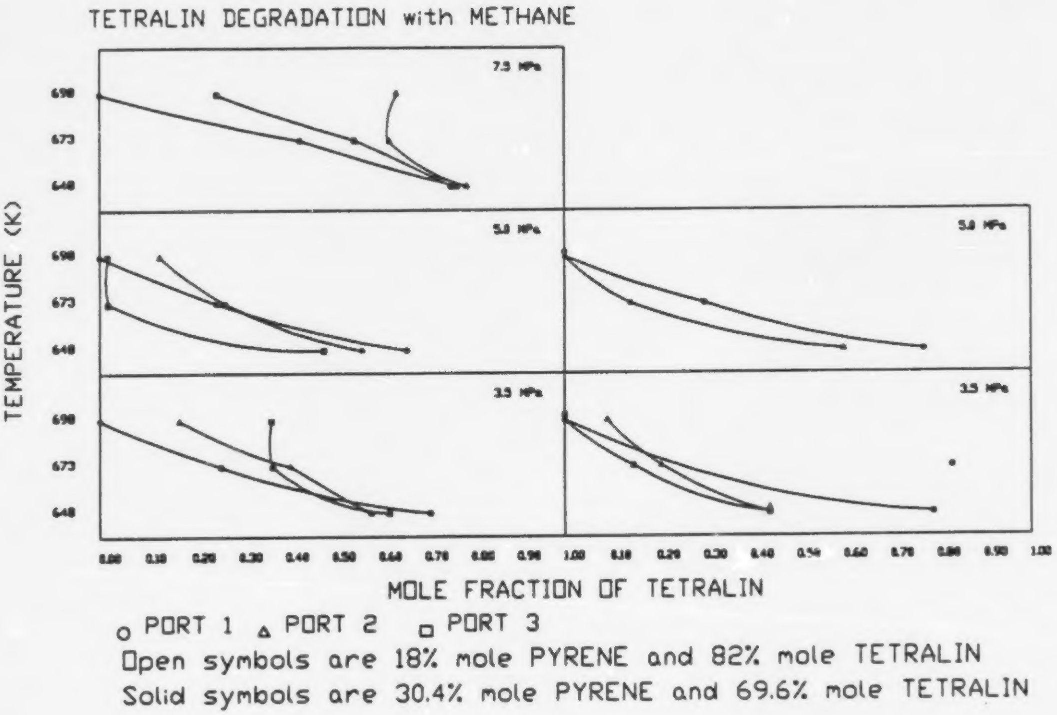
TETRALIN DEGRADATION with METHANE
7.5 MPa
5.0 MPa
5.0 MPa
3.5 MPa
3.5 MPa
698
673
648
TEMPERATURE (K)
0.00 0.10 0.20 0.30 0.40 0.50 0.60 0.70 0.80 0.90 1.00 0.10 0.20 0.30 0.40 0.50 0.60 0.70 0.80 0.90 1.00
MOLE FRACTION OF TETRALIN
○ PORT 1 △ PORT 2 □ PORT 3
Open symbols are 18% mole PYRENE and 82% mole TETRALIN
Solid symbols are 30.4% mole PYRENE and 69.6% mole TETRALIN

Figure 4.3

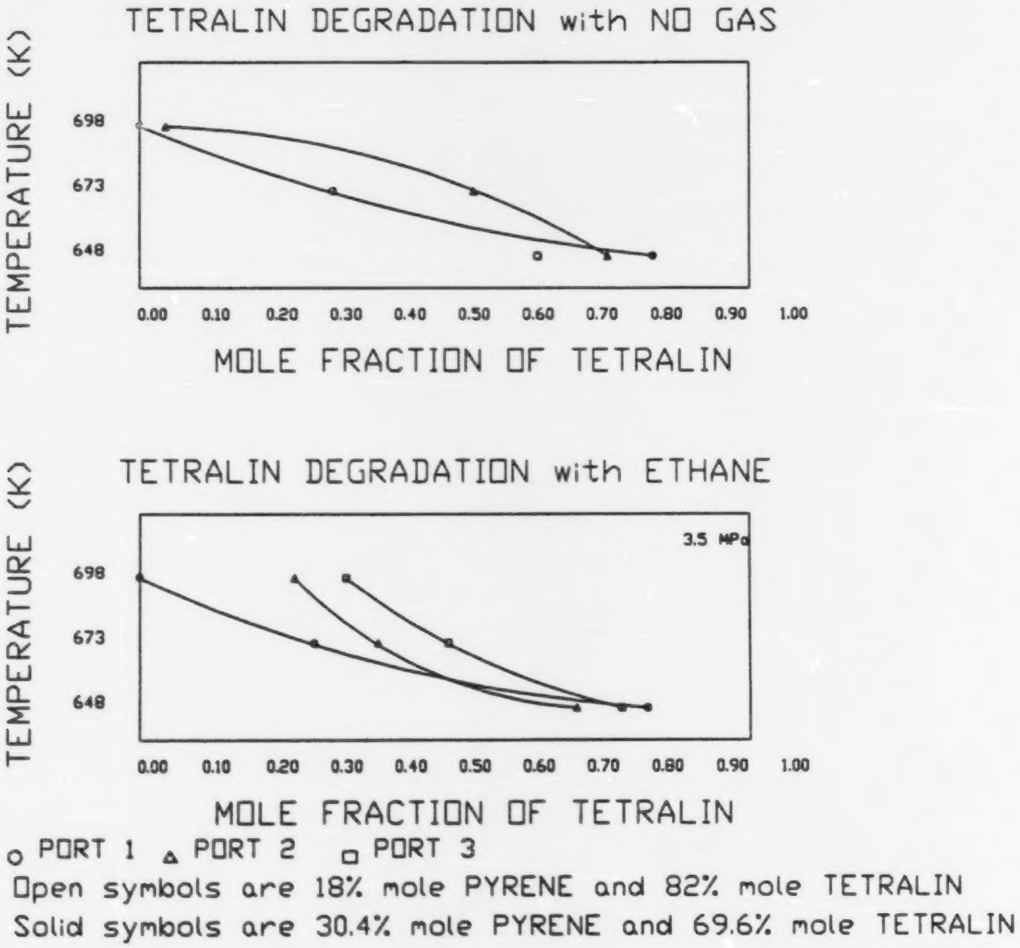

Open symbols are 18% mole PYRENE and 82% mole TETRALIN

Solid symbols are 30.4% mole PYRENE and 69.6% mole TETRALIN

Figure 4.4

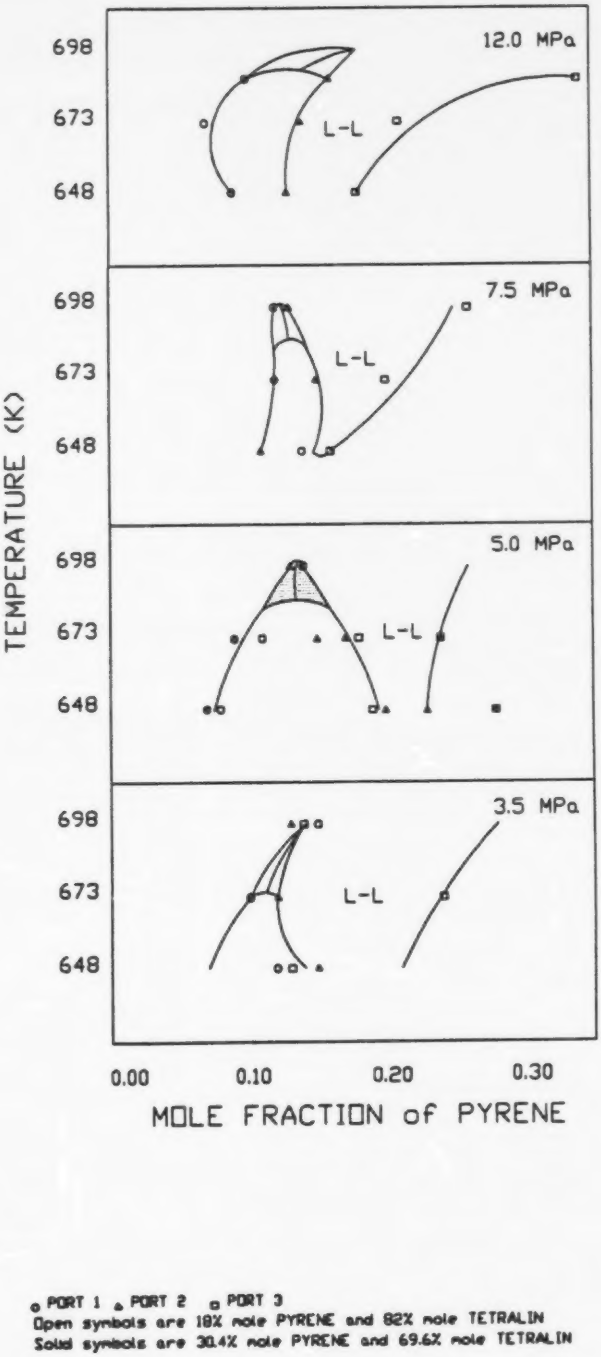

Figure 4.5 : Partial phase diagram (isobars) for pyrene - tetralin with nitrogen.

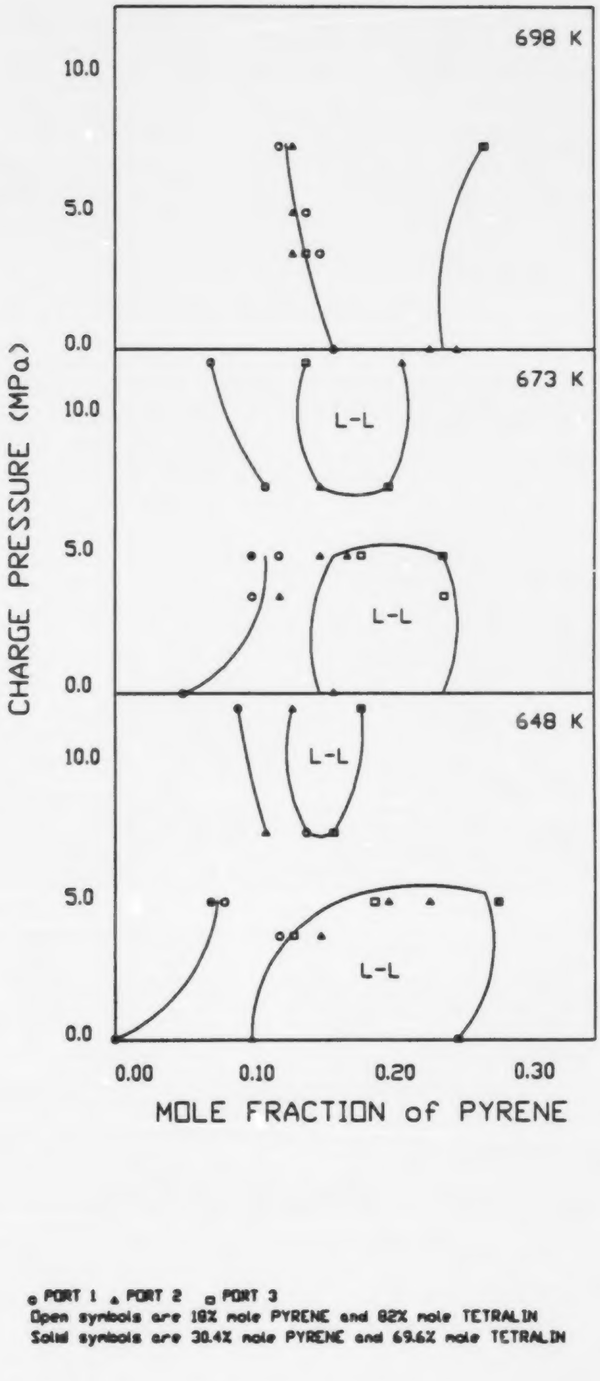

Figure 4.6 : Partial phase diagram (isotherms) for pyrene - tetralin with nitrogen.

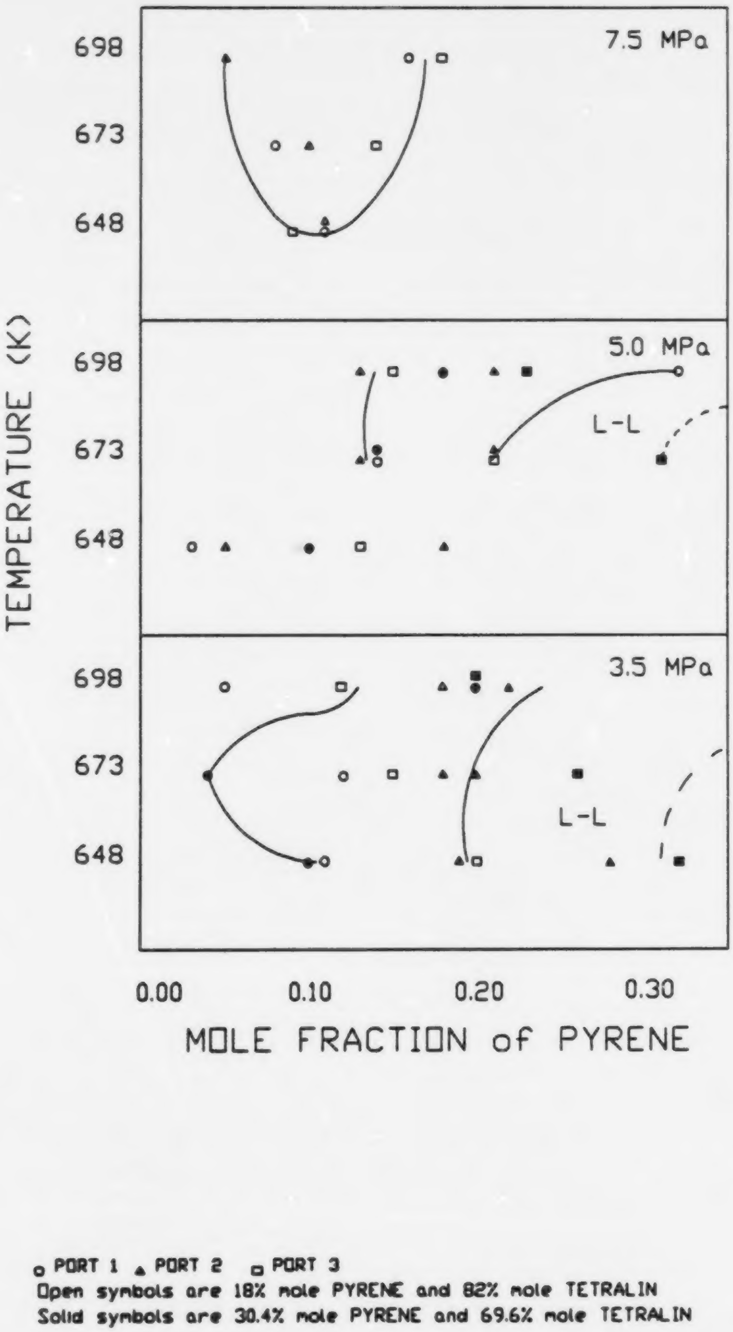

Figure 4.7 : Partial phase diagram (isobars) for pyrene - tetralin system with methane.

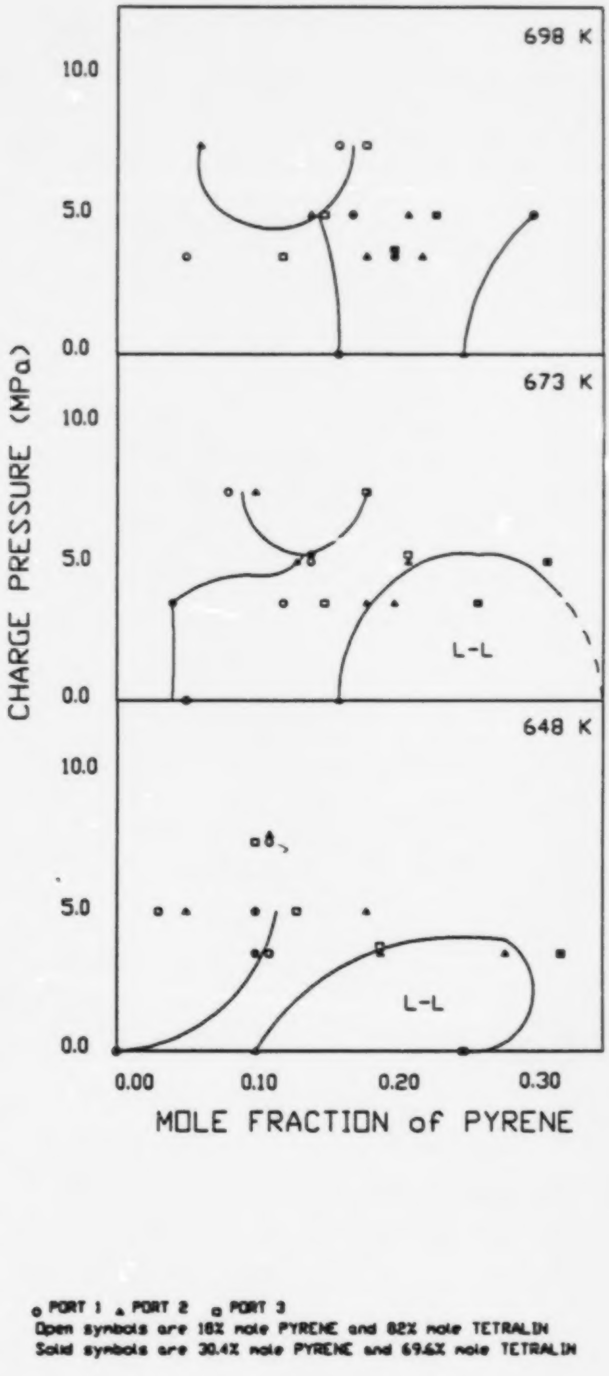

Figure 4.8 : Partial phase diagram (isotherms) for pyrene - tetralin with methane.

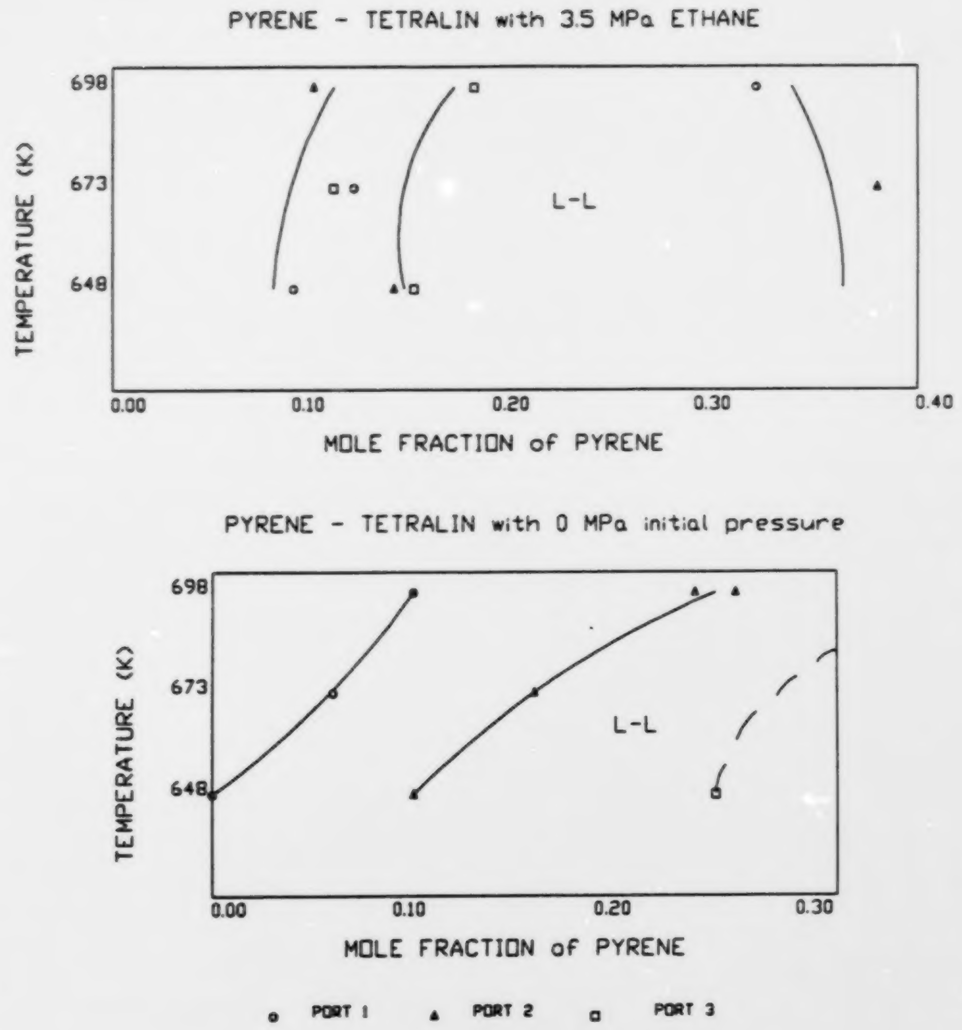

PYRENE - TETRALIN with 3.5 MPa ETHANE

PYRENE - TETRALIN with 0 MPa initial pressure

Figure 4.9 : Partial phase diagram (isobar) for pyrene - tetralin with a) 3.5 MPa ethane and b) no gas.

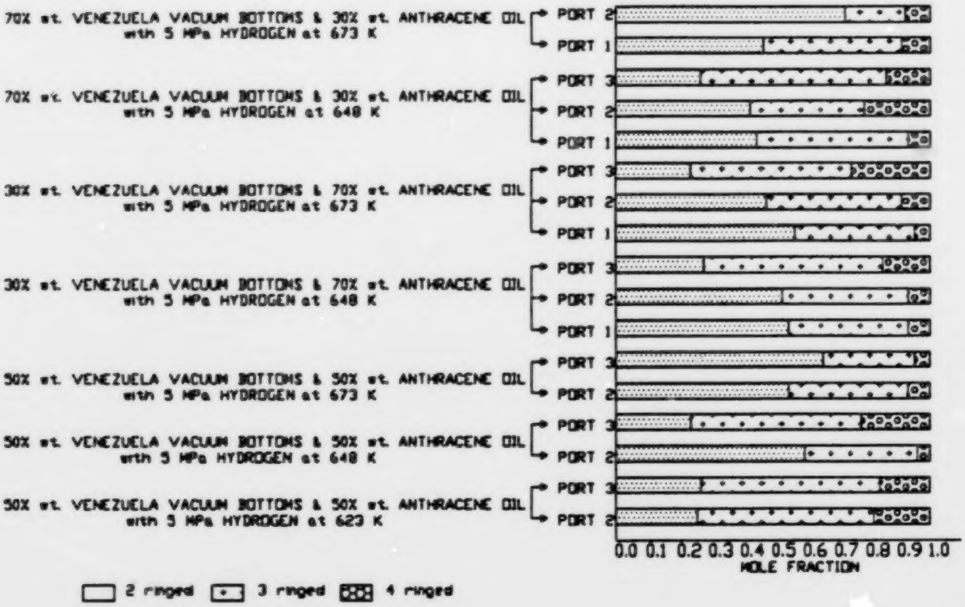

Figure 4.10 : Compositions (in terms of 2, 3 and 4 or more fused ringed material) retrieved from ports 1,2 and 3 of the reactor for Venezuela Vacuum Bottoms (blend 24) and Anthracene Oil with Hydrogen.

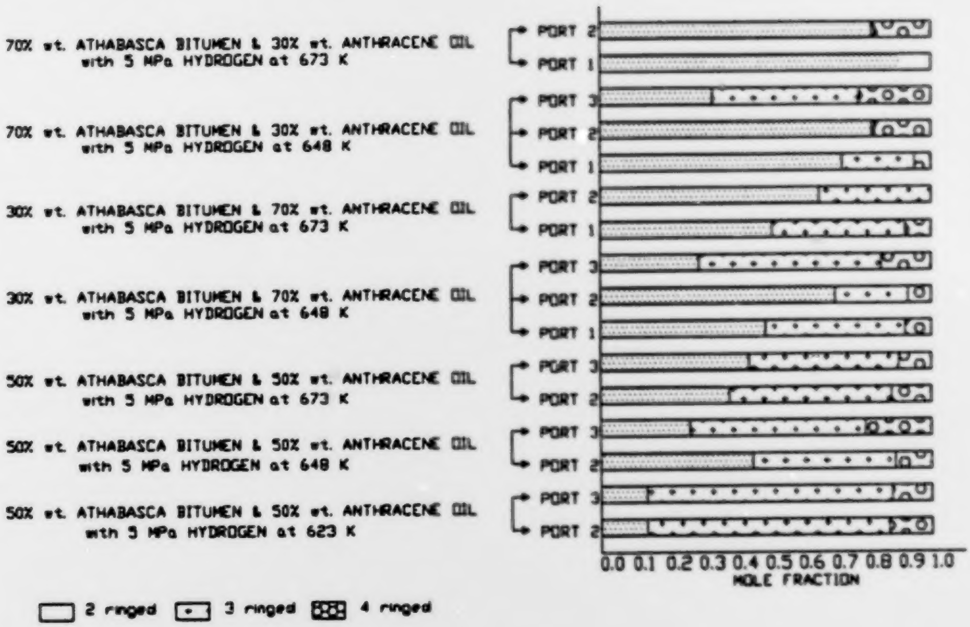

Figure 4.11 : Compositions (in terms of 2, 3 and 4 or more fused ringed material) retrieved from ports 1, 2 and 3 of the reactor for Athabasca Bitumen and Anthracene oil with Hydrogen.

Table 4.1 : Systems that did not exhibit phase splitting. All systems were charged with 5 MPa hydrogen (cold)

SYSTEM	WEIGHT %	MOLE %	TEMPERATURE (K)
1	60 % Decalin 40 % Naphthalene	58 % Decalin 42 % Naphthalene	< 673
2	63 % Decalin 37 % Naphthalene	61 % Decalin 39 % Naphthalene	< 698
3	69 % Decalin 28 % Naphthalene 3 % Pyrene	68 % Decalin 30 % Naphthalene 2 % Pyrene	< 698
4	25 % Decalin 75 % Indene	22 % Decalin 78 % Indene	< 698
5	50 % Decalin 50 % Indene	46 % Decalin 54 % Indene	< 698
6	65 % Decalin 35 % Indene	61 % Decalin 39 % Indene	< 698
7	25 % Indene 25 % Decalin 50 % Anthracene	80 % 2-Ringed 16 % 3-Ringed 4 % 4-Ringed	< 698

Table 4.2 a.

18 mole % PYRENE - 82 mole % TETRALIN with 7.5 MPa NITROGEN (cold) at 623 K

PRESSURE (MPa) = 16 MPa	MOLE FRACTION		
COMPOUND	PORT 1	PORT 2	PORT 3
INDENE or BENZENE derivative(C_9H_8)	0.00	0.00	0.00
INDENE or BENZENE derivative($C_{10}H_{12}$)	0.00	0.00	0.00
TETRALIN ($C_{10}H_{12}$)	0.65	0.83	0.82
NAPHTHALENE ($C_{10}H_8$)	0.29	0.00	0.00
DIHYDROPYRENE ($C_{16}H_{12}$)	0.00	0.00	0.00
PYRENE ($C_{16}H_{10}$)	0.06	0.17	0.18

Figure 4.2 b.

18 mole % PYRENE - 82 mole % TETRALIN with 7.5 MPa NITROGEN (cold) at 648 K

PRESSURE (MPa) = 18.5 MPa	MOLE FRACTION		
COMPOUND	PORT 1	PORT 2	PORT 3
INDENE or BENZENE derivative(C_9H_8)	0.00	0.00	0.00
INDENE or BENZENE derivative($C_{10}H_{12}$)	0.00	0.13	0.11
TETRALIN ($C_{10}H_{12}$)	0.78	0.70	0.68
NAPHTHALENE ($C_{10}H_8$)	0.08	0.06	0.05
DIHYDROPYRENE ($C_{16}H_{12}$)	0.00	0.00	0.00
PYRENE ($C_{16}H_{10}$)	0.14	0.11	0.16

Table 4.2 c.

18 mole % PYRENE - 82 mole % TETRALIN with 7.5 MPa NITROGEN (cold) at 673 K

PRESSURE (MPa) = 20.5 MPa	MOLE FRACTION		
COMPOUND	PORT 1	PORT 2	PORT 3
INDENE or BENZENE derivative (C_9H_{10})	0.03	0.03	0.03
INDENE or BENZENE derivative ($C_{10}H_{12}$)	0.21	0.27	0.26
TETRALIN ($C_{10}H_{12}$)	0.37	0.34	0.25
NAPHTHALENE ($C_{10}H_8$)	0.28	0.21	0.24
DIHYDROPYRENE ($C_{16}H_{12}$)	0.00	0.00	0.01
PYRENE ($C_{16}H_{10}$)	0.11	0.15	0.20

Table 4.2 d.

18 mole % PYRENE - 82 mole % TETRALIN with 7.5 MPa NITROGEN (cold) at 698 K

PRESSURE (MPa) = 22.5 MPa	MOLE FRACTION		
COMPOUND	PORT 1	PORT 2	PORT 3
INDENE or BENZENE derivative (C_9H_{10})	0.03	0.06	0.05
INDENE or BENZENE derivative ($C_{10}H_{12}$)	0.22	0.24	0.03
TETRALIN ($C_{10}H_{12}$)	0.37	0.23	0.09
NAPHTHALENE ($C_{10}H_8$)	0.26	0.34	0.56
DIHYDROPYRENE ($C_{16}H_{12}$)	0.00	0.00	0.00
PYRENE ($C_{16}H_{10}$)	0.12	0.13	0.26

Table 4.3 : PYRENE - TETRALIN with NITROGEN

SYSTEM	PRESSURE (MPa)	TEMPERATURE (K)	MOLE FRACTION OF PYRENE		
			PORT 1	PORT 2	PORT 3
18 mole % PYRENE and 82 mole % TETRALIN	3.5	648	0.12	0.15	0.13
		673	0.10	0.12	0.24
		698	0.15	0.13	0.14
	5.0	648	0.08	0.23	0.19
		673	0.11	0.17	0.18
		698	0.14	0.13	***
	7.5	648	0.14	0.11	0.16
		673	0.11	0.15	0.22
		698	0.12	0.13	0.27
	12.0	648	0.09	0.13	0.19
		673	0.07	0.21	0.14
		688	0.10	0.16	0.34
30.4 mole % PYRENE and 69.6 mole % TETRALIN	5.0	648	0.07	0.20	0.28
		673	0.09	0.15	0.24
		698	N/A	N/A	N/A

*** - Sample was not obtained due to coking

N/A - Sample not obatined due to experimental difficulty

Table 4.4 : PYRENE - TETRALIN with METHANE

SYSTEM	PRESSURE (MPa)	TEMPERATURE (K)	MOLE FRACTION OF PYRENE		
			PORT 1	PORT 2	PORT 3
18 mole % PYRENE and 82 mole % TETRALIN	3.5	648	0.11	0.19	0.19
		673	0.12	0.18	0.15
		698	0.05	0.18	0.12
	5.0	648	0.03	0.05	0.13
		673	0.14	0.13	0.21
		698	0.30	0.13	0.15
	7.5	648	0.11	0.11	0.09
		673	0.08	0.10	0.14
		698	0.16	0.05	0.18
30.4 mole % PYRENE and 69.6 mole % TETRALIN	3.5	648	0.10	0.28	0.32
		673	0.04	0.20	0.26
		698	0.20	0.22	0.20
	5.0	648	0.10	0.18	N/A
		673	0.14	0.21	0.31
		698	0.17	0.17	0.23

*** - Sample was not obtained due to coking

N/A - Sample not obatined due to experimental difficulty

Table 4.5 : PYRENE - TETRALIN with ETHANE

SYSTEM	PRESSURE (MPa)	TEMPERATURE (K)	MOLE FRACTION OF PYRENE		
			PORT 1	PORT 2	PORT 3
18 mole % PYRENE and 82 mole % TETRALIN	3.5	648	0.09	0.14	0.15
		673	0.12	0.36	0.12
		698	0.32	0.10	0.18

*** - Sample was not obtained due to coking

N/A - Sample not obatined due to experimental difficulty

Table 4.6 : PYRENE - TETRALIN with NO GAS

SYSTEM	PRESSURE (MPa)	TEMPERATURE (K)	MOLE FRACTION OF PYRENE		
			PORT 1	PORT 2	PORT 3
18 mole % PYRENE and 82 mole % TETRALIN	NO GAS	648	0.00	0.10	0.25
		673	0.05	0.16	***
		698	0.16	0.25	***

*** - Sample was not obtained due to coking

N/A - Sample not obatined due to experimental difficulty

Table 4.7 : 50 wt. % Venezuela Vaacuum Bottoms (blend 24) and 50 wt. % Anthracene oil with 5 MPa Hydrogen (cold)

		MOLE FRACTION		
TEMPERATURE (K)	COMPOUND	PORT 1	PORT 2	PORT 3
623	2 RINGED	N/A	0.26	0.27
	3 RINGED	N/A	0.56	0.57
	4 RINGED	N/A	0.18	0.16
648	2 RINGED	N/A	0.60	0.24
	3 RINGED	N/A	0.36	0.54
	4 RINGED	N/A	0.04	0.22
673	2 RINGED	N/A	0.55	0.66
	3 RINGED	N/A	0.38	0.29
	4 RINGED	N/A	0.07	0.05

N/A - Sample not obtained due to experimental difficulty

Table 4.8 : 30 wt. % Venezuela Vacuum Bottom (blend 24) and 70 wt. % Anthracene oil with 5 MPa Hydrogen (cold)

		MOLE FRACTION		
TEMPERATURE (K)	COMPOUND	PORT 1	PORT 2	PORT 3
648	2 RINGED	0.55	0.53	0.28
	3 RINGED	0.38	0.40	0.57
	4 RINGED	0.07	0.07	0.15
673	2 RINGED	0.57	0.48	0.24
	3 RINGED	0.38	0.43	0.52
	4 RINGED	0.05	0.09	0.25

Table 4.9 : 70 wt. % Venezuela Vacuum Bottoms (blend 24) and 30 wt. % Anthracene oil with 5 MPa Hydrogen (cold)

		MOLE FRACTION		
TEMPERATURE (K)	COMPOUND	PORT 1	PORT 2	PORT 3
648	2 RINGED	0.45	0.43	0.27
	3 RINGED	0.47	0.36	0.59
	4 RINGED	0.08	0.21	0.14
673	2 RINGED	0.47	0.73	***
	3 RINGED	0.44	0.19	***
	4 RINGED	0.09	0.08	***

Table 4.10 : 50 wt. % Athabasca Bitumen and 50 wt. % Anthracene oil with 5 MPa Hydrogen (cold)

		MOLE FRACTION		
TEMPERATURE (K)	COMPOUND	PORT 1	PORT 2	PORT 3
623	2 RINGED	N/A	0.14	0.13
	3 RINGED	N/A	0.73	0.75
	4 RINGED	N/A	0.13	0.12
648	2 RINGED	N/A	0.41	0.27
	3 RINGED	N/A	0.48	0.53
	4 RINGED	N/A	0.11	0.20
673	2 RINGED	N/A	0.39	0.45
	3 RINGED	N/A	0.49	0.45
	4 RINGED	N/A	0.12	0.10

N/A - Sample not obtained due to experimental difficulty

Table 4.11 : 30 wt. % Athabasca Bitumen and 70 wt. % Anthracene oil with 5 MPa Hydrogen (cold)

		MOLE FRACTION		
TEMPERATURE (K)	COMPOUND	PORT 1	PORT 2	PORT 3
648	2 RINGED	0.50	0.71	0.30
	3 RINGED	0.42	0.22	0.55
	4 RINGED	0.08	0.07	0.15
673	2 RINGED	0.52	0.66	***
	3 RINGED	0.41	0.34	***
	4 RINGED	0.07	0.00	***

Table 4.12 : 70 wt. % Athabasca Bitumen and 30 wt. % Anthracene oil with 5 MPa Hydrogen (cold)

		MOLE FRACTION		
TEMPERATURE (K)	COMPOUND	PORT 1	PORT 2	PORT 3
648	2 RINGED	0.73	0.82	0.34
	3 RINGED	0.22	0.01	0.45
	4 RINGED	0.05	0.17	0.21
673	2 RINGED	1.00	0.82	***
	3 RINGED	0.00	0.01	***
	4 RINGED	0.00	0.16	***

Table 4.13 a : 25 wt. % Indene - 25 wt. % Decalin - 50 wt. % Anthracene Oil with 5 MPa Hydrogen

TEMPERATURE (K) = 648 K		MOLE FRACTION	
COMPOUND	PORT 1	PORT 2	PORT 3
INDENE or BENZENE derivative ($C_9 H_{10}$)	0.641	0.510	0.533
DECALIN (cis & trans) ($C_{10} H_8$)	0.186	0.166	0.171
INDENE or BENZENE derivative ($C_{10} H_{12}$)	0.000	0.013	0.016
SPIRO (4,5) DECANE ($C_{10} H_8$)	0.030	0.030	0.035
TETRALIN ($C_{10} H_{12}$)	0.000	0.010	0.012
NAPHTHALENE ($C_{10} H_8$)	0.073	0.084	0.119
NAPHTHALENE derivative ($C_{11} H_{10}$)	0.011	0.012	0.018
NAPHTHALENE derivative ($C_{12} H_{12}$)	0.000	0.000	0.000
ACENAPTHENE ($C_{12} H_{10}$)	0.017	0.025	0.028
DIBENZOFURAN ($C_{12} H_8 O$)	0.009	0.099	0.013
9-H FLUORENE ($C_{13} H_{10}$)	0.011	0.022	0.015
DIBENZOFURAN derivative ($C_{13} H_{10} O$)	0.000	0.002	0.002
ANTHRACENE ($C_{14} H_{10}$)	0.021	0.015	0.031
PYRENE or FLUORANTHENE ($C_{16} H_{10}$)	0.000	0.011	0.008
2 RINGED	0.941	0.825	0.903
3 RINGED	0.058	0.163	0.089
4 RINGED	0.000	0.011	0.008

Table 4.13 b: 25 wt. % Indene - 25 wt. % Decalin - 50 wt. % Anthracene oil with 5 MPa Hydrogen

TEMPERATURE (K) = 673 K		MOLE FRACTION	
COMPOUND	PORT 1	PORT 2	PORT 3
INDENE or BENZENE derivative (C_9H_{10})	0.542	0.543	0.269
DECALIN (cis & trans) ($C_{10}H_{18}$)	0.039	0.116	0.031
INDENE or BENZENE derivative ($C_{10}H_{12}$)	0.023	0.013	0.000
SPIRO (4,5) DECANE ($C_{10}H_{18}$)	0.000	0.015	0.000
TETRALIN ($C_{10}H_{12}$)	0.010	0.000	0.000
NAPHTHALENE ($C_{10}H_8$)	0.228	0.171	0.450
NAPHTHALENE derivative ($C_{11}H_{10}$)	0.032	0.021	0.046
NAPHTHALENE derivative ($C_{12}H_{12}$)	0.022	0.000	0.000
ACENAPTHENE ($C_{12}H_{10}$)	0.016	0.023	0.000
DIBENZOFURAN ($C_{12}H_8O$)	0.019	0.023	0.039
9-H FLUORENE ($C_{13}H_{10}$)	0.030	0.030	0.053
DIBENZOFURAN derivative ($C_{13}H_{10}O$)	0.000	0.000	0.000
ANTHRACENE ($C_{14}H_{10}$)	0.024	0.028	0.061
PYRENE or FLUORANTHENE ($C_{16}H_{10}$)	0.015	0.016	0.051
2 RINGED	0.896	0.879	0.796
3 RINGED	0.089	0.104	0.153
4 RINGED	0.015	0.016	0.051

Table 4.13 c : 25 wt. % Indene - 25 wt. % Decalin - 50 wt. % Anthracene oil with 5 MPa Hydrogen

TEMPERATURE (K) = 698 K	MOLE FRACTION		
COMPOUND	PORT 1	PORT 2	PORT 3
INDENE or BENZENE derivative (C_9 H_{10})	0.269	0.224	0.205
DECALIN (cis & trans) (C_{10} H_8)	0.000	0.000	0.000
INDENE or BENZENE derivative (C_{10} H_{12})	0.000	0.000	0.000
SPIRO (4,5) DECANE (C_{10} H_8)	0.000	0.000	0.000
TETRALIN (C_{10} H_{12})	0.000	0.000	0.000
NAPHTHALENE (C_{10} H_8)	0.575	0.584	0.608
NAPHTHALENE derivative (C_{11} H_{10})	0.040	0.050	0.034
NAPHTHALENE derivative (C_{12} H_{12})	0.000	0.000	0.000
ACENAPTHENE (C_{12} H_{10})	0.000	0.000	0.000
DIBENZOFURAN (C_{12} H_8 O)	0.000	0.032	0.000
9-H FLUORENE (C_{13} H_{10})	0.036	0.033	0.053
DIBENZOFURAN derivative (C_{13} H_{10} O)	0.000	0.000	0.000
ANTHRACENE (C_{14} H_{10})	0.080	0.035	0.058
PYRENE or FLUORANTHENE (C_{16} H_{10})	0.000	0.042	0.018
2 RINGED	0.884	0.858	0.847
3 RINGED	0.116	0.100	0.111
4 RINGED	0.000	0.042	0.041

5. DISCUSSION :

This project has been purely experimental with the objective of answering the following questions: Can the phase behaviour of complex hydrocarbon systems i.e. those associated with coal liquefaction, co-processing and heavy crude oil upgrading be predicted and how can this be connected to the reported synergy? What are the implications for maximizing yields by optimizing solvent systems and defining operating conditions during processing.

5.1 : Gas phase composition

The results for the pyrene - tetralin - hydrogen system previously investigated by Derbyshire et al., (1982) and Shaw et al., (1988) led to the following questions : Is this system an anomalie in terms of its phase behaviour and how does the initial gas phase affect the phase behaviour? It was initially thought that the critical properties of the gas phase affected the phase behaviour of the system. Based on a simple group contribution method for estimating the critical properties of a mixture (Li, 1971, The Properties of Gases and Liquids, 1987) one would expect that with a gas of higher critical temperature the onset of phase splitting would occur at a higher temperature. Hence phase splitting would occur at higher temperatures in the order of hydrogen, nitrogen, methane and ethane. This trend was not observed. The results show that in all cases phase splitting occurs at temperatures in excess of 623 K. However phase behaviour is clearly dependent on the initial gas phase since systems with methane and nitrogen show very different phase behaviour. All gases investigated are often typical constituents in processing and the results provide examples of the most extreme cases.

The effect of gas phase solubility on phase splitting must also be addressed. The solubility of gases in hydrocarbon liquid is a function of many variables and exhibit complex relationships with temperature, pressure and concentration. A survey of the literature (Lin et al., 1981, Sebastian et al., 1981, and Svrcek et al., 1982 and Shaw et al., 1987) shows that in the temperature range of 303 K - 573 K the solubility of hydrogen, nitrogen, methane and ethane in heptane and benzene demonstrate the following trend : ethane > methane > nitrogen > hydrogen. A similar trend was reported for methane and nitrogen in Athabasca bitumen. These trends are based on absolute values and do not reflect the complex dependency of solubility on temperature and composition. Hydrogen and nitrogen solubilities increase as temperature increases while methane solubility decreases or stays constant as temperature increases and ethane solubility decreases as temperature increases. Comparing the results obtained in the investigation of these gases it appears that the greater the solubility of the gas in the liquid the wider the zone of phase splitting. Pyrene - tetralin systems exhibited liquid - liquid equilibrium between approximately 15 - 36 mole % pyrene with 3.5 MPa ethane, 20 - 35 mole % pyrene with 3.5 MPa methane and 15 - 25 mole % pyrene with 3.5 MPa nitrogen. With ethane and methane (at pressures lower than 7.5 MPa) gas - liquid - liquid equilibrium existed for temperature up to 698 K whereas with the nitrogen gas - liquid - liquid equilibrium led to fluid - fluid equilibria at 698 K at all pressures investigated. This may suggest that the less soluble the gas is in the liquid phase the greater the tendency for the system to approach supercritical phase behaviour. Carbon monoxide and dioxide are two gases which are also present in substantial amounts during coal liquefaction. Carbon dioxide solubility declines rapidly as temperature increases. One would expect that in a carbon dioxide atmosphere the system would tend to supercritical behaviour at lower temperatures when compared to methane or ethane.

5.2 : Phase Splitting Systems

Phase splitting phenomena was only exhibited with mixtures where the amount of 4 or more fused ringed material (for example pyrene) was in excess of 10 mole %. depending on the temperature, pressure and initial gas phase. Phase splitting was not encountered in any of the model systems that consisted of mainly 2 fused ringed material (Table 4.1). In the indene - decalin - anthracene system which consisted of 80 mole % of 2 or less fused ringed, 16 mole % of 3 fused ringed and 4 mole % of 4 or more fused ringed material did not phase split. Heavy oil systems investigated exhibited phase splitting that were consistent with the results obtained from the model systems. These systems contained a high concentration of 4 or more fused ringed material. It is well known that liquid - liquid immiscibility arises due to the difference in chemical types and may explain the phase splitting phenomena encountered with 4 or more fused ringed material.

5.3 : Synergy and Phase Splitting

Phase splitting may account for some aspects of the synergistic effect that has been reported. In a system where phase splitting has occurred the change in hydrogen solubility, hydrogen donor ability and dissolution properties of each phase may account for the swings in conversions that have been observed.

Synergistic behaviour reported by Chiba et al., (1985) cannot be explained by phase splitting of the solvent system. Investigation of the indene - decalin system did not show liquid -liquid immiscibility. It is suggested that complex phase behaviour between the coal derived liquids produced during processing and the solvent system may explain the synergistic behaviour.

Work done by Rincon et al., (1986 and 1987) is consistent with phase splitting. It has been shown that phase splitting arises in petroleum heavy oil (PHO) - anthracene oil solvent (AO) systems. Mixtures of 30, 50, 70 wt. % of PHO in AO exhibited phase splitting at temperatures greater than 648 K. In Figure 2.3 at a residence time of approximately 30 minutes (similar to experimental conditions employed in this project) and at 633 K coal conversions decrease as the mass fraction of AO in the system increases. This type of behaviour is consistent with type "A" behaviour (see Figure 2.7). Anthracene oil has good coal liquid dissolution properties but poor hydrogen donor abilities whereas petroleum heavy oil has more donatable hydrogen but is a poor coal liquid solvent. In a single solvent phase system as the mass fraction of AO increases a decrease in coal conversion is expected. At 633 K phase splitting was not observed in the heavy oil systems. As the temperature increased to 673 K a synergistic effect was observed and this is consistent with the onset of liquid immiscibility and the existence of two liquid phases. As the solvent switches from a AO rich continuous phase to a PHO rich continuous phase a decrease in coal conversion is expected. As the temperatures increases the AO - PHO solvent system may now exist in subcritical and critical regions as shown with the model solvent systems where the transition from liquid -

liquid equilibria to supercritical fluid occurs.

In Figure 2.4 b. at 673 K an overall decrease in coal conversion is observed and this is consistent with an increase in polymerization reactions leading to "coke" formation. At higher temperatures where thermal cleavage of the coal particles is greater an increase in a coal liquid derived solvent will increase coal conversions and may explain the increase in conversion with the addition of AO at 673 K. Figure 2.4 a. shows the effect of pressure on coal conversions and these results are also consistent with phase splitting. At higher pressures the synergistic effect is no longer observed and a more additive behaviour dominates. By operating at higher pressures the zone of phase splitting is avoided. Operating in a single critical fluid phase is optimal since supercritical solvent exhibit increased diffusivity and solubility powers (Penninger et al., 1983).

The effect of coal concentration on coprocessing experiments investigated by Fouda et al., 1988 showed a decrease in pitch conversion from approximately 70 to 50 wt. % as coal concentrations increased from approximately 30 to 40 wt. %. In the same range coal conversions were relatively constant at 85 wt. % and this corresponded to 25 - 35 wt. % of coal derived species in the mixture. Phase splitting has been shown in 30 wt. % mixtures of coal like liquids in heavy oil and may explain the decrease in pitch conversions. The concentration of larger molecules in a dispersed phase subjected to poor liquid - liquid mass transfer rates and lack of available hydrogen can promote the formation of "coke" and a subsequent decreases in conversion. At lower coal concentration, pitch conversions were relatively constant and reflected the existence of a single liquid phase.

The work done by Curtis et al., (1987) also demonstrates the effect of phase splitting of the solvent system on coal conversion in coprocessing experiments. Coal conversions (at 698 K) showed a decrease from 60 - 45 wt.% as the concentration of V1067 (a coal derived solvent) increased from 0 - 35 wt.% in a Maya TLR (a petroleum resid). This corresponds to approximately 20 - 60 wt. % of coal derived species in the mixture. Phase splitting has been shown to occur in mixtures of coal liquids in petroleum heavy oils in the range between 30 - 70 wt. %. This decrease in coal conversion reflects the existence of two phases, a heavier coal oil dispersed phase in a continuous petroleum rich phase. As more coal oil is added the dispersed phase is extended where poor dissolution of the coal in the petroleum rich continuous phase and possible "coking" in the dispersed phase lead to a decrease in coal conversion. Further addition of coal oil may cause the phases to switch and a continuous phase rich in coal oil allows for enhanced coal dissolution and subsequent increases in coal conversions. This switch occurs at approximately 60 wt.% of coal derived liquids and shows an increase in coal conversions to 75 wt.%.

5.4 Solvent Design and Operating Conditions

Phase splitting has been shown to be a significant factor when considering solvent mixtures and operating conditions in coprocessing and coal liquefaction reactions. Solvent mixtures being employed must not exceed solubility limits of coal derived liquids in the systems. Solvent immiscibility arises with 25 - 30 wt. % of coal derived liquids in mixtures whereas at lower concentrations this problem is not encountered. Although at higher concentration of coal liquids phase splitting may still persist the effect on conversion may not be as dramatic since the higher concentration of coal liquids would ensure that the continuous phase would exhibit better coal solvating properties.

The lowering of severity in processing conditions for coal liquefaction and coprocessing while maintaining optimum conversions has been extensively investigated. However the onset of phase splitting must be avoided. By determining the zone of liquid - liquid immiscibility for solvent systems high conversions can be maintained. The results have shown that phase splitting occurs in the temperature range between 648 K - 698 K for the solvent systems investigated. The effect of pressure on phase splitting has not led to any conclusive results and requires further investigation. It is suggested that at higher pressures subcritical and critical behaviour would persist. By avoiding zones of phase splitting and operating in critical and supercritical regions better conversions would be obtained since mass transfer resistances are minimized in a single fluid. Derbyshire et al., (1982) reported a significant increase in coal conversion by the Exxon Donor Solvent process as hydrogen pressure was marginally increased from 10.34 MPa to 13.78 MPa. This may reflect an increase in conversion by avoiding the zone of phase splitting and operating in the supercritical region of the mixture.

6.0 CONCLUSIONS and RECOMMENDATIONS :

1. Model solvent systems of indene - decalin, decalin - naphthalene and indene - decalin - anthracene oil do not exhibit phase splitting in the temperature range between 623 K - 698 K.
2. The pyrene - tetralin solvent system exhibits phase splitting at temperatures in excess of 648 K. Transitions from gas - liquid - liquid to gas - liquid and fluid - fluid equilibria is demonstrated by the pyrene - tetralin system.
3. The gas phase composition affects the phase behaviour of the pyrene - tetralin system. Apparent trends show that the greater the solubility of the gas in the liquid phase the broader the zone of liquid - liquid immiscibility and the wider the temperature range for which for liquid - liquid phase behaviour to exist before leading to supercritical phase behaviour.
4. Phase splitting is only evident with mixtures of 2 and 4 fused ringed compounds.
5. Mixtures of 30, 50 and 70 wt. % of bitumen and heavy oil in anthracene oil exhibit phase splitting at temperatures in excess of 623 K.
6. Phase splitting can account for some aspects of the synergistic effects reported with model and complex solvent systems. The shifts in hydrogen solubility, hydrogen donor ability and coal dissolution properties that occur with liquid - liquid immiscibility had previously been unpredictable.
7. Predictions of optimum solvent design and operating conditions must consider the effect of possible phase splitting. Mixtures with 20 - 30 wt. % of coal derived species in solvent mixtures in the temperature range between 648 K - 698 K must be avoided.

- 698 K must be avoided.

8. The effect of carbon monoxide and dioxide on phase splitting in coal/oil coprocessing and coal liquefaction should be investigated.
9. The experimental results reported in this thesis should be modelled theorecitcally.

7. REFERENCES :

Benjamin, B.M., Hagaman, E.W., Raaen, V.F. and Collins, C.J., " Pyrolysis of Tetralin", FUEL, 58, 386 - 390, (1979)

Chiba, K., Tagaya, H., Sato, S. and Ito, K., "Coal Liquefaction Using Indene - Tetralin and Indene - Decalin Mixtures as Solvents", FUEL, 65, 68 -73, (1985)

Curtis, C.W., Tsai, K. and Guin, J.A., "Effects of Solvent Composition on Coprocessing Coal with Petroleum Residua", Fuel Processing Tech., 16, 71 - 87, (1987)

Derbyshire, F.J., Varghese, P. and Whitehurst, D.D., "Synergistic Effects Between Light and Heavy Solvent Components During Coal Liquefaction ", Fuel, 61, 859 - 864, (1982)

Dukhedin - Lalla, L., Yushun, S., Shaw, J.M. and Rahimi, P.M., "Phase Splitting of Complex Hydrocarbon Mixtures", poster presented at the Fifth International Conference on Fluid Properties & Phase Equilibria for Chemical Process Design, Banff, April,1989.

Dukhedin - Lalla, L., Rahimi, P.M.and Shaw, J.M., "Phase Splitting of Complex Hydrocarbon Mixtures", Fluid Phase Equilibria, 53, 415 - 422, (1989)

Dukhedin - Lalla, L., Rahimi, P.M.and Shaw, J.M., "Phase Splitting and Synergy in Coal Oil Coprocessing and Coal Liquefaction", Paper to be presented at the ACS Conference in Washington, August, 1990.

Fouda, S.A., Kelly, J.F. and Rahimi, " The Effects of Coal Concentration on Coprocessing Performance ", ACS Fuel Chem. Symp. Series, 33, 178 - 184,(1988)

Hooper, R.J., Battaerd, A.J. and Evans, D.G., "Thermal Dissociation of Tetralin

Between 300 and 450 °C ", FUEL, 58, 132 - 138, (1979)

Greer, S.C. and Moldover, M.R., "Thermodynamic Anomalies at Critical Points of Fluids" , Ann. Rev. Phys. Chem., 32, 233 - 265, (1981)

Gudzinowicz, B.J., Gudzinowicz, M.J. and Martin, H.F., " Fundamentals of Intergrated GC-MS ", Marcel Decker, New York, (1977)

Gulari, E., Saad, H. and Bae, Y.C., " Effect of Critical Phenomena on Transport Properties in Supercritical Region ", Supercritical Fluids Chemical Engineering Principles and Applications by Squires, T.G and Paulaitis, M.E., ACS, (1987)

Paulaitis, M.E., Lin, H., Sebastian, H.M., Simnick, J.J. and Chao, K.C., " Solubilities of Hydrogen and Methane in Coal liquids ", Ind. Eng. Chem. Process Des. Dev., 20, 253 - 256, 1981

Novak, J.P, Jaroslav, M. and Pick, J., " Liquid - Liquid Equilibria ", Studies in Thermodynamics, Vol 7, Elsevier Science Inc., New York, (1987)

Penninger, J.M.L. and Gray R.D., " Chemical Engineering at Supercritical Fluid Conditions ", Ann Arbor Science, Michigan, (1983)

Penninger, J.M.L. and Slatboom H.W., " Industrial and Laboratory Pyrolyses", (Eds. L.F. Allbright and B.L. Crynes), ACS Symposium Series 32, 444 -449, (1976)

Reid, R., Prausnitz, J. and Poling, B., "The Properties of Gases and Liquids ", 4th ed., McGraw - Hill, (1987)

Rincon, J.E. and Angulo R., " Petroleum heavy oil mixtures as a source of hydrogen in liquefaction of Cerrejon coal ", FUEL, 65, 899 - 902, (1986)

Rincon, J.E. and Angulo R.," Synergism in coal liquefaction using petroleum heavy oil mixtures for the liquefaction of Cerrejon coal ", Proc. 1987 Int. Conf. Coal Sci.", 375 - 378, (1987)

Sebastian, H.M., Lin, H.and Chao, K.C., " Correlation of the Solubility of Methane in hydrocarbon solvents ", Ind. Eng. Chem. Fundam., 20, 346 - 349, (1981)

Shaw, J.M., " A Correlation for Hydrogen solubility in Alicyclic and Aromatic Solvents ", Can. J. Chem. Eng., 65, 293 - 298, (1987)

Shaw, J.M., Gaikwad, R.P. and Stowe, D.A., " Phase Splitting of Pyrene - Tetralin Mixtures under Coal Liquefaction Conditions ", FUEL, 67, 1554 - 1559, (1988)

Shaw, J.M and Peters, E., " A General Model for Coal Dissolution Reactions ", Ind. Eng. Chem. Res., 28, 1795 - 1801, (1989)

Shaw, J.M and Peters, E., " The Role of Initial Reaction Conditions in Direct Coal Liquefaction ", Ing. Eng. Chem. Res., 28, 976 - 982, (1989)

Solubility Data Series, " Solubility of Hydrocarbons ", Vol. 6 Stanley, H.E, "Introduction to Phase Transitions and Critical Phenomena ", Clarendon Press, Oxford, (1971)

Subramaniam, B. and McHugh, M.A., " Reactions in Supercritical Fluids ", Ind. Eng. Chem. Proc. Des. Dev., 25, 1-6, (1986)

Svrcek, W.Y. and Mehrotra, A.K., " Gas solubility, viscosity and density measurements for Athabasca bitumen ", Journal of Canadian Petroleum, July - August, 31-38, (1982)

Wilson, M.A., Foster, N.R., Vaughan, R.P. and Cosstick, R., " Surface changes in coal hydrogenation autoclaves that affect autoclave reactions ", Fuel Processing Technology, 5, 267 - 279, (1982)

8. BIBLIOGRAPHY

dePablo, J.J. and Prausnitz, J.M., " Thermodynamics of Liquid - Liquid Equilibria Including the Critical Region " AIChE Journal, 34, 10, 1595 - 1606, 1988

Choa, K.C.and Greenkorn, R.A., " Thermodynamics of Fluids : An Introduction to Equilibrium Theory ", Chemical Processing and Process Thermodynamics: an international series, (Ed. Lyle F., Albright, R.N. Maddox and J.J. McKetta) Vol. 4., (1975)

Kara, M., Sung, S., Klinzing, G.E. and Chiang, S.H., " Hydrogen mass transfer in liquid hydrocarbons at elevated temperatures and pressures ", FUEL, 62, 1492 - 1500, (1983)

Kyle, B.G., " Chemical and Process Thermodynamics ", Prentice - Hall, New Jersey, (1984)

Modell, M. and Reid, R., " Thermodynamics and Its Applications " 2nd ed., Prentice - Hall, 1983

Paulaitis, M.E, Penninger, J.M.L and Gray, R.D., "Chemical Engineering at Supercritical Fluids Conditions ", Ann Arbor Science, Michigan, (1983)

Perry, R.H., "Perry's Chemical Engineers Handbook ", 6th ed., McGraw - Hill, Toronto, (1984)

Whitehurst, D.D., Mitchell, T.O. and Farasin, M., " Coal Liquefaction : The Chemistry and Technology of Thermal Process ", Academic Press, London, U.K. (1980)

Woodfine, B., Kemp, W. and Stiedman, W., " Donor Solvent Interactions in Direct Coal Liquefaction ", 1987 International Conference on Coal Science.

Appendix A : Sample composition for model solvent systems

Table A1

18 mole % PYRENE & 82 mole % TETRALIN with no gas at 648 K

PRESSURE (MPa) = 2.5 MPa	MOLE FRACTION		
COMPOUND	PORT 1	PORT 2	PORT 3
INDENE or BENZENE derivative (C_9H_{10})	0.00	0.00	0.00
INDENE or BENZENE derivative ($C_{10}H_{12}$)	0.11	0.09	0.06
TETRALIN ($C_{10}H_{12}$)	0.80	0.73	0.61
NAPHTHALENE ($C_{10}H_8$)	0.10	0.08	0.08
DIHYDROPYRENE ($C_{16}H_{12}$)	0.00	0.00	0.00
PYRENE ($C_{16}H_{10}$)	0.00	0.10	0.25

18 mole % PYRENE & 82 mole % TETRALIN with no gas at 673 K

PRESSURE (MPa) = 4.4 MPa	MOLE FRACTION		
COMPOUND	PORT 1	PORT 2	PORT 3
INDENE or BENZENE derivative (C_9H_{10})	0.08	0.00	***
INDENE or BENZENE derivative ($C_{10}H_{12}$)	0.23	0.13	***
TETRALIN ($C_{10}H_{12}$)	0.30	0.52	***
NAPHTHALENE ($C_{10}H_8$)	0.30	0.19	***
DIHYDROPYRENE ($C_{16}H_{12}$)	0.00	0.00	***
PYRENE ($C_{16}H_{10}$)	0.05	0.16	***

18 mole % PYRENE & 82 mole % TETRALIN with no gas at 698 K

PRESSURE (MPa) = 5.5 MPa	MOLE FRACTION		
COMPOUND	PORT 1	PORT 2	PORT 3
INDENE or BENZENE derivative (C_9H_{10})	0.12	0.08	***
INDENE or BENZENE derivative ($C_{10}H_{12}$)	0.00	0.13	***
TETRALIN ($C_{10}H_{12}$)	0.00	0.04	***
NAPHTHALENE ($C_{10}H_8$)	0.73	0.51	***
DIHYDROPYRENE ($C_{16}H_{12}$)	0.00	0.00	***
PYRENE ($C_{16}H_{10}$)	0.16	0.25	***

Table A2

18 mole % PYRENE & 82 mole % TETRALIN with 3.5 MPa ETHANE (cold) at 648 K

PRESSURE (MPa) = 11 MPa	MOLE FRACTION		
COMPOUND	PORT 1	PORT 2	PORT 3
INDENE or BENZENE derivative (C_9H_{10})	0.00	0.00	0.00
INDENE or BENZENE derivative ($C_{10}H_{12}$)	0.06	0.13	0.10
TETRALIN ($C_{10}H_{12}$)	0.79	0.68	0.75
NAPHTHALENE ($C_{10}H_8$)	0.06	0.05	0.00
DIHYDROPYRENE ($C_{16}H_{12}$)	0.00	0.00	0.00
PYRENE ($C_{16}H_{10}$)	0.09	0.14	0.15

18 mole % PYRENE & 82 mole % TETRALIN with 3.5 MPa ETHANE (cold) at 673 K

PRESSURE (MPa) = 4.4 MPa	MOLE FRACTION		
COMPOUND	PORT 1	PORT 2	PORT 3
INDENE or BENZENE derivative (C_9H_{10})	0.06	0.01	0.00
INDENE or BENZENE derivative ($C_{10}H_{12}$)	0.25	0.00	0.23
TETRALIN ($C_{10}H_{12}$)	0.27	0.37	0.48
NAPHTHALENE ($C_{10}H_8$)	0.30	0.26	0.18
DIHYDROPYRENE ($C_{16}H_{12}$)	0.00	0.00	0.00
PYRENE ($C_{16}H_{10}$)	0.12	0.36	0.12

18 mole % PYRENE & 82 mole % TETRALIN with 3.5 MPa ETHANE (cold) at 698 K

PRESSURE (MPa) = 5.5 MPa	MOLE FRACTION		
COMPOUND	PORT 1	PORT 2	PORT 3
INDENE or BENZENE derivative (C_9H_{10})	0.09	0.06	0.05
INDENE or BENZENE derivative ($C_{10}H_{12}$)	0.00	0.09	0.13
TETRALIN ($C_{10}H_{12}$)	0.00	0.24	0.32
NAPHTHALENE ($C_{10}H_8$)	0.59	0.51	0.32
DIHYDROPYRENE ($C_{16}H_{12}$)	0.00	0.00	0.00
PYRENE ($C_{16}H_{10}$)	0.32	0.10	0.18

Table A3

18 mole % PYRENE & 82 mole % TETRALIN with 3.5 MPa NITROGEN (cold) at 648 K

PRESSURE (MPa) = 9.0 MPa	MOLE FRACTION		
COMPOUND	PORT 1	PORT 2	PORT 3
INDENE or BENZENE derivative (C_9H_{10})	0.00	0.00	0.00
INDENE or BENZENE derivative ($C_{10}H_{12}$)	0.08	0.13	0.13
TETRALIN ($C_{10}H_{12}$)	0.68	0.66	0.74
NAPHTHALENE ($C_{10}H_8$)	0.12	0.06	0.00
DIHYDROPYRENE ($C_{16}H_{12}$)	0.00	0.00	0.00
PYRENE ($C_{16}H_{10}$)	0.12	0.15	0.13

18 mole % PYRENE & 82 mole % TETRALIN with 3.5 MPa NITROGEN (cold) at 673 K

PRESSURE (MPa) = 10.0 MPa	MOLE FRACTION		
COMPOUND	PORT 1	PORT 2	PORT 3
INDENE or BENZENE derivative (C_9H_{10})	0.09	0.05	0.05
INDENE or BENZENE derivative ($C_{10}H_{12}$)	0.23	0.23	0.21
TETRALIN ($C_{10}H_{12}$)	0.20	0.39	0.23
NAPHTHALENE ($C_{10}H_8$)	0.37	0.21	0.27
DIHYDROPYRENE ($C_{16}H_{12}$)	0.00	0.00	0.00
PYRENE ($C_{16}H_{10}$)	0.10	0.12	0.24

18 mole % PYRENE & 82 mole % TETRALIN with 3.5 MPa NITROGEN (cold) at 698 K

PRESSURE (MPa) = 10.0 MPa	MOLE FRACTION		
COMPOUND	PORT 1	PORT 2	PORT 3
INDENE or BENZENE derivative (C_9H_{10})	0.09	0.07	0.07
INDENE or BENZENE derivative ($C_{10}H_{12}$)	0.00	0.17	0.18
TETRALIN ($C_{10}H_{12}$)	0.00	0.36	0.17
NAPHTHALENE ($C_{10}H_8$)	0.76	0.27	0.44
DIHYDROPYRENE ($C_{16}H_{12}$)	0.00	0.00	0.00
PYRENE ($C_{16}H_{10}$)	0.15	0.13	0.14

Table A4

18 mole % PYRENE & 82 mole % TETRALIN with 5.0 MPa NITROGEN (cold) at 648 K

PRESSURE (MPa) = 12.5 MPa	MOLE FRACTION		
COMPOUND	PORT 1	PORT 2	PORT 3
INDENE or BENZENE derivative (C_9H_{10})	0.00	0.00	0.00
INDENE or BENZENE derivative ($C_{10}H_{12}$)	0.07	0.09	0.09
TETRALIN ($C_{10}H_{12}$)	0.72	0.68	0.72
NAPHTHALENE ($C_{10}H_8$)	0.13	0.00	0.00
DIHYDROPYRENE ($C_{16}H_{12}$)	0.00	0.00	0.00
PYRENE ($C_{16}H_{10}$)	0.08	0.23	0.19

18 mole % PYRENE & 82 mole % TETRALIN with 5.0 MPa NITROGEN (cold) at 673 K

PRESSURE (MPa) = 15.0 MPa	MOLE FRACTION		
COMPOUND	PORT 1	PORT 2	PORT 3
INDENE or BENZENE derivative (C_9H_{10})	0.07	0.05	0.00
INDENE or BENZENE derivative ($C_{10}H_{12}$)	0.23	0.25	0.17
TETRALIN ($C_{10}H_{12}$)	0.22	0.28	0.52
NAPHTHALENE ($C_{10}H_8$)	0.37	0.26	0.14
DIHYDROPYRENE ($C_{16}H_{12}$)	0.00	0.00	0.00
PYRENE ($C_{16}H_{10}$)	0.12	0.17	0.18

18 mole % PYRENE & 82 mole % TETRALIN with 5.0 MPa NITROGEN (cold) at 698 K

PRESSURE (MPa) = 15.3 MPa	MOLE FRACTION		
COMPOUND	PORT 1	PORT 2	PORT 3
INDENE or BENZENE derivative (C_9H_{10})	0.12	0.08	***
INDENE or BENZENE derivative ($C_{10}H_{12}$)	0.00	0.06	***
TETRALIN ($C_{10}H_{12}$)	0.00	0.10	***
NAPHTHALENE ($C_{10}H_8$)	0.74	0.63	***
DIHYDROPYRENE ($C_{16}H_{12}$)	0.00	0.00	***
PYRENE ($C_{16}H_{10}$)	0.14	0.13	***

*** - Sample not obtained due to coking

Table A5

18 mole % PYRENE & 82 mole % TETRALIN with 7.5 MPa NITROGEN (cold) at 648 K

PRESSURE (MPa) = 18.5 MPa	MOLE FRACTION		
COMPOUND	PORT 1	PORT 2	PORT 3
INDENE or BENZENE derivative (C_9H_{10})	0.00	0.00	0.00
INDENE or BENZENE derivative ($C_{10}H_{12}$)	0.00	0.13	0.11
TETRALIN ($C_{10}H_{12}$)	0.78	0.70	0.68
NAPHTHALENE ($C_{10}H_8$)	0.08	0.06	0.05
DIHYDROPYRENE ($C_{16}H_{12}$)	0.00	0.00	0.00
PYRENE ($C_{16}H_{10}$)	0.14	0.11	0.16

18 mole % PYRENE & 82 mole % TETRALIN with 7.5 MPa NITROGEN (cold) at 673 K

PRESSURE (MPa) = 20.5 MPa	MOLE FRACTION		
COMPOUND	PORT 1	PORT 2	PORT 3
INDENE or BENZENE derivative (C_9H_{10})	0.03	0.03	0.03
INDENE or BENZENE derivative ($C_{10}H_{12}$)	0.21	0.27	0.26
TETRALIN ($C_{10}H_{12}$)	0.37	0.34	0.25
NAPHTHALENE ($C_{10}H_8$)	0.28	0.21	0.24
DIHYDROPYRENE ($C_{16}H_{12}$)	0.00	0.00	0.01
PYRENE ($C_{16}H_{10}$)	0.11	0.15	0.20

18 mole % PYRENE & 82 mole % TETRALIN with 7.5 MPa NITROGEN (cold) at 698 K

PRESSURE (MPa) = 22.5 MPa	MOLE FRACTION		
COMPOUND	PORT 1	PORT 2	PORT 3
INDENE or BENZENE derivative (C_9H_{10})	0.03	0.06	0.05
INDENE or BENZENE derivative ($C_{10}H_{12}$)	0.22	0.24	0.03
TETRALIN ($C_{10}H_{12}$)	0.37	0.23	0.09
NAPHTHALENE ($C_{10}H_8$)	0.26	0.34	0.56
DIHYDROPYRENE ($C_{16}H_{12}$)	0.00	0.00	0.00
PYRENE ($C_{16}H_{10}$)	0.12	0.13	0.26

Table A6

18 mole % PYRENE & 82 mole % TETRALIN with 12 MPa NITROGEN (cold) at 648 K

PRESSURE (MPa) = 23.4 MPa	MOLE FRACTION		
COMPOUND	PORT 1	PORT 2	PORT 3
INDENE or BENZENE derivative (C_9H_{10})	0.00	0.00	0.00
INDENE or BENZENE derivative ($C_{10}H_{12}$)	0.10	0.29	0.24
TETRALIN ($C_{10}H_{12}$)	0.67	0.41	0.45
NAPHTHALENE ($C_{10}H_8$)	0.13	0.16	0.12
DIHYDROPYRENE ($C_{16}H_{12}$)	0.00	0.00	0.00
PYRENE ($C_{16}H_{10}$)	0.09	0.13	0.18

18 mole % PYRENE & 82 mole % TETRALIN with 12 MPa NITROGEN (cold) at 673 K

PRESSURE (MPa) = 25.0 MPa	MOLE FRACTION		
COMPOUND	PORT 1	PORT 2	PORT 3
INDENE or BENZENE derivative (C_9H_{10})	0.10	0.11	0.13
INDENE or BENZENE derivative ($C_{10}H_{12}$)	0.18	0.17	0.20
TETRALIN ($C_{10}H_{12}$)	0.17	0.05	0.03
NAPHTHALENE ($C_{10}H_8$)	0.48	0.47	0.51
DIHYDROPYRENE ($C_{16}H_{12}$)	0.00	0.00	0.00
PYRENE ($C_{16}H_{10}$)	0.07	0.21	0.14

18 mole % PYRENE & 82 mole % TETRALIN with 12 MPa NITROGEN (cold) at 688 K

PRESSURE (MPa) = 24.0 MPa	MOLE FRACTION		
COMPOUND	PORT 1	PORT 2	PORT 3
INDENE or BENZENE derivative (C_9H_{10})	0.15	0.08	0.00
INDENE or BENZENE derivative ($C_{10}H_{12}$)	0.00	0.00	0.00
TETRALIN ($C_{10}H_{12}$)	0.00	0.00	0.00
NAPHTHALENE ($C_{10}H_8$)	0.75	0.76	0.66
DIHYDROPYRENE ($C_{16}H_{12}$)	0.00	0.00	0.00
PYRENE ($C_{16}H_{10}$)	0.10	0.16	0.34

Table A7

30.4 mole % PYRENE & 69.6 mole % TETRALIN with 5 MPa NITROGEN (cold) at 648 K

PRESSURE (MPa) = 10.0 MPa	MOLE FRACTION		
COMPOUND	PORT 1	PORT 2	PORT 3
INDENE or BENZENE derivative(C[illegible] H[illegible])	0.00	0.00	0.00
INDENE or BENZENE derivative(C[illegible] H[illegible])	0.15	0.25	0.16
TETRALIN (C[illegible] H[illegible])	0.64	0.36	0.42
NAPHTHALENE (C[illegible] H[illegible])	0.14	0.18	0.12
DIHYDROPYRENE (C[illegible] H[illegible])	0.00	0.02	0.02
PYRENE (C[illegible] H[illegible])	0.07	0.20	0.28

30.4 mole % PYRENE & 69.6 mole % TETRALIN with 5 MPa NITROGEN (cold) at 673 K

PRESSURE (MPa) = 11.5 MPa	MOLE FRACTION		
COMPOUND	PORT 1	PORT 2	PORT 3
INDENE or BENZENE derivative(C[illegible] H[illegible])	0.05	0.06	0.00
INDENE or BENZENE derivative(C[illegible] H[illegible])	0.17	0.30	0.21
TETRALIN (C[illegible] H[illegible])	0.34	0.30	0.37
NAPHTHALENE (C[illegible] H[illegible])	0.35	0.29	0.16
DIHYDROPYRENE (C[illegible] H[illegible])	0.00	0.00	0.02
PYRENE (C[illegible] H[illegible])	0.10	0.15	0.24

Table A8

18 mole % PYRENE & 82 mole % TETRALIN with 3.5 MPa METHANE (cold) at 648 K

PRESSURE (MPa) = 7.5 MPa	MOLE FRACTION		
COMPOUND	PORT 1	PORT 2	PORT 3
INDENE or BENZENE derivative(C_9H_{10})	0.00	0.15	0.00
INDENE or BENZENE derivative($C_{10}H_{12}$)	0.00	0.00	0.12
TETRALIN ($C_{10}H_{12}$)	0.79	0.44	0.44
NAPHTHALENE ($C_{10}H_8$)	0.11	0.10	0.09
DIHYDROPYRENE ($C_{16}H_{12}$)	0.00	0.03	0.03
PYRENE ($C_{16}H_{10}$)	0.10	0.28	0.31

18 mole % PYRENE & 82 mole % TETRALIN with 3.5 MPa METHANE (cold) at 673 K

PRESSURE (MPa) = 9.0 MPa	MOLE FRACTION		
COMPOUND	PORT 1	PORT 2	PORT 3
INDENE or BENZENE derivative(C_9H_{10})	0.00	0.04	0.04
INDENE or BENZENE derivative($C_{10}H_{12}$)	0.04	0.25	0.21
TETRALIN ($C_{10}H_{12}$)	0.83	0.21	0.15
NAPHTHALENE ($C_{10}H_8$)	0.09	0.28	0.33
DIHYDROPYRENE ($C_{16}H_{12}$)	0.00	0.01	0.02
PYRENE ($C_{16}H_{10}$)	0.04	0.20	0.26

18 mole % PYRENE & 82 mole % TETRALIN with 3.5 MPa METHANE (cold) at 698 K

PRESSURE (MPa) =	MOLE FRACTION		
COMPOUND	PORT 1	PORT 2	PORT 3
INDENE or BENZENE derivative(C_9H_{10})	0.07	0.03	0.09
INDENE or BENZENE derivative($C_{10}H_{12}$)	0.00	0.10	0.00
TETRALIN ($C_{10}H_{12}$)	0.00	0.09	0.00
NAPHTHALENE ($C_{10}H_8$)	0.73	0.56	0.71
DIHYDROPYRENE ($C_{16}H_{12}$)	0.00	0.00	0.00
PYRENE ($C_{16}H_{10}$)	0.20	0.22	0.20

Table A9

18 mole % PYRENE & 82 mole % TETRALIN with 5.0 MPa METHANE (cold) at 648 K

PRESSURE (MPa) = 13.5 MPa	MOLE FRACTION		
COMPOUND	PORT 1	PORT 2	PORT 3
INDENE or BENZENE derivative (C_9H_{10})	0.00	0.00	0.00
INDENE or BENZENE derivative ($C_{10}H_{12}$)	0.19	0.30	0.25
TETRALIN ($C_{10}H_{12}$)	0.66	0.56	0.48
NAPHTHALENE ($C_{10}H_8$)	0.05	0.09	0.12
DIHYDROPYRENE ($C_{16}H_{12}$)	0.00	0.00	0.02
PYRENE ($C_{16}H_{10}$)	0.10	0.05	0.13

18 mole % PYRENE & 82 mole % TETRALIN with 5.0 MPa METHANE (cold) at 673 K

PRESSURE (MPa) = 13.0 MPa	MOLE FRACTION		
COMPOUND	PORT 1	PORT 2	PORT 3
INDENE or BENZENE derivative (C_9H_{10})	0.06	0.05	0.14
INDENE or BENZENE derivative ($C_{10}H_{12}$)	0.24	0.28	0.12
TETRALIN ($C_{10}H_{12}$)	0.25	0.27	0.02
NAPHTHALENE ($C_{10}H_8$)	0.31	0.27	0.51
DIHYDROPYRENE ($C_{16}H_{12}$)	0.00	0.00	0.00
PYRENE ($C_{16}H_{10}$)	0.14	0.13	0.21

18 mole % PYRENE & 82 mole % TETRALIN with 5.0 MPa METHANE (cold) at 698 K

PRESSURE (MPa) = 12.6 MPa	MOLE FRACTION		
COMPOUND	PORT 1	PORT 2	PORT 3
INDENE or BENZENE derivative (C_9H_{10})	0.13	0.25	0.30
INDENE or BENZENE derivative ($C_{10}H_{12}$)	0.00	0.19	0.11
TETRALIN ($C_{10}H_{12}$)	0.00	0.13	0.03
NAPHTHALENE ($C_{10}H_8$)	0.56	0.30	0.41
DIHYDROPYRENE ($C_{16}H_{12}$)	0.00	0.00	0.00
PYRENE ($C_{16}H_{10}$)	0.30	0.13	0.14

Table A10

18 mole % PYRENE & 82 mole % TETRALIN with 7.5 MPa METHANE (cold) at 648 K

PRESSURE (MPa) = 20.5 MPa	MOLE FRACTION		
COMPOUND	PORT 1	PORT 2	PORT 3
INDENE or BENZENE derivative (C_9H_{10})	0.00	0.00	0.00
INDENE or BENZENE derivative ($C_{10}H_{12}$)	0.00	0.10	0.10
TETRALIN ($C_{10}H_{12}$)	0.77	0.79	0.76
NAPHTHALENE ($C_{10}H_8$)	0.11	0.00	0.05
DIHYDROPYRENE ($C_{16}H_{12}$)	0.00	0.00	0.00
PYRENE ($C_{16}H_{10}$)	0.11	0.11	0.09

18 mole % PYRENE & 82 mole % TETRALIN with 7.5 MPa METHANE (cold) at 673 K

PRESSURE (MPa) = 22.5 MPa	MOLE FRACTION		
COMPOUND	PORT 1	PORT 2	PORT 3
INDENE or BENZENE derivative (C_9H_{10})	0.04	0.00	0.00
INDENE or BENZENE derivative ($C_{10}H_{12}$)	0.21	0.16	0.18
TETRALIN ($C_{10}H_{12}$)	0.38	0.62	0.55
NAPHTHALENE ($C_{10}H_8$)	0.29	0.12	0.14
DIHYDROPYRENE ($C_{16}H_{12}$)	0.00	0.00	0.00
PYRENE ($C_{16}H_{10}$)	0.08	0.10	0.14

18 mole % PYRENE & 82 mole % TETRALIN with 7.5 MPa METHANE (cold) at 698 K

PRESSURE (MPa) = 25.0 MPa	MOLE FRACTION		
COMPOUND	PORT 1	PORT 2	PORT 3
INDENE or BENZENE derivative (C_9H_{10})	0.11	0.00	0.04
INDENE or BENZENE derivative ($C_{10}H_{12}$)	0.00	0.16	0.12
TETRALIN ($C_{10}H_{12}$)	0.00	0.64	0.25
NAPHTHALENE ($C_{10}H_8$)	0.73	0.15	0.41
DIHYDROPYRENE ($C_{16}H_{12}$)	0.00	0.00	0.00
PYRENE ($C_{16}H_{10}$)	0.16	0.05	0.18

Table A11

18 mole % PYRENE & 82 mole % TETRALIN with 3.5 MPa METHANE (cold) at 648 K

PRESSURE (MPa) = 10.2 MPa	MOLE FRACTION		
COMPOUND	PORT 1	PORT 2	PORT 3
INDENE or BENZENE derivative (C_9H_{10})	0.00	0.00	0.00
INDENE or BENZENE derivative ($C_{10}H_{12}$)	0.10	0.16	0.14
TETRALIN ($C_{10}H_{12}$)	0.71	0.58	0.62
NAPHTHALENE ($C_{10}H_8$)	0.08	0.06	0.05
DIHYDROPYRENE ($C_{16}H_{12}$)	0.00	0.00	0.00
PYRENE ($C_{16}H_{10}$)	0.11	0.19	0.19

18 mole % PYRENE & 82 mole % TETRALIN with 3.5 MPa METHANE (cold) at 673 K

PRESSURE (MPa) = 10.8 MPa	MOLE FRACTION		
COMPOUND	PORT 1	PORT 2	PORT 3
INDENE or BENZENE derivative (C_9H_{10})	0.06	0.00	0.04
INDENE or BENZENE derivative ($C_{10}H_{12}$)	0.24	0.22	0.24
TETRALIN ($C_{10}H_{12}$)	0.26	0.41	0.37
NAPHTHALENE ($C_{10}H_8$)	0.32	0.19	0.19
DIHYDROPYRENE ($C_{16}H_{12}$)	0.00	0.00	0.01
PYRENE ($C_{16}H_{10}$)	0.12	0.18	0.15

18 mole % PYRENE & 82 mole % TETRALIN with 3.5 MPa METHANE (cold) at 698 K

PRESSURE (MPa) = 10.8 MPa	MOLE FRACTION		
COMPOUND	PORT 1	PORT 2	PORT 3
INDENE or BENZENE derivative (C_9H_{10})	0.68	0.09	0.04
INDENE or BENZENE derivative ($C_{10}H_{12}$)	0.00	0.10	0.24
TETRALIN ($C_{10}H_{12}$)	0.00	0.17	0.37
NAPHTHALENE ($C_{10}H_8$)	0.27	0.46	0.19
DIHYDROPYRENE ($C_{16}H_{12}$)	0.00	0.00	0.00
PYRENE ($C_{16}H_{10}$)	0.05	0.18	0.12

Table A12

30.4 mole % PYRENE & 69.6 mole % TETRALIN with 5.0 MPa METHANE (cold) at 648 K

PRESSURE (MPa) = 12.5 MPa	MOLE FRACTION		
COMPOUND	PORT 1	PORT 2	PORT 3
INDENE or BENZENE derivative (C_9H_{10})	0.00	0.00	N/A
INDENE or BENZENE derivative ($C_{10}H_{12}$)	0.00	0.14	N/A
TETRALIN ($C_{10}H_{12}$)	0.77	0.60	N/A
NAPHTHALENE ($C_{10}H_8$)	0.13	0.08	N/A
DIHYDROPYRENE ($C_{16}H_{12}$)	0.00	0.00	N/A
PYRENE ($C_{16}H_{10}$)	0.10	0.18	N/A

30.4 mole % PYRENE & 69.6 mole % TETRALIN with 5.0 MPa METHANE (cold) at 673 K

PRESSURE (MPa) = 14.5 MPa	MOLE FRACTION		
COMPOUND	PORT 1	PORT 2	PORT 3
INDENE or BENZENE derivative (C_9H_{10})	0.03	0.08	0.04
INDENE or BENZENE derivative ($C_{10}H_{12}$)	0.17	0.25	0.16
TETRALIN ($C_{10}H_{12}$)	0.30	0.14	0.20
NAPHTHALENE ($C_{10}H_8$)	0.36	0.32	0.27
DIHYDROPYRENE ($C_{16}H_{12}$)	0.00	0.00	0.02
PYRENE ($C_{16}H_{10}$)	0.14	0.22	0.31

30.4 mole % PYRENE & 69.6 mole % TETRALIN with 5.0 MPa METHANE (cold) at 698 K

PRESSURE (MPa) = 17.3 MPa	MOLE FRACTION		
COMPOUND	PORT 1	PORT 2	PORT 3
INDENE or BENZENE derivative (C_9H_{10})	0.00	0.06	0.04
INDENE or BENZENE derivative ($C_{10}H_{12}$)	0.00	0.00	0.11
TETRALIN ($C_{10}H_{12}$)	0.00	0.00	0.30
NAPHTHALENE ($C_{10}H_8$)	0.83	0.73	0.33
DIHYDROPYRENE ($C_{16}H_{12}$)	0.00	0.00	0.00
PYRENE ($C_{16}H_{10}$)	0.17	0.21	0.23

Appendix B : Sample compositions from heavy oils

Table B1 : 50 wt. % Venezuela Vacuum Bottoms (blend 24) and 50 wt. % Anthracene oil with 5 MPa hydrogen at 623 K.

TEMPERATURE (K) = 623 K PRESSURE (MPa) = 9.8 MPa	MOLE FRACTION		
COMPOUND	PORT 1	PORT 2	PORT 3
INDENE or BENZENE derivative (C_9H_{10})	N/A	0.00	0.00
INDENE or BENZENE derivative ($C_{10}H_{14}$)	N/A	0.02	0.01
INDENE or BENZENE derivative ($C_{10}H_{12}$)	N/A	0.03	0.05
BENZENE DERIVATIVE ($C_{10}H_{14}$)	N/A	0.00	0.00
TETRALIN ($C_{10}H_{12}$)	N/A	0.00	0.00
NAPHTHALENE ($C_{10}H_8$)	N/A	0.16	0.17
NAPHTHALENE or INDENE deriv. ($C_{11}H_{10}$)	N/A	0.03	0.03
METHYL NAPHTHALENE ($C_{11}H_{10}$)	N/A	0.00	0.00
NAPHTHALENE or INDENE deriv. ($C_{11}H_{10}$)	N/A	0.02	0.01
NAPHTHALENE deriv. ($C_{12}H_{10}$) & ($C_{12}H_{12}$)	N/A	0.00	0.00
ACENAPTHENE ($C_{12}H_{10}$)	N/A	0.10	0.11
DIBENZOFURAN ($C_{12}H_8O$)	N/A	0.08	0.08
9-H FLUORENE ($C_{13}H_{10}$)	N/A	0.04	0.04
9-H FLUORENE METHYL ($C_{14}H_{12}$)	N/A	0.00	0.00
DIBENZOFURAN METHYL ($C_{13}H_{10}O$)	N/A	0.00	0.00
PHENANTHRENE derivative ($C_{14}H_{12}$)	N/A	0.00	0.00
PHENANTHRENE or ANTHRACENE ($C_{14}H_{10}$)	N/A	0.34	0.34
PYRENE or FLUORANTHENE ($C_{16}H_{10}$)	N/A	0.18	0.16

Table B2 : 50 wt. % Venezuela Vacuum Bottoms (blend 24) and 50 wt. % Anthracene Oil with 5 MPa hydrogen at 648 K.

TEMPERATURE (K) = 648 K PRESSURE (MPa) = 10.7 MPa	MOLE FRACTION		
COMPOUND	PORT 1	PORT 2	PORT 3
INDENE or BENZENE derivative ($C_9 H_{10}$)	N/A	0.00	0.00
INDENE or BENZENE derivative ($C_{10} H_{14}$)	N/A	0.07	0.00
INDENE or BENZENE derivative ($C_{10} H_{12}$)	N/A	0.07	0.00
BENZENE DERIVATIVE ($C_{10} H_{14}$)	N/A	0.00	0.00
TETRALIN ($C_{10} H_{12}$)	N/A	0.00	0.00
NAPHTHALENE ($C_{10} H_8$)	N/A	0.37	0.17
NAPHTHALENE or INDENE deriv. ($C_{11} H_{10}$)	N/A	0.05	0.04
METHYL NAPHTHALENE ($C_{11} H_{10}$)	N/A	0.00	0.00
NAPHTHALENE or INDENE deriv. ($C_{11} H_{10}$)	N/A	0.04	0.03
NAPHTHALENE deriv. ($C_{12} H_{10}$) & ($C_{12} H_{12}$)	N/A	0.00	0.00
ACENAPTHENE ($C_{12} H_{10}$)	N/A	0.09	0.05
DIBENZOFURAN ($C_{12} H_8 O$)	N/A	0.06	0.08
9-H FLUORENE ($C_{13} H_{10}$)	N/A	0.02	0.07
9-H FLUORENE METHYL ($C_{14} H_{12}$)	N/A	0.00	0.00
DIBENZOFURAN METHYL ($C_{13} H_{10} O$)	N/A	0.00	0.00
PHENANTHRENE derivative ($C_{14} H_{12}$)	N/A	0.00	0.00
PHENANTHRENE or ANTHRACENE ($C_{14} H_{10}$)	N/A	0.19	0.34
PYRENE or FLUORANTHENE ($C_{16} H_{10}$)	N/A	0.04	0.22

Table B3 : 50 wt. % Venezuela Vacuum Bottoms (blend 24) and 50 wt. % Anthracene oil with 5 MPa hydrogen at 673 K.

TEMPERATURE (K) = 673 K PRESSURE (MPa) = 13.0 MPa	MOLE FRACTION		
COMPOUND	PORT 1	PORT 2	PORT 3
INDENE or BENZENE derivative (C_9 H_{10})	N/A	0.00	0.00
INDENE or BENZENE derivative (C_{10} H_{14})	N/A	0.00	0.27
INDENE or BENZENE derivative (C_{10} H_{12})	N/A	0.00	0.00
BENZENE DERIVATIVE (C_{10} H_{14})	N/A	0.00	0.00
TETRALIN (C_{10} H_{12})	N/A	0.00	0.00
NAPHTHALENE (C_{10} H_8)	N/A	0.35	0.37
NAPHTHALENE or INDENE deriv. (C_{11} H_{10})	N/A	0.09	0.00
METHYL NAPHTHALENE (C_{11} H_{10})	N/A	0.00	0.00
NAPHTHALENE or INDENE deriv. (C_{11} H_{10})	N/A	0.04	0.02
NAPHTHALENE deriv. (C_{12} H_{10}) & (C_{12} H_{12})	N/A	0.00	0.00
ACENAPTHENE (C_{12} H_{10})	N/A	0.07	0.00
DIBENZOFURAN (C_{12} H_8 O)	N/A	0.05	0.20
9-H FLUORENE (C_{13} H_{10})	N/A	0.08	0.02
9-H FLUORENE METHYL (C_{14} H_{12})	N/A	0.06	0.00
DIBENZOFURAN METHYL (C_{13} H_{10} O)	N/A	0.00	0.00
PHENANTHRENE derivative (C_{14} H_{12})	N/A	0.00	0.00
PHENANTHRENE or ANTHRACENE (C_{14} H_{10})	N/A	0.19	0.07
PYRENE or FLUORANTHENE (C_{16} H_{10})	N/A	0.07	0.03

Table B4 : 70 wt. % Venezuela Vacuum Bottoms (blend 24) and 30 wt. % Anthracene oil with 5 MPa hydrogen at 648 K.

TEMPERATURE (K) = 648 K PRESSURE (MPa) = 12.5 MPa	MOLE FRACTION		
COMPOUND	PORT 1	PORT 2	PORT 3
INDENE or BENZENE derivative (C_9H_{10})	0.00	0.00	0.00
INDENE or BENZENE derivative ($C_{10}H_{14}$)	0.00	0.00	0.00
INDENE or BENZENE derivative ($C_{10}H_{12}$)	0.04	0.07	0.00
BENZENE DERIVATIVE ($C_{10}H_{14}$)	0.03	0.00	0.00
TETRALIN ($C_{10}H_{12}$)	0.00	0.04	0.00
NAPHTHALENE ($C_{10}H_8$)	0.23	0.25	0.21
NAPHTHALENE or INDENE deriv. ($C_{11}H_{10}$)	0.00	0.04	0.04
METHYL NAPHTHALENE ($C_{11}H_{10}$)	0.05	0.00	0.00
NAPHTHALENE or INDENE deriv. ($C_{11}H_{10}$)	0.03	0.03	0.00
NAPHTHALENE deriv. ($C_{12}H_{10}$) & ($C_{12}H_{12}$)	0.07	0.00	0.02
ACENAPTHENE ($C_{12}H_{10}$)	0.07	0.10	0.00
DIBENZOFURAN ($C_{12}H_8O$)	0.07	0.05	0.20
9-H FLUORENE ($C_{13}H_{10}$)	0.06	0.03	0.07
9-H FLUORENE METHYL ($C_{14}H_{12}$)	0.02	0.00	0.08
DIBENZOFURAN METHYL ($C_{13}H_{10}O$)	0.02	0.00	0.00
PHENANTHRENE derivative ($C_{14}H_{12}$)	0.02	0.00	0.00
PHENANTHRENE or ANTHRACENE ($C_{14}H_{10}$)	0.21	0.18	0.24
PYRENE or FLUORANTHENE ($C_{16}H_{10}$)	0.08	0.21	0.14

Table B5 : 70 wt. % Venezuela Vacuum Bottoms (blend 24) and 30 wt. % Anthracene oil with 5 MPa hydrogen at 673 K.

TEMPERATURE (K) = 673 K PRESSURE (MPa) = 15.0 MPa	MOLE FRACTION		
COMPOUND	PORT 1	PORT 2	PORT 3
INDENE or BENZENE derivative (C_9H_{10})	0.00	0.00	***
INDENE or BENZENE derivative ($C_{10}H_{14}$)	0.00	0.00	***
INDENE or BENZENE derivative ($C_{10}H_{12}$)	0.00	0.15	***
BENZENE DERIVATIVE ($C_{10}H_{14}$)	0.00	0.00	***
TETRALIN ($C_{10}H_{12}$)	0.00	0.05	***
NAPHTHALENE ($C_{10}H_8$)	0.25	0.45	***
NAPHTHALENE or INDENE deriv. ($C_{11}H_{10}$)	0.09	0.03	***
METHYL NAPHTHALENE ($C_{11}H_{10}$)	0.00	0.00	***
NAPHTHALENE or INDENE deriv. ($C_{11}H_{10}$)	0.04	0.05	***
NAPHTHALENE deriv. ($C_{12}H_{10}$) & ($C_{12}H_{12}$)	0.09	0.00	***
ACENAPTHENE ($C_{12}H_{10}$)	0.06	0.06	***
DIBENZOFURAN ($C_{12}H_8O$)	0.08	0.03	***
9-H FLUORENE ($C_{13}H_{10}$)	0.07	0.00	***
9-H FLUORENE METHYL ($C_{14}H_{12}$)	0.01	0.00	***
DIBENZOFURAN METHYL ($C_{13}H_{10}O$)	0.01	0.00	***
PHENANTHRENE derivative ($C_{14}H_{12}$)	0.02	0.00	***
PHENANTHRENE or ANTHRACENE ($C_{14}H_{10}$)	0.19	0.10	***
PYRENE or FLUORANTHENE ($C_{16}H_{10}$)	0.09	0.08	***

*** - Sample not obtained due to coking

Table B6 : 30 wt. % Venezuela Vacuum Botttoms (blend 24) and 70 wt. % Anthracene oil with 5 MPa hydrogen at 648 K.

TEMPERATURE (K) = 648 K PRESSURE (MPa) = 13.0 MPa	MOLE FRACTION		
COMPOUND	PORT 1	PORT 2	PORT 3
INDENE or BENZENE derivative (C_9H_{10})	0.00	0.00	0.00
INDENE or BENZENE derivative ($C_{10}H_{14}$)	0.00	0.00	0.00
INDENE or BENZENE derivative ($C_{10}H_{12}$)	0.00	0.00	0.00
BENZENE DERIVATIVE ($C_{10}H_{14}$)	0.00	0.00	0.00
TETRALIN ($C_{10}H_{12}$)	0.00	0.00	0.00
NAPHTHALENE ($C_{10}H_8$)	0.47	0.38	0.21
NAPHTHALENE or INDENE deriv. ($C_{11}H_{10}$)	0.08	0.00	0.00
METHYL NAPHTHALENE ($C_{11}H_{10}$)	0.00	0.10	0.06
NAPHTHALENE or INDENE deriv. ($C_{11}H_{10}$)	0.00	0.03	0.01
NAPHTHALENE deriv. ($C_{12}H_{10}$) & ($C_{12}H_{12}$)	0.00	0.02	0.00
ACENAPTHENE ($C_{12}H_{10}$)	0.12	0.03	0.08
DIBENZOFURAN ($C_{12}H_8O$)	0.08	0.08	0.08
9-H FLUORENE ($C_{13}H_{10}$)	0.03	0.06	0.07
9-H FLUORENE METHYL ($C_{14}H_{12}$)	0.00	0.00	0.00
DIBENZOFURAN METHYL ($C_{13}H_{10}O$)	0.00	0.00	0.00
PHENANTHRENE derivative ($C_{14}H_{12}$)	0.00	0.00	0.00
PHENANTHRENE or ANTHRACENE ($C_{14}H_{10}$)	0.15	0.23	0.34
PYRENE or FLUORANTHENE ($C_{16}H_{10}$)	0.07	0.07	0.15

Table B7 : 30 wt. % Venezuela Vacuum Bottoms (blend 24) and 70 wt. % Anthracene oil with 5 MPa hydrogen at 673 K.

TEMPERATURE (K) = 648 K PRESSURE (MPa) = 14.5 MPa	MOLE FRACTION		
COMPOUND	PORT 1	PORT 2	PORT 3
INDENE or BENZENE derivative (C_9 H_{10})	0.00	0.00	0.00
INDENE or BENZENE derivative (C_{10} H_{14})	0.00	0.00	0.00
INDENE or BENZENE derivative (C_{10} H_{12})	0.00	0.00	0.00
BENZENE DERIVATIVE (C_{10} H_{14})	0.00	0.00	0.00
TETRALIN (C_{10} H_{12})	0.02	0.00	0.00
NAPHTHALENE (C_{10} H_8)	0.43	0.37	0.20
NAPHTHALENE or INDENE deriv. (C_{11} H_{10})	0.09	0.09	0.00
METHYL NAPHTHALENE (C_{11} H_{10})	0.00	0.00	0.03
NAPHTHALENE or INDENE deriv. (C_{11} H_{10})	0.03	0.00	0.00
NAPHTHALENE deriv. (C_{12} H_{10}) & (C_{12} H_{12})	0.00	0.02	0.00
ACENAPTHENE (C_{12} H_{10})	0.04	0.02	0.02
DIBENZOFURAN (C_{12} H_8 O)	0.09	0.09	0.07
9-H FLUORENE (C_{13} H_{10})	0.06	0.06	0.05
9-H FLUORENE METHYL (C_{14} H_{12})	0.00	0.00	0.00
DIBENZOFURAN METHYL (C_{13} H_{10} O)	0.00	0.00	0.00
PHENANTHRENE derivative (C_{14} H_{12})	0.00	0.00	0.00
PHENANTHRENE or ANTHRACENE (C_{14} H_{10})	0.19	0.26	0.38
PYRENE or FLUORANTHENE (C_{16} H_{10})	0.05	0.09	0.25

Table B8 : 50 wt. % Athabasca Bitumen and 50 wt. % Anthracene Oil with 5 MPa Hydrogen at 623 K

TEMPERATURE (K) = 623 K PRESSURE (MPa) = 14.0 MPa	MOLE FRACTION		
COMPOUND	PORT 1	PORT 2	PORT 3
INDENE or BENZENE derivative (C_9H_{10})	N/A	0.00	0.00
INDENE or BENZENE derivative ($C_{10}H_{14}$)	N/A	0.00	0.00
INDENE or BENZENE derivative ($C_{10}H_{12}$)	N/A	0.00	0.00
BENZENE DERIVATIVE ($C_{10}H_{14}$)	N/A	0.00	0.00
TETRALIN ($C_{10}H_{12}$)	N/A	0.00	0.00
NAPHTHALENE ($C_{10}H_8$)	N/A	0.11	0.10
NAPHTHALENE or INDENE deriv. ($C_{11}H_{10}$)	N/A	0.00	0.00
METHYL NAPHTHALENE ($C_{11}H_{10}$)	N/A	0.00	0.00
NAPHTHALENE or INDENE deriv. ($C_{11}H_{10}$)	N/A	0.01	0.01
NAPHTHALENE deriv. ($C_{12}H_{10}$) & ($C_{12}H_{12}$)	N/A	0.02	0.02
ACENAPTHENE ($C_{12}H_{10}$)	N/A	0.12	0.14
DIBENZOFURAN ($C_{12}H_8O$)	N/A	0.13	0.11
9-H FLUORENE ($C_{13}H_{10}$)	N/A	0.16	0.17
9-H FLUORENE METHYL ($C_{14}H_{12}$)	N/A	0.00	0.00
DIBENZOFURAN METHYL ($C_{13}H_{10}O$)	N/A	0.00	0.00
PHENANTHRENE derivative ($C_{14}H_{12}$)	N/A	0.00	0.00
PHENANTHRENE or ANTHRACENE ($C_{14}H_{10}$)	N/A	0.32	0.33
PYRENE or FLUORANTHENE ($C_{16}H_{10}$)	N/A	0.13	0.12

Table B9: 50 wt. % Athabasca Bitumen and 50 wt. % Anthracene Oil with 5 MPa Hydrogen at 648 K

TEMPERATURE (K) = 648 K PRESSURE (MPa) = 15.2 MPa	MOLE FRACTION		
COMPOUND	PORT 1	PORT 2	PORT 3
INDENE or BENZENE derivative (C_9 H_{10})	N/A	0.00	0.00
INDENE or BENZENE derivative (C_{10} H_{14})	N/A	0.00	0.00
INDENE or BENZENE derivative (C_{10} H_{12})	N/A	0.00	0.00
BENZENE DERIVATIVE (C_{10} H_{14})	N/A	0.00	0.00
TETRALIN (C_{10} H_{12})	N/A	0.00	0.00
NAPHTHALENE (C_{10} H_8)	N/A	0.26	0.18
NAPHTHALENE or INDENE deriv. (C_{11} H_{10})	N/A	0.08	0.06
METHYL NAPHTHALENE (C_{11} H_{10})	N/A	0.00	0.00
NAPHTHALENE or INDENE deriv. (C_{11} H_{10})	N/A	0.04	0.03
NAPHTHALENE deriv. (C_{12} H_{10}) & (C_{12} H_{12})	N/A	0.03	0.00
ACENAPTHENE (C_{12} H_{10})	N/A	0.10	0.03
DIBENZOFURAN (C_{12} H_8 O)	N/A	0.11	0.08
9-H FLUORENE (C_{13} H_{10})	N/A	0.12	0.06
9-H FLUORENE METHYL (C_{14} H_{12})	N/A	0.00	0.00
DIBENZOFURAN METHYL (C_{13} H_{10} O)	N/A	0.00	0.00
PHENANTHRENE derivative (C_{14} H_{12})	N/A	0.00	0.00
PHENANTHRENE or ANTHRACENE (C_{14} H_{10})	N/A	0.15	0.36
PYRENE or FLUORANTHENE (C_{16} H_{10})	N/A	0.11	0.20

Table B10 : 50 wt. % Athabasca Bitumen and 50 wt. % Anthracene Oil with 5 MPa Hydrogen at 673 K

TEMPERATURE (K) = 648 K PRESSURE (MPa) = 15.2 MPa	MOLE FRACTION		
COMPOUND	PORT 1	PORT 2	PORT 3
INDENE or BENZENE derivative (C_9H_{10})	N/A	0.00	0.00
INDENE or BENZENE derivative ($C_{10}H_{14}$)	N/A	0.00	0.00
INDENE or BENZENE derivative ($C_{10}H_{12}$)	N/A	0.00	0.00
BENZENE DERIVATIVE ($C_{10}H_{14}$)	N/A	0.00	0.00
TETRALIN ($C_{10}H_{12}$)	N/A	0.00	0.00
NAPHTHALENE ($C_{10}H_8$)	N/A	0.26	0.18
NAPHTHALENE or INDENE deriv. ($C_{11}H_{10}$)	N/A	0.08	0.06
METHYL NAPHTHALENE ($C_{11}H_{10}$)	N/A	0.00	0.00
NAPHTHALENE or INDENE deriv. ($C_{11}H_{10}$)	N/A	0.04	0.03
NAPHTHALENE deriv. ($C_{12}H_{10}$) & ($C_{12}H_{12}$)	N/A	0.03	0.00
ACENAPTHENE ($C_{12}H_{10}$)	N/A	0.10	0.03
DIBENZOFURAN ($C_{12}H_8O$)	N/A	0.11	0.08
9-H FLUORENE ($C_{13}H_{10}$)	N/A	0.12	0.06
9-H FLUORENE METHYL ($C_{14}H_{12}$)	N/A	0.00	0.00
DIBENZOFURAN METHYL ($C_{13}H_{10}O$)	N/A	0.00	0.00
PHENANTHRENE derivative ($C_{14}H_{12}$)	N/A	0.00	0.00
PHENANTHRENE or ANTHRACENE ($C_{14}H_{10}$)	N/A	0.15	0.36
PYRENE or FLUORANTHENE ($C_{16}H_{10}$)	N/A	0.11	0.20

Table B11 : 70 wt. % Athabasca Bitumen and 30 wt. % Anthracene oil with 5 MPa Hydrogen at 648 K

TEMPERATURE (K) = 648 K PRESSURE (MPa) = 10.5 MPa	MOLE FRACTION		
COMPOUND	PORT 1	PORT 2	PORT 3
INDENE or BENZENE derivative (C_9H_{10})	0.00	0.00	0.00
INDENE or BENZENE derivative ($C_{10}H_{14}$)	0.00	0.00	0.00
INDENE or BENZENE derivative ($C_{10}H_{12}$)	0.00	0.10	0.00
BENZENE DERIVATIVE ($C_{10}H_{14}$)	0.00	0.00	0.00
TETRALIN ($C_{10}H_{12}$)	0.00	0.06	0.02
NAPHTHALENE ($C_{10}H_8$)	0.38	0.47	0.20
NAPHTHALENE or INDENE deriv. ($C_{11}H_{10}$)	0.08	0.08	0.05
METHYL NAPHTHALENE ($C_{11}H_{10}$)	0.00	0.00	0.00
NAPHTHALENE or INDENE deriv. ($C_{11}H_{10}$)	0.04	0.00	0.03
NAPHTHALENE deriv. ($C_{12}H_{10}$) & ($C_{12}H_{12}$)	0.00	0.00	0.00
ACENAPTHENE ($C_{12}H_{10}$)	0.10	0.00	0.08
DIBENZOFURAN ($C_{12}H_8O$)	0.07	0.05	0.08
9-H FLUORENE ($C_{13}H_{10}$)	0.06	0.04	0.08
9-H FLUORENE METHYL ($C_{14}H_{12}$)	0.00	0.00	0.00
DIBENZOFURAN METHYL ($C_{13}H_{10}O$)	0.00	0.00	0.00
PHENANTHRENE derivative ($C_{14}H_{12}$)	0.00	0.00	0.00
PHENANTHRENE or ANTHRACENE ($C_{14}H_{10}$)	0.19	0.13	0.31
PYRENE or FLUORANTHENE ($C_{16}H_{10}$)	0.08	0.07	0.15

Table B10 : 70 wt. % Athabasca Bitumen and 30 wt. % Anthracene Oil with 5 MPa Hydrogen at 673 K

TEMPERATURE (K) = 673 K PRESSURE (MPa) = 12.0 MPa	MOLE FRACTION		
COMPOUND	PORT 1	PORT 2	PORT 3
INDENE or BENZENE derivative (C_9 H_{10})	0.00	0.00	***
INDENE or BENZENE derivative (C_{10} H_{14})	0.00	0.00	***
INDENE or BENZENE derivative (C_{10} H_{12})	0.00	0.00	***
BENZENE DERIVATIVE (C_{10} H_{14})	0.00	0.00	***
TETRALIN (C_{10} H_{12})	0.00	0.00	***
NAPHTHALENE (C_{10} H_8)	0.37	0.55	***
NAPHTHALENE or INDENE deriv. (C_{11} H_{10})	0.08	0.11	***
METHYL NAPHTHALENE (C_{11} H_{10})	0.00	0.00	***
NAPHTHALENE or INDENE deriv. (C_{11} H_{10})	0.07	0.00	***
NAPHTHALENE deriv. (C_{12} H_{10}) & (C_{12} H_{12})	0.00	0.00	***
ACENAPTHENE (C_{12} H_{10})	0.06	0.00	***
DIBENZOFURAN (C_{12} H_8 O)	0.08	0.08	***
9-H FLUORENE (C_{13} H_{10})	0.06	0.03	***
9-H FLUORENE METHYL (C_{14} H_{12})	0.00	0.00	***
DIBENZOFURAN METHYL (C_{13} H_{10} O)	0.00	0.00	***
PHENANTHRENE derivative (C_{14} H_{12})	0.00	0.00	***
PHENANTHRENE or ANTHRACENE (C_{14} H_{10})	0.21	0.23	***
PYRENE or FLUORANTHENE (C_{16} H_{10})	0.07	0.00	***

*** - Sample not obtained due to coking

Table B11 : 30 wt. % Athasbaca Bitumen and 70 wt. % Anthracene oil with 5 MPa Hydrogen at 648 K

TEMPERATURE (K) = 648 K PRESSURE (MPa) = 13.0 MPa	MOLE FRACTION		
COMPOUND	PORT 1	PORT 2	PORT 3
INDENE or BENZENE derivative (C_9H_{10})	0.06	0.07	0.00
INDENE or BENZENE derivative ($C_{10}H_{14}$)	0.00	0.03	0.00
INDENE or BENZENE derivative ($C_{10}H_{12}$)	0.09	0.34	0.00
BENZENE DERIVATIVE ($C_{10}H_{14}$)	0.00	0.00	0.00
TETRALIN ($C_{10}H_{12}$)	0.07	0.16	0.02
NAPHTHALENE ($C_{10}H_8$)	0.43	0.22	0.24
NAPHTHALENE or INDENE deriv. ($C_{11}H_{10}$)	0.05	0.00	0.05
METHYL NAPHTHALENE ($C_{11}H_{10}$)	0.00	0.00	0.00
NAPHTHALENE or INDENE deriv. ($C_{11}H_{10}$)	0.03	0.00	0.03
NAPHTHALENE deriv. ($C_{12}H_{10}$) & ($C_{12}H_{12}$)	0.00	0.00	0.00
ACENAPTHENE ($C_{12}H_{10}$)	0.06	0.01	0.10
DIBENZOFURAN ($C_{12}H_8O$)	0.04	0.00	0.05
9-H FLUORENE ($C_{13}H_{10}$)	0.00	0.00	0.05
9-H FLUORENE METHYL ($C_{14}H_{12}$)	0.00	0.00	0.00
DIBENZOFURAN METHYL ($C_{13}H_{10}O$)	0.00	0.00	0.00
PHENANTHRENE derivative ($C_{14}H_{12}$)	0.00	0.00	0.25
PHENANTHRENE or ANTHRACENE ($C_{14}H_{10}$)	0.12	0.00	0.21
PYRENE or FLUORANTHENE ($C_{16}H_{10}$)	0.05	0.17	0.15

Table B12 : 30 wt. % Athabasca Bitumen and 70 wt. % Anthracene oil with 5 MPa Hydrogen at 673 K

TEMPERATURE (K) = 673 K PRESSURE (MPa) = 15.5 MPa	MOLE FRACTION		
COMPOUND	PORT 1	PORT 2	PORT 3
INDENE or BENZENE derivative (C_9H_{10})	0.11	0.06	***
INDENE or BENZENE derivative ($C_{10}H_{14}$)	0.00	0.03	***
INDENE or BENZENE derivative ($C_{10}H_{12}$)	0.13	0.31	***
BENZENE DERIVATIVE ($C_{10}H_{14}$)	0.00	0.00	***
TETRALIN ($C_{10}H_{12}$)	0.08	0.17	***
NAPHTHALENE ($C_{10}H_8$)	0.58	0.24	***
NAPHTHALENE or INDENE deriv. ($C_{11}H_{10}$)	0.10	0.01	***
METHYL NAPHTHALENE ($C_{11}H_{10}$)	0.00	0.00	***
NAPHTHALENE or INDENE deriv. ($C_{11}H_{10}$)	0.00	0.00	***
NAPHTHALENE deriv. ($C_{12}H_{10}$) & ($C_{12}H_{12}$)	0.00	0.00	***
ACENAPTHENE ($C_{12}H_{10}$)	0.00	0.01	***
DIBENZOFURAN ($C_{12}H_8O$)	0.00	0.00	***
9-H FLUORENE ($C_{13}H_{10}$)	0.00	0.00	***
9-H FLUORENE METHYL ($C_{14}H_{12}$)	0.00	0.00	***
DIBENZOFURAN METHYL ($C_{13}H_{10}O$)	0.00	0.00	***
PHENANTHRENE derivative ($C_{14}H_{12}$)	0.00	0.00	***
PHENANTHRENE or ANTHRACENE ($C_{14}H_{10}$)	0.00	0.02	***
PYRENE or FLUORANTHENE ($C_{16}H_{10}$)	0.00	0.15	***

*** - Sample not obtained due to coking

Appendix C : Calibrations curves

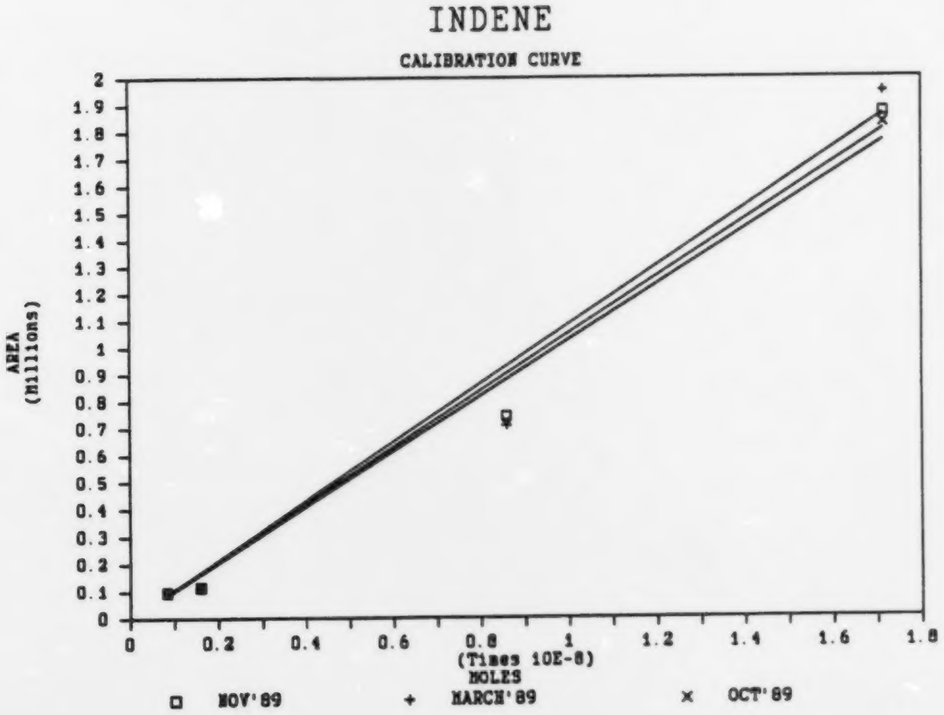

Figure C1 : Calibration curve for indene

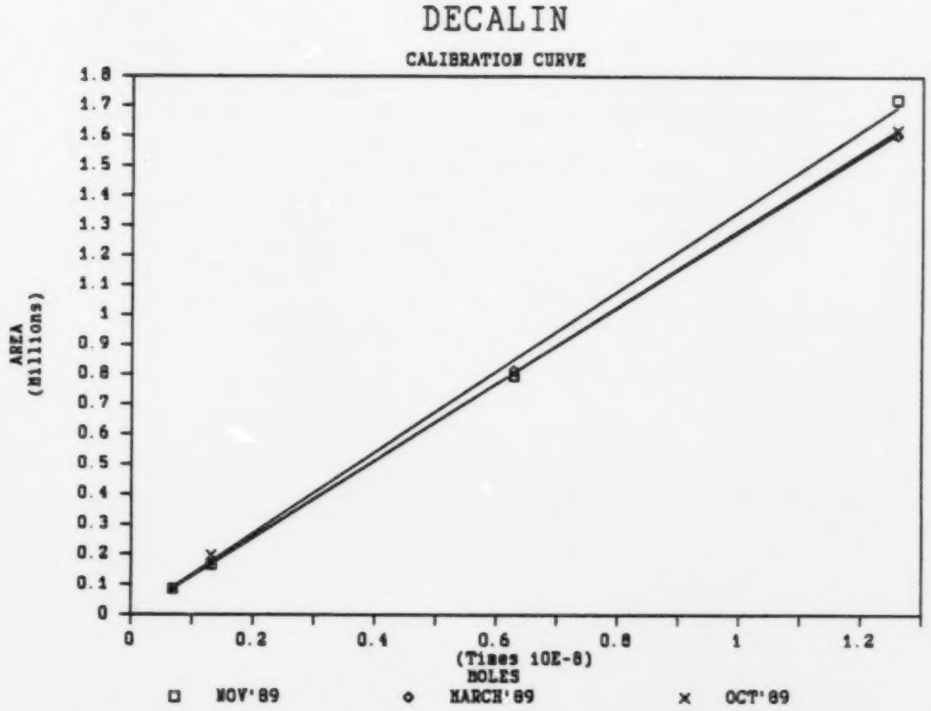

Figure D2 : Calibration curve for decalin (cis and trans)

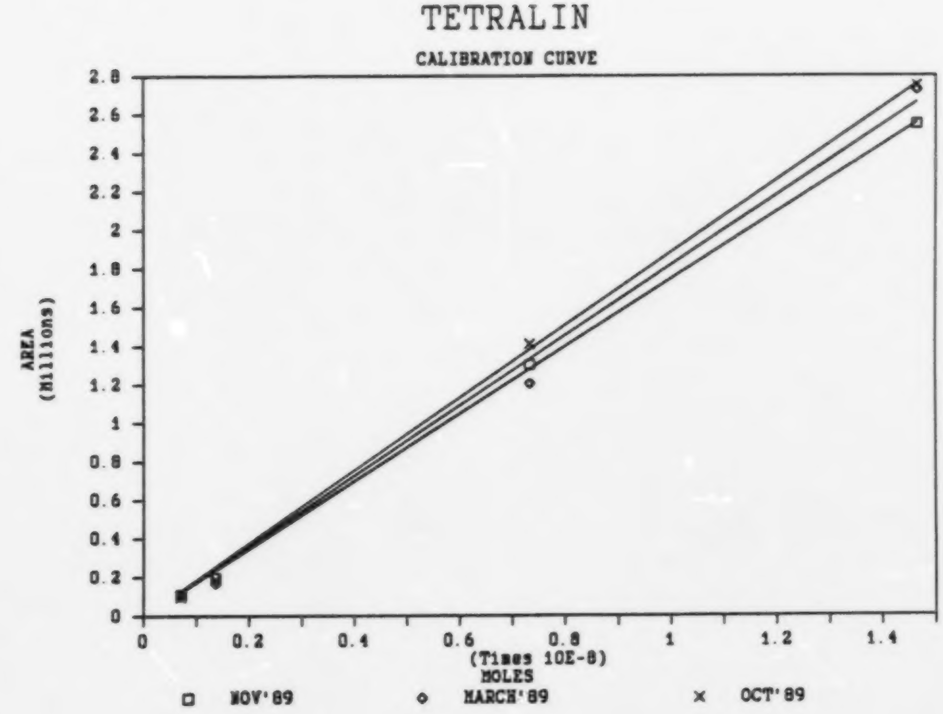

Figure D3 : Calibration curve for tetralin

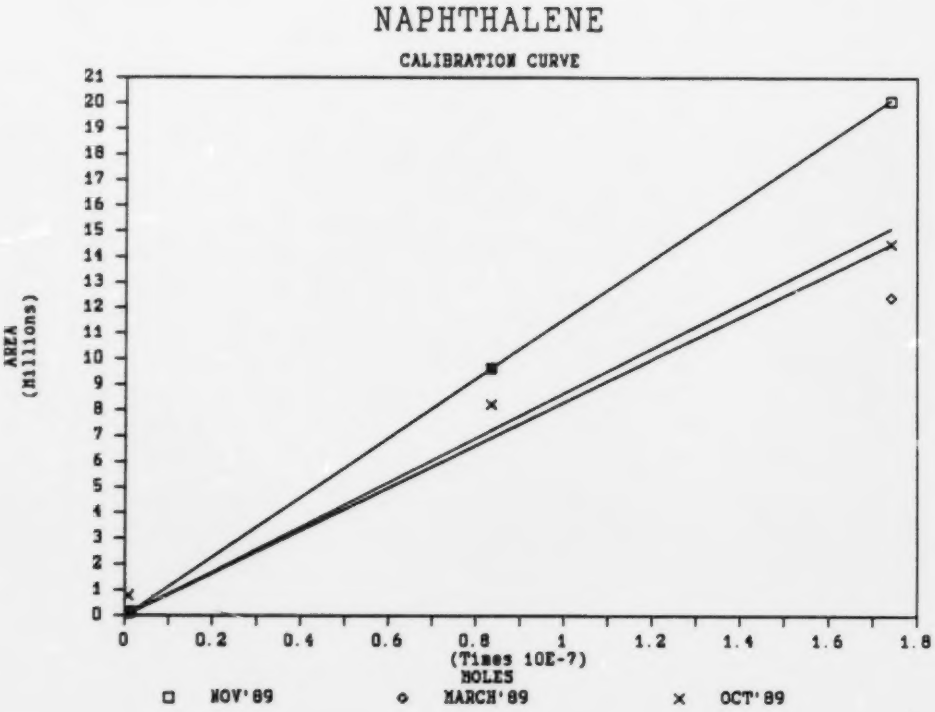

Figure D4 : Calibratino curve for naphthalene

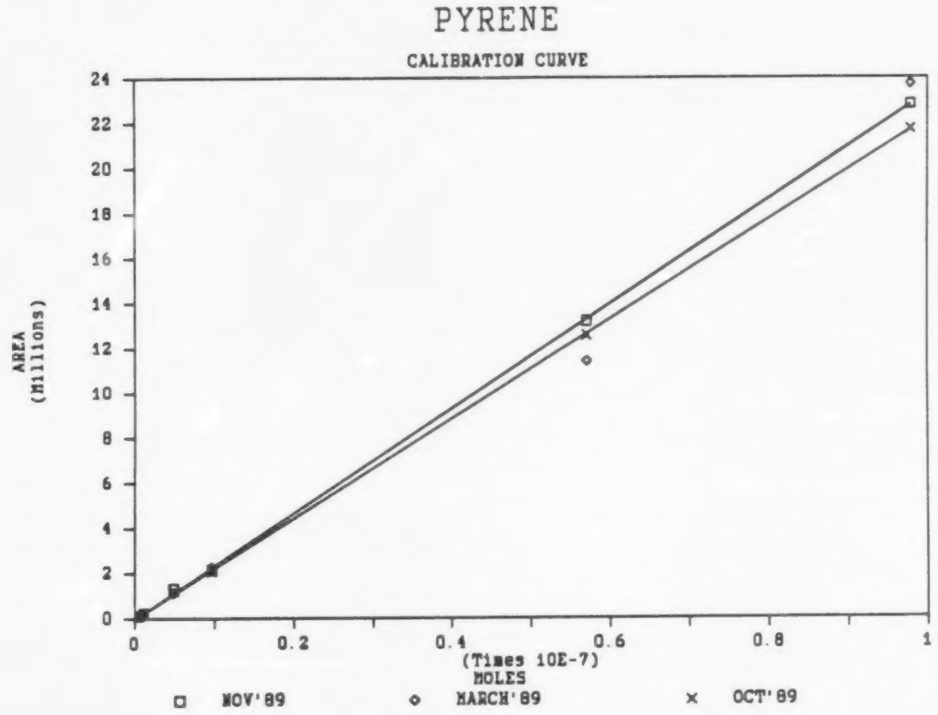

Figure D5 : Calibration curve for pyrene

Appendix D : Sample calculation for port placement

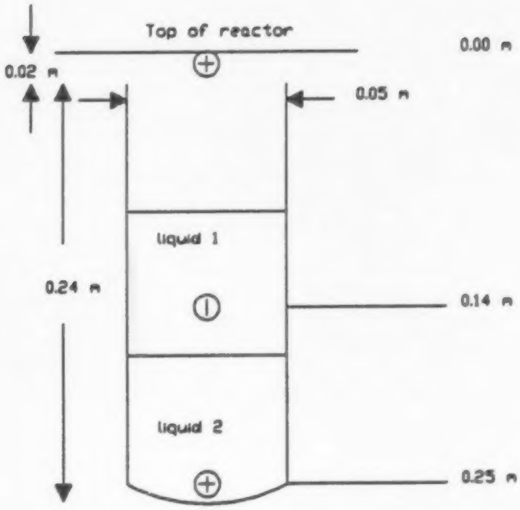
Top of reactor
0.00 m
0.02 m
0.05 m
0.24 m
liquid 1
0.14 m
liquid 2
0.25 m

Cross sectional area of insert $= \frac{\pi D^2}{4} = 0.0019635\ m^2$

Density of tetralin at 700 K = 0.5 g/cm³

Mass of fluid = 180 g

Height of fluid = 0.18 m

Assume each liquid phase is approximately 0.09 m

Place port 2 2/3 into liquid 1.

⊕ -- position of a sample port

Figure D1 : Sample calculation of port placement for model solvent systems

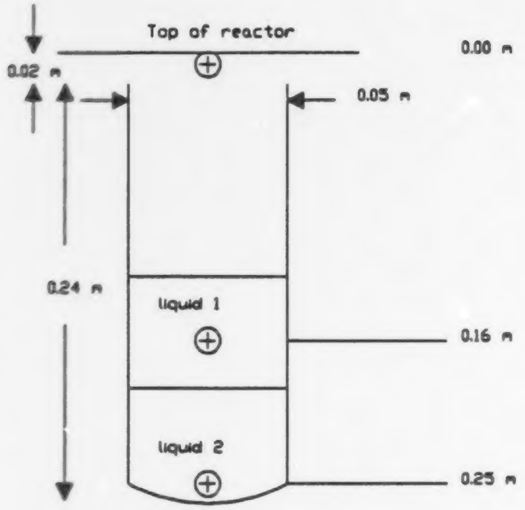
Top of reactor
0.00 m
0.02 m
0.05 m
0.24 m
liquid 1
0.16 m
liquid 2
0.25 m

Cross sectional area of insert = $\frac{\pi D^2}{4}$ = 0.0019635 m^2

Approximate density of heavy oil at 700 K = 0.75 g/cm

Approximate density of anthracene oil = 0.63 g/cm^3

Mass of fluid = 200 g

Assume each liquid phase is approximately 0.07 m

Place port 2 2/3 into liquid 1.

⊕ -- position of a sample port

Figure D2 : Sample calculation of port placement for heavy oil systems